ROLE OF PROTEIN O-MANNOSYLATION IN NERVOUS SYSTEM DEVELOPMENT USING *DROSOPHILA* AS A MODEL

A Dissertation

by

ISHITA CHANDEL

Submitted to the Office of Graduate and Professional Studies of
Texas A&M University
in partial fulfillment of the requirements for the degree of

DOCTOR OF PHILOSOPHY

Chair of Committee,	Dorothy Shippen
Committee Members,	Vlad Panin
	Hubert Amrein
	Junjie Zhang
Head of Department,	Josh A. Wand

December 2020

Major Subject: Biochemistry

ABSTRACT

Protein O-mannosylation (POM) is a post translational modification where enzymes add O-mannose to serine and threonine residues of proteins in the ER. Two well studied enzymes that work as a complex to add O-mannose sugar to Ser/Thr of proteins are protein –O-mannosyltransferase 1 and 2 (POMT1/2). Mutations in *Pomt1/2* cause congenital muscular dystrophies (CMDs) in humans. Although substantial research has been done to elucidate the role of POMT1/2 in muscles, little is known about their role in neural development.

In my dissertation, I used *Drosophila* as a model system to study the functions of POMT1/2 in nervous system development. *Drosophila* has orthologs of *pomt1* and *pomt2* called Rotated Abdomen (*rt*) and Twisted (*tw*), respectively. Mutations in *rt* and *tw* cause a clockwise rotation of abdominal segments in adult flies and embryos. I studied axon morphology of different types of sensory neurons which regulate muscle contraction, body position, pain and locomotion behavior in *rt* and *tw* mutants. I found that both genes are required to maintain axon connections of a class of multidendritic sensory neurons (Class IV) in the ventral nerve cord of *Drosophila.*

Rescue results, RNAi experiments and mosaic analysis with a repressible cell marker (MARCM) revealed that the function of *rt* and *tw* in maintaining axon morphology is cell autonomous.

I further studied the functionally relevant substrates of RT and TW. Dystroglycan (DG) is the only well-studied substrate of POMT1/2 in both humans and *Drosophila*. I found

that *Dystroglycan* mutants do not fully recapitulate the defects seen in *rt* and *tw* mutants. This indicated the importance of other unknown substrates of RT and TW. To that end, I studied a group of transmembrane signal transduction proteins called receptor protein tyrosine phosphatases (RPTPs). Genetic interactions between *tw* and *rptp* mutants revealed synergistic roles in maintaining axon morphology. Mass spectrometry of the RPTP69D protein revealed that it is modified by RT and TW and co-overexpression of RT and TW adds extra O-mannose to RPTP69D. Further biochemical evidence revealed that O-mannose may protect RPTP69D from proteolysis.

Overall, this research work established novel functions and novel substrates of POMT1/2, which might be evolutionarily conserved and shed light on the CMD mechanisms in humans.

DEDICATION

Dedicated to my parents, sister and all my friends..

ACKNOWLEDGEMENTS

I would like to thank my doctoral advisor, Dr. Vladislav Panin, for his constant support and guidance through the years. He has been a great mentor and I learned a lot from him. I would also like to thank my committee members, Dr. Hubert Amrein, Dr. Dorothy Shippen and Dr. Junjie Zhang for their valuable feedback and advice during graduate school.

I also thank the members of the Panin Lab, former and current especially Dr. Boris Novikov, Dr. Brooke Howell, Dr. Ryan Baker, Kacy Petersen and Melissa Koff . I extend a special thanks to Dr. Hillary Scott for her help and friendship. I would also like to thank the faculty and staff of Department of biochemistry and biophysics, especially Rafael Almanzar, Dr. Mary Bryk, Dr. Craig Kaplan and the late Dr. Jim Hu for helping me and teaching me a lot during graduate school.

Finally, I thank my parents and my sister for their moral support and all my friends for keeping me sane during graduate school. Some deserve a special mention; I thank Divya Rathi, Diana Juarez, Daman Brar, Megalakshmi Suresh, Kiran Vasan, Jasmine Yu, Nairita Maitra, Neha Deshpande and Miguel Gonzales for their love and affection.

CONTRIBUTORS AND FUNDING SOURCES

Contributors

This work was supervised by a dissertation committee consisting of Dr. Vlad Panin, Dr. Dorothy Shippen and Dr. Junjie Zhang of the Department of biochemistry and biophysics and Dr. Hubert Amrein of the Department of Molecular and cellular medicine.

The data analyzed for Chapter 4 was provided by Dr. Ryan Baker.

All other work conducted for the dissertation was completed by the student independently.

Funding Sources

This work was made possible in part by NIH grant numbers NIH/NS075534 and NIH/NS099409 to Vlad Panin. Its contents are solely the responsibility of the authors and do not necessarily represent the official views of the NIH.

TABLE OF CONTENTS

Page

LIST OF FIGURES

Page

LIST OF TABLES

Page

CHAPTER I

INTRODUCTION

Protein O-mannosylation (POM) is an evolutionarily conserved posttranslational modification, widely distributed from yeast to mammals(1-3). O-mannosyl glycans on proteins in mammals were first discovered about 40 years ago in rat brain lysate(4), eliciting an interest and intrigue in its function in the nervous system. Moreover, deficiencies in the enzymes that catalyze the addition of O-mannose on proteins were found to cause congenital muscular dystrophies (CMDs) and neurodevelopmental disorders in humans(5). CMDs are a group of debilitating neuromuscular disorders present at birth or early infancy. Interestingly, patients with CMDs exhibit striking neurological abnormalities(6). Despite POM's conservation across species and its association with human diseases the role of POM in the nervous system is still elusive. One of the many challenges that remain is the elucidation of biological roles of O-mannose linked to proteins and the uncovering of identities of proteins that have this modification. Dystroglycan (DG), an extracellular peripheral membrane glycoprotein, is the only well studied protein with characterized structure and function of complex O-mannose modifications on its extracellular domain; these glycans were shown to be important for its interaction with laminin. Several other proteins have recently been shown to have O-mannose sugar on their Ser/Thr residues(7), however the functional purpose it serves or how it's loss could be linked to neurological disorders is unknown. In this section, I attempt to introduce the possible roles of POM with an emphasis on its importance in the nervous system across species. Additionally, I discuss gaps in our

understanding of the neurological functions of O-mannosylation and posit how POM affects neurodevelopment.

Protein O-mannosylation pathways: from yeast to mammals

Protein O-mannosylation pathway is quite diverse, elaborate and compounded in certain cases. The canonical pathway was first discovered in yeast(8) and involves the transfer of mannose from dolichol phosphate β-D-mannose(DPM) to serine and threonine amino acids of proteins, a conserved reaction carried out by Protein-O-mannosyltransferases(9, 10), referred to as PMTs in fungi and POMTs in mammals(11). Two POMTs, POMT1 and POMT2(PMT1-2 in yeast) work as a complex(12) to initialize O-mannosylation in the lumen of ER(Fig. 1).

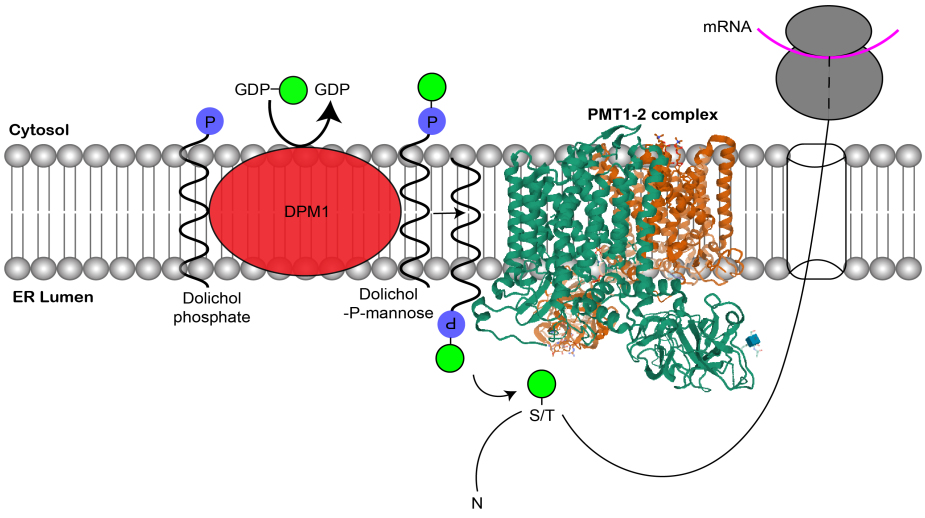

Figure 1. Schematic representation of Protein-O Mannosylation. Initial steps of O Mannosylation are conserved in all species. In yeast, Pmt1-2 work as a complex in the ER lumen to transfer mannose from Dolichol phosphate mannose(DPM) to Ser/Thr of proteins entering the secretory pathway. DPM formation is catalyzed in yeast, by Dpm1p(red) from GDP-mannose (Green circles) and dolichol phosphate on the cytosolic face of the ER and flip flops into the ER lumen. Dark grey, ribosomes; nascent polypeptide (black) shown entering ER lumen. Pmt1 is shown in green and Pmt2 in orange in the ribbon diagram, PDB ID 6P25.

The initial mannose can be then extended in the Golgi by the addition of other sugar moieties making oligo mannose structures in yeast and more complex, heterogeneous structures in mammals(Fig. 2)(11, 13). The oligo mannose structures are found on several cell wall and plasma membrane proteins(14) in yeast, but in mammals Dystroglycan, a membrane glycoprotein involved in cell adhesion is the only well-known and well-studied substrate with highly branched and extended O-mannosyl glycans. Recently, KIAA1549, a protein implicated in pediatric central nervous system tumors(15), was discovered to be a POMT1/2 target in humans(7, 16), however it's functions are unknown. O-mannose was discovered on the extracellular subunit of Dystroglycan called α-Dystroglycan(α-DG) in bovine peripheral nerve and the extended O-mannose oligosaccharide was found to be essential for binding to laminin in the extracellular matrix(17). Interestingly, α-Dystroglycan's O-mannose is differentially elongated based on the tissue indicating the specific roles played by heterogeneous sugar extensions(18). To organize and ease our understanding of the complexities of O-mannose extensions, a nomenclature has been devised(19)(Fig 2), wherein:

1. Single, unextended O-mannose are referred to as Core M0 (catalyzed by POMT1/POMT2).
2. Core M0 modified by β1,2-linked N-Acetylglucosamine (GlcNAc) are M1(catalyzed by Protein O-Linked Mannose N-Acetyl glucosaminyltransferase 1, POMGNT1).
3. Core M1 structure modified with β1,6-linked GlcNAc are M2(catalyzed by Mannosyl (α1,6)-Glycoprotein β1,6-N-Acetyl-Glucosaminyltransferase MGAT5B).

4. Core M0 modified by addition of β1,4-linked GlcNAc are M3(catalyzed by Protein O-Linked Mannose N-Acetyl-glucosaminyltransferase 2 (POMGnT2).

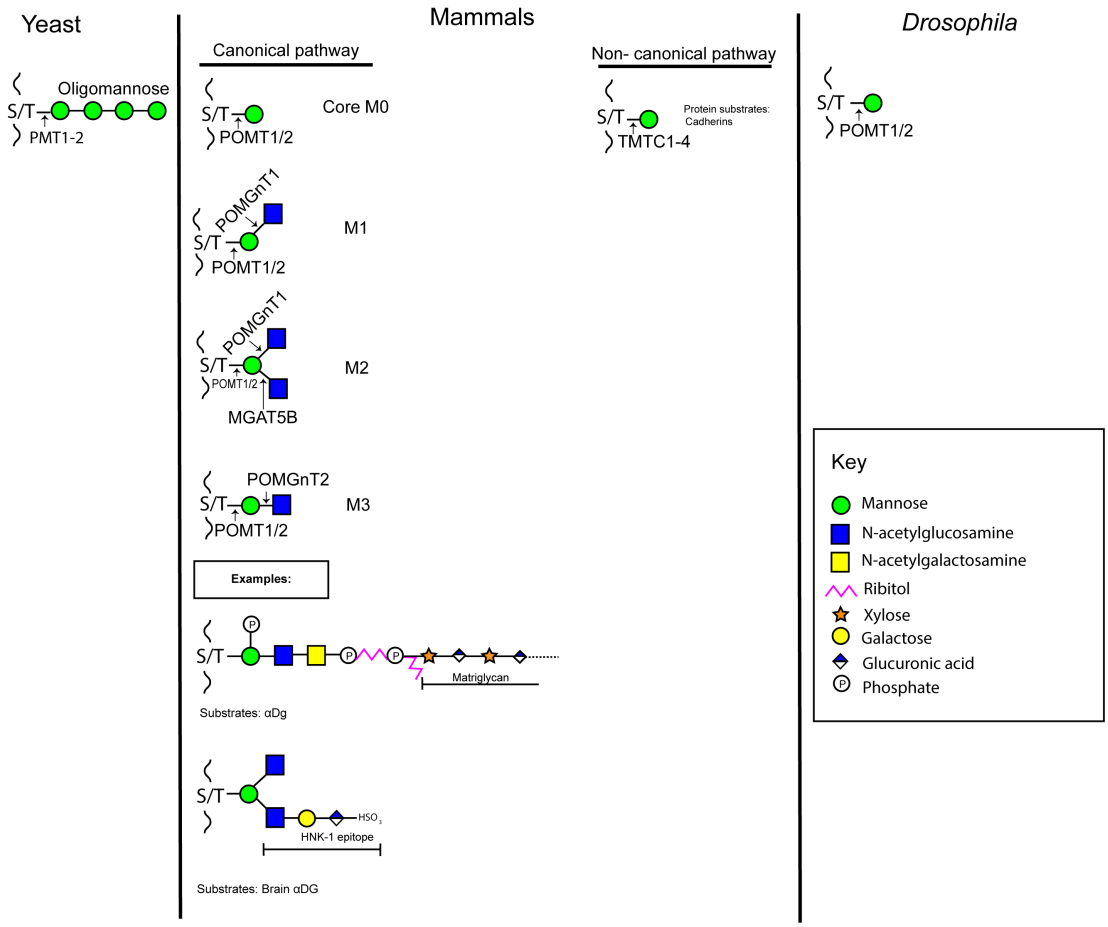

Figure 2. Types of O-mannosylation in different species. After initial O-mannose is added in the ER, it can be extended in the Golgi lumen. In yeast, oligomannose structures are built by Pmt1-7 enzyme family. In mammals, various extended structures classified as M1,M2,M3 are generated by specific enzymes indicated. Examples of M3 functional glycan and M2 glycan (Matriglycan and HNK-1 epitope, respectively) are shown. Non-canonical initial O-mannosylation occurs in ER lumen by TMTC1-4 on cadherins and plexins and is not known to be elongated. In *Drosophila*, elongated O-mannose structures or substrates other than αDG, have not been reported.

Core M1 and M2 structures are further elongated into linear or bisected highly branched O-mannosyl glycans(20). Most commonly studied M1 and M2 structures include the HNK1 epitope found on α-DG isolated from rat brain but not muscles(21) and the Lewis X epitope also found on sheep brain α-DG(22). Both these epitopes are modifications of a common O-mannosylated structure Siaα3Galβ4GlcNAcβ2Manα -Ser/Thr(23), also found on bovine peripheral nerve α-DG(17), wherein HNK-1 epitope has sulfoglucuronic acid in place of sialic acid and Lewis X epitope is a trisaccharide with fucose in between galactose and N-acetylglucosamine(23). Both epitopes are essential for the developing mammalian brain. However, HNK-1 epitope has also been reported on N-linked glycans(24). More recently, terminal sulfoglucuronic acid, a hallmark of HNK-1 epitope was discovered on M3 glycan of α-DG(25). The presence of different O-mannose initiated structures on one substrate α-DG raises an important question about their specific roles in the nervous system.

Core M3 structures are elaborately elongated by a cascade of enzymes and in some cases, form a long, GAG (Glycosaminoglycan)-like, phosphorylated, polysaccharide wherein the GAG-like structure is called “Matriglycan” (19). It consists of Xylose and Glucuronic acid disaccharide repeating units, which are terminally sulfated by HNK-1 Sulfotransferase to form a sulfoglucuronic acid at the end. Matriglycan is only found so far on α-DG isolated from mammalian skeletal muscles(26), although some studies suggest it’s presence on Glypicans. Matriglycan is important for laminin binding(27) and has not been reported on brain α-DG raising an important question of whether different O-mannose structures interact with different ligands in a tissue specific manner. In

general, elaborate core M3 structures are far less abundant in the brain than the M1 and M2 structures(28, 29) indicating that diverse, branched O-mannosyl glycans have distinct functions.

The non-canonical pathway of protein O-mannosylation, recently discovered in human cell lines, adds O-mannose to Ser/Thr of a different set of proteins, Cadherins, Plexins and Receptor tyrosine kinases(RTKs), not α-DG (Fig. 2) (7). Interestingly, the enzymes that add O-mannose to each of these are proteins are different. Cadherins are O-mannosylated by a group of enzymes called transmembrane and tetratricopeptide repeat containing protein 1-4 (TMTC1-4), in the ER lumen. Remarkably, TMTC1-4 are conserved across species (Fig. 3) indicating the significance of this previously overlooked O-mannosylation pathway.

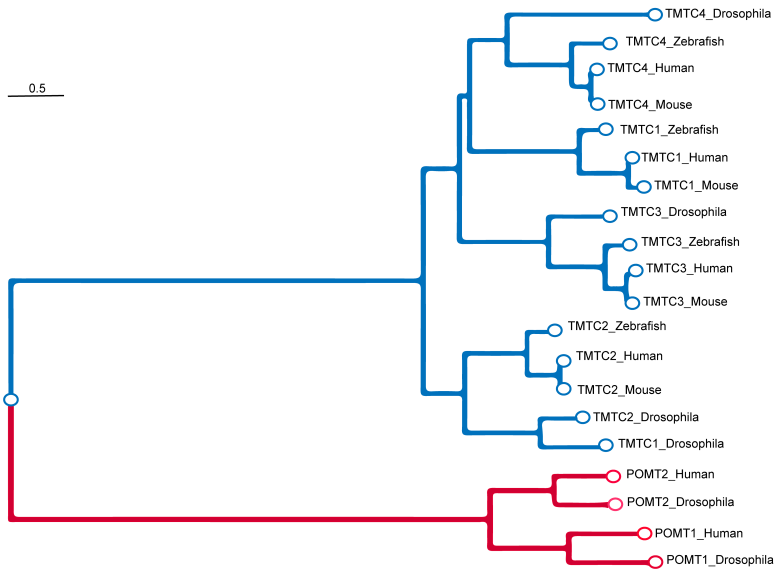

Figure 3. TMTC and POMT evolution across species. Multiple sequence alignments of TMTC1-4 orthologues from human, mouse, zebrafish and Drosophila with POMT1/2 from human and Drosophila. Alignments were generated using CLUSTALW algorithm, distance based phylogenic trees were constructed by an NJ image method (GenomeNet CLUSTALW of Kyoto University Bioinformatics Center.)

It remains to be seen, however, if TMTC1-4 O-mannosylate conserved domains on cadherins in other species. It is unclear why 4 enzymes are needed to O-mannosylate the extracellular cadherin (EC) domains, although it has been hypothesized that individual TMTCs O-mannosylate different β strands on the EC domains (13). Whether TMTC1-4, like POMT1-POMT2 also work together as a complex is a mystery. The enzymes that O-mannosylate the IPT domains of plexins and RTKs are currently unknown. Rather surprisingly, the O-mannose on Cadherins and plexins was shown to be unbranched and unextended quite opposite to what is seen in α-DG O-mannosylation in mammals. Core M1-M3 structures or oligomannoses are not seen on the cadherins, plexins and RTKs. In the same vein, Dystroglycan from *Drosophila* is O-mannosylated but not extended(30), however *Drosophila* does not have homologs of all glycosyltransferases responsible for extension and branching, making this finding easier to comprehend. Nevertheless, it raises another important question of how a single mannose impacts the functions of each of these proteins. More studies are needed to understand if there are tissue specific differences in the O-mannosylation sites of cadherins, plexins and RTKs to better understand their individual functions. Other proteins in mammals that have been shown to possess O-mannosyl glycans on their Ser/Thr are RPTPζ(31), CD24(32), Neurofascin(33) and lecticans(34). It is unclear whether they are O-mannosylated by POMT1/2 or TMTC1-4 or by the still unknown enzyme(s). Strikingly, CD24, a cell adhesion molecule is modified with M1 glycans and Receptor protein tyrosine phosphatase ζ is decorated with HNK1 core M2 glycan. Evidence suggests Neurofascins and lecticans also possess extended O-mannosyl glycans, raising the possibility that

proteins with extended O-mannose structures might be modified by the canonical POMT1/2 pathway. Cadherins, plexins, α-DG, RPTPζ , CD24, Neurofascin and lecticans all have enormous roles especially in the developing nervous system, hence more research on how O-mannose, single or extended, affects their function is imperative.

Yet another non-canonical O-mannosylation pathway so far reported only in yeast adds O-mannose to Ser/Thr of nucleocytoplasmic and mitochondrial proteins(35). The significance of this pathway and the enzymes required are currently unknown. The variety of O-mannosylation pathways that exist across species and the substrates they differentially modify clearly indicates the significance of this glycosylation. It is also interesting to note that known POM targets are enriched in the nervous system and O-mannosyl glycans are highly abundant in the brain, a driving force to advance research in this area.

Structure-function relationship of O-mannose: Emphasis on the nervous system

Different O-mannosyl glycan structures described above, serve different functions. In yeast, single O-mannose added by Pmt1-2 in the ER acts a timer and stops prolonged folding of proteins or folding that takes too many, eventually unproductive cycles(36). It increases solubility of proteins and decreases aggregation. Hence, O-mannosylation not only keeps the protein soluble (required for ER exit), but prevents further folding and perhaps stimulates unfolding, and flags the protein for elimination(37). The rapid O-mannosylation of peptides by mammalian orthologs of PMT1/2 (POMT1/2) is consistent with this(36). Interestingly, in yeast, ER O-mannosylation is a common post

translational mechanism for ER associated degradation(ERAD) substrates, even if their native, folded counterparts are not O-mannosylated. This is known as Unfolded Protein O-mannosylation(UPOM) and is carried out by PMT1/2 complex(38). Although the ER O-mannosylation machinery is conserved in mammals, there are no reports of an equivalent UPOM activity in higher eukaryotes(37). Studies in yeast indicate that UPOM disrupts intrinsic folding capacity of substrates, reduces substrate interactions with chaperones and thus has a role in removing substrates from futile protein folding cycles. Thus, O-mannosylation is an integral part of ER protein homoeostasis(37). The linear oligomannose structures found in yeast vary in length from 1 to 5 mannoses and are frequently found on cell wall and plasma membrane proteins(39). The O-mannosylation of these proteins is indispensable for cell viability and cell wall integrity(14). Furthermore, O-mannosylation of Axl2/Bud10p has been shown to be required for its stability, localization and function in daughter cells(40).

In mammals, the only best-studied O-mannosylated glycoprotein is α-dystroglycan(α-DG), a substrate of POMT1/2. It is an extracellular component of the dystrophin–glycoprotein complex, common to several tissues, and is implicated in the interconnection of the cytoskeleton of muscle cells and neurons with proteins of the extracellular matrix (ECM)(41). The extensively glycosylated α-DG acts as a receptor for LG(Laminin-G-like)-domain-containing ECM proteins that are major constituents of the basement membrane of skeletal muscle and other tissues: laminin, agrin and perlecan(42). The ECM-binding modification of α-DG also mediates interactions with the LG domains of neurexins, pikachurin and Slit, thereby contributing to synapse

formation and axon guidance(41). Abnormalities in the post-translational processing of α-DG that disrupt the interaction with the basement membrane result in various congenital and limb-girdle muscular dystrophies, referred to collectively as secondary dystroglycanopathies(43). One of the most common brain malformation seen in patients with defective O-mannosylation pathways is cobblestone lissencephaly(6, 44, 45). Humans are gyrencephalic species meaning we have convolutions in our cortex which allow us to expand surface area in limited skull volumes and exhibit complex cognitive behaviors(46). The cerebral cortex is the apex of neural learning and processing in mammalian brain(47). It is a highly ordered structure comprised of six layers of neurons defined by their different morphology, physiology and connectivity(48). Post mitotic neurons are generated in the innermost layer called the ventricular zone (VZ) by the proliferation of neural progenitor cells(49) (Fig. 4). During development, the post mitotic neurons migrate into their particular layer to send axons to defined areas of the cortex and sub cortex in order to establish proper connectivity. Correct cell divisions of neural progenitors and migration of neurons in specific cortex layers contributes to cortical growth and folding(46). Cobblestone lissencephaly results from over migration of neurons beyond the marginal zone (outermost layer) into meninges through gaps in the external/pial basement membrane(50). Basement membranes are thin sheets of extracellular matrix composed of members of laminin family(51).

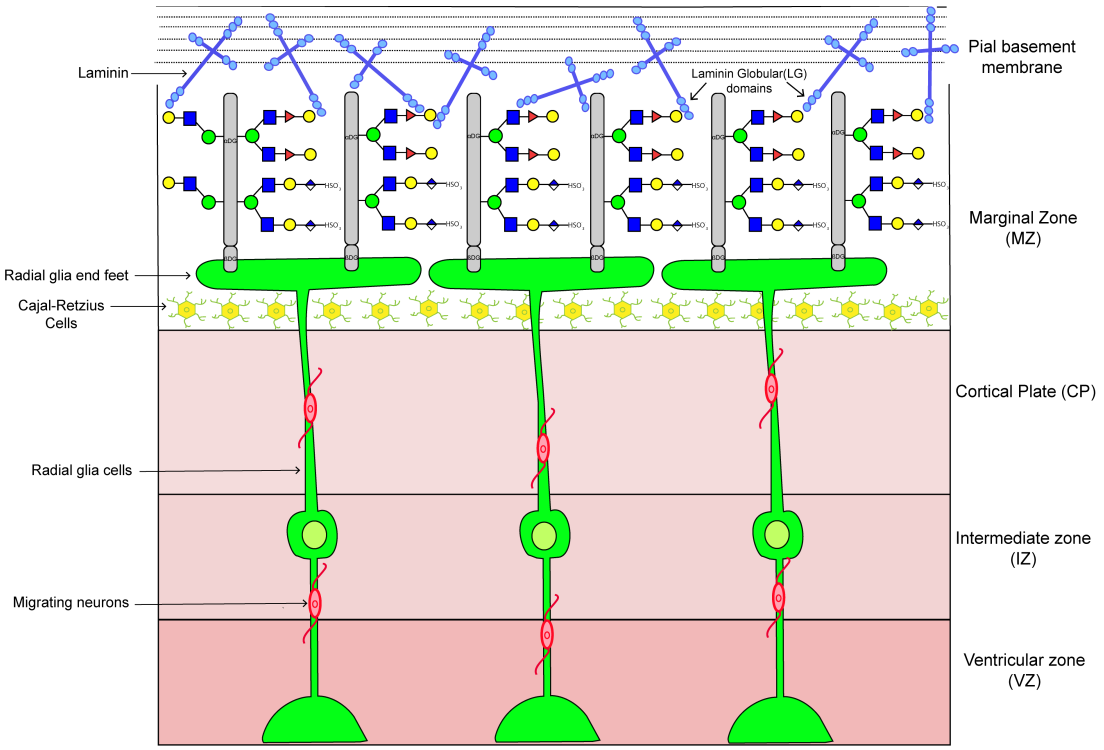

Figure 4. O-mannosylation in human cerebral cortex. M1 and M2 O-mannosyl glycans present on αDG are important for interaction with LG domains of extracellular matrix molecules such as laminin, agrin, perlecan etc. This helps in maintaining the integrity of pial basement membrane and proper migration of neurons during development. αDG (grey) is highly expressed in radial glial end feet in the marginal zone. Layers of cerebral cortex and cell types are shown.

Brain specific deletion of POMT2 in mice results in disruptions of radial glial cells (neural progenitors) and Cajal-Retzius cells (cells of the marginal zone) in the cerebral cortex and abolishes laminin binding of Dystroglycan(52) (Fig 4). It is speculated that O-mannosylation of DG is required for laminin binding which plays a role in maintaining pial basement membrane integrity(53). It is also speculated that O-mannosylation deficiency may lead to formation of a weak membrane during rapid brain expansion, due to reduced binding of extracellular matrix molecules(52).

DG O-mannosylation is highly branched, extended and varies according to tissue. Brain DG mostly comprises of Lewis and HNK-1 epitopes on O-mannosyl glycan and muscle DG has an extended matriglycan structure. However, mono-O-mannosyl glycans were also identified in all cerebral layers of the mouse cerebral cortex, cerebellum and were found particularly enriched in the GABAergic inhibitory interneurons(54). Proteins identified to possess the mono-O-mannosyl glycans include members of the cadherin and plexin superfamilies, perineural net protein neurocan and a cell adhesion protein involved in synaptic plasticity, Neurexin(54). Neurexins have an elaborate, well-developed role as a pre-synaptic adhesion molecule(55) and O-mannosyl glycans on neurexins likely help maintain its association with post synaptic molecules such as Dystroglycan, neuroligins etc. but the exact role of single O-mannose on neurexins is unknown.

Cadherins, a substrate of TMTC1-4 is also required to maintain the structure of cerebral cortex in mammals. N-cadherin dependent adhesiveness of neurons is required to stop them from over migrating. Certain signaling cascades(e.g. Reelin) promote the function of cadherins of mediating cell- cell interactions between migrating neurons and cells of the marginal zone causing neurons to aggregate and not enter the marginal zone(56, 57). It has been reported that O-mannosyl glycans on E-cadherins are essential for cell adhesion in mouse embryos(58). In this study, defects in cell adhesion were found in *pomt2* mutant embryos although cadherins are not a substrate for POMT1/2. This may indicate a crosstalk between different O-mannosylation pathways. Cadherins also maintain a morphogenic gradient across the cortical layers in gyrencephalic species

suggesting that they are important in mediating interactions between neurons and their environment to guide them through the migration process and to help them make correct axon connectivity in a layer specific manner(59). All types of cadherins have enormous roles in cortex development(60-63), however it is unknown how the single, unbranched O-mannosylation of the EC domains (extracellular domain) of cadherins might mediate cell-cell adhesion between neurons.

O-mannosyl glycans have a prominent role in maintaining synapses. Synapses are intercellular junctions specialized for fast, point-to-point information transfer from a presynaptic neuron to a postsynaptic cell(64). Dystroglycan ligand, pikachurin, an extracellular matrix protein, has been shown to be important for the formation of photoreceptor ribbon synapse in mice(65). It was also shown that presynaptic interaction between dystroglycan and pikachurin is required to maintain synaptic connection between photoreceptor and bipolar cells(66). Interestingly, defective O-mannosylation of dystroglycan diminished the interaction between dystroglycan and pikachurin(67)(Fig. 5). This indicates that elaborate O-mannosylation of αDG is important for maintenance of synapses.

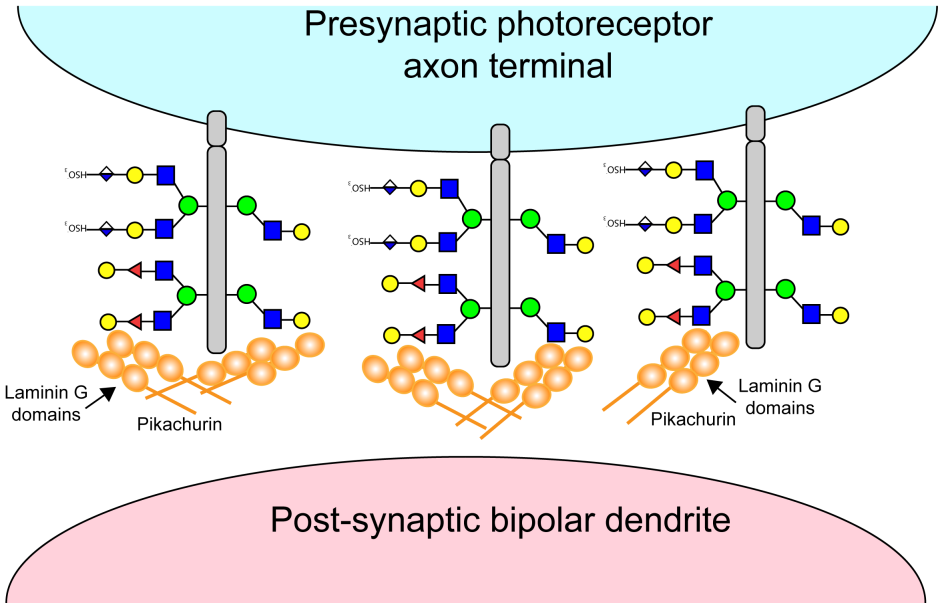

Figure 5. O-mannosylation of DG is required to maintain synapses. Branched O-mannosylation of αDG is required for its interaction with laminin G domains of pikachurin to stabilize the photoreceptor ribbon synapse.

Remarkably, the loss of the extended O-mannosyl glycosylation of dystroglycan in mice leads to severe defects in the development of longitudinal axon tracts and in the formation of the dorsal funiculus by central projections of dorsal root ganglion sensory neurons(68). Glycosylated dystroglycan is also required to interact with Slit, an important and well conserved axon guidance molecule, and regulate slit-mediated axon guidance(68).

Other O-mannosylated molecules such as plexins, RPTPs have crucial roles in the nervous system but the significance of the O-mannose glycans on them is not yet explored. For e.g. RPTPζ, a brain specific chondroitin sulfate proteoglycan, which is O-mannosylated(31, 69) is expressed predominantly in the CNS, especially during development, where it localizes mainly to the ventricular and subventricular zone of the

cerebral cortex. During brain development, RPTPζ is expressed on neurons and glia and can bind several other ligands, including contactin, Nr-CAM, N-CAM, L1/Ng-CAM, and TAG-1/axonin(70). RPTPζ also modulates dendritogenesis and synaptogenesis(71). But whether the O-mannosylation is required for these CNS functions is unknown and the enzyme that O-mannosylates RPTPζ is unknown. Intriguingly, it has been shown that the loss of branched O-mannosyl glycans on RPTPβ/ζ accelerates the process of remyelination on axons in mice corpus callosum(72). Failure to remyelinate is a critical issue in neurodegenerative diseases and injury, as myelin sheath protects axons from degeneration and restores conduction deficits. Removal of chondroitin sulfate proteoglycans in the nervous system has shown to be a promising way to help neurons regenerate(73). This study has shown that removal of branched O-mannosyl glycans might be sufficient to aid regeneration, as a novel therapeutic strategy. This also indicates that O-mannosyl glycans have different roles on different substrates, such as αDG and RPTPβ/ζ.

Investigating the need for O-mannose on these proteins may help us better understand the multitude of inexplicable, clinical, neurological phenotypes associated with the loss of O-mannosylation pathways in humans.

Drosophila: a model for neuromuscular roles associated with CMDs

To fill the gaps in our understanding of the significance of O-mannosylation in the nervous system we turn to model organisms such as *Drosophila. Drosophila* is an excellent model system to study neurological abnormalities caused by POM defects due to evolutionarily conserved genes of POM pathway, simpler glycosylation patterns and

efficient genetic approaches. *Drosophila* has orthologs of vertebrate *pomt1/2* known as *rt* (rotated abdomen) and *tw* (twisted) respectively(74), named due to the adult abdomen rotation phenotype seen in mutants (Fig. 6).

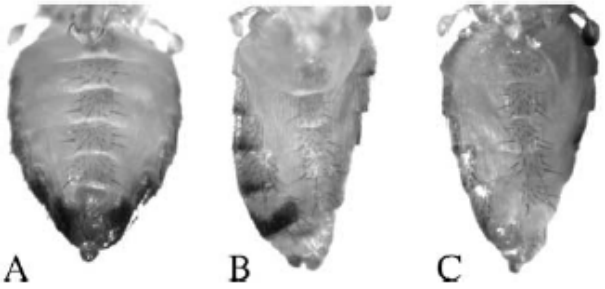

Figure 6. Adult *pomt1/2* mutants. A, WT abdomen B, $rt^{-/-}$ abdomen C, $tw^{-/-}$ abdomen. (Adapted from (74)).

Studies in *Drosophila* have shown that POMT1/2 are required to maintain the functionality of neuromuscular junction(NMJ), a well-studied synapse, by maintaining glutamate receptor subunit composition and increasing neurotransmitter release(75). In *rt* mutants, the level of synaptic DGluRIIB was decreased with no detectable change in the level of DGluRIIA. The decreased levels of DGluRIIB subunit impaired the ability of NMJ synapse to release neurotransmitter. Similar phenotypes were seen in *Dg(*dystroglycan*)* mutants as well and hence defects seen in *rt* mutants were attributed to the possible loss of *Dg* function. However, it was not clear how the hypoglycosylation of *Dg* can affect subunit composition and neurotransmitter release. DG is the only known substrate of POMT1/2 in *Drosophila* and likely possesses only single, unextended O-mannose(30). In *Drosophila*, dystroglycan has been shown to regulate axon projections of photoreceptor retinal cells into the lamina and medulla of third instar larval brains(76). However, the effect of glycosylated DG in axon guidance in *Drosophila* is

unclear. *Pomt1/2* defects in *Drosophila* have also shown a clockwise rotation of abdomen in adult flies. In addition, studies have shown that *rt* and *tw* mutants exhibit larval and adult muscle abnormalities such as muscle morphology defects including missing muscles, sarcomere disarray, irregular Z-lines, filament disorganization, accumulation of glycogen granules, enlargement of mitochondria and duplication of basement membrane(77, 78). Similar muscle defects are also seen in human patients with CMDs. Previous studies in the lab have shown that *rt* and *tw* mutant flies have problems with heavy exercises such as climbing and flying but no problems with light movements such as locomotion(79). Defective motor function in mutants appears after enclosure and progresses in an age dependent manner. These findings might suggest that *pomt* mutant flies have a high myoblast density and position derangements which cause apoptosis, muscle disorganization and muscle cell defects(79). However, previous studies in the lab also point out that DG alone may not be accountable for the multitude of neuromuscular phenotypes seen in *pomt1/2* mutant flies. In humans, SUCO and KIAA1549 were identified as POMT1/2 substrates (7)and both these proteins have homologues of unknown function in *Drosophila*. Cadherins and plexins are important O-mannosylated proteins of the nervous system however both are not modified by POMT1/2. This leaves us to identify functionally relevant substrates of POMT1/2 in *Drosophila*, other than DG to better understand the role of POMTs in neuromuscular development.

Dissertation overview

To understand the role of O-mannosyl glycans in *Drosophila*, I focused on the neural development function of *Drosophila* O-mannosyltransferase genes, DmPOMT1(*rt*) and DmPOMT2(*tw*), as it relates more closely to the congenital defects seen in muscular dystrophy patients. Although substantial research has been done to understand the role of O-mannosylation in muscles, little is known about its role in neurons. At the beginning of my PhD project, previous studies in the lab had discovered an embryonic posture defect seen in *rt/tw* mutants that seemed to be largely neural in nature. In Chapter II, I show that *rt/tw* have a novel function in regulating connectivity of a specific class of sensory neurons responsible for sensing locomotion, heat and pain responses that may explain the posture defect of *rt/tw* mutant embryos. Despite the importance of O-mannosylation and relevance in diseases, only one substrate DG (Dystroglycan) is well studied in both mammals and *Drosophila*. In Chapter III, I use the neuronal wiring defect as a tool to identify candidate genes that interact with *rt/tw* . I identify novel genes *rptps* (receptor protein tyrosine phosphatases) that interact with *rt/tw* to regulate sensory axon morphology and I present biochemical evidence that one of them, RPTP69D is indeed O-mannosylated by RT/TW. In Chapter IV, in collaboration with Dr. Baker I present a method to analyze muscle contractions live in *Drosophila* embryos using fluorescence. These studies help understand the role of O-mannosyl glycans in *Drosophila* neural development and may help us understand muscular dystrophies better.

CHAPTER II

PROTEIN O-MANNOSYLTRANSFERASES 1/2 (POMT 1/2) REGULATE SENSORY AXON WIRING IN *DROSOPHILA*[*]

Introduction

Protein O-mannosylation (POM) represents a prominent example of protein glycosylation with crucial biological functions(80). Two protein O-mannosyltransferases (POMTs) that mediate POM, POMT1 and POMT2, are conserved in all animals. Enzymatic POM activity requires the formation of a complex between POMT1 and POMT2 that functions in the endoplasmic reticulum (ER). POM affects the development and physiology of mammalian muscular and nervous systems, while genetic inactivation of POMT1 or POMT2 results in early embryonic lethality in mice(52, 81, 82). The best characterized O-mannosylation substrate is dystroglycan (Dg), a glycoprotein that serves as a cell membrane-spanning bridge linking the ECM and cytoskeleton(18, 26). Defects in POM compromise interactions between Dg and its extracellular ligands, which causes congenital muscular dystrophies termed dystroglycanopathies(43). These dystrophies are associated with neurological abnormalities, including brain developmental defects, which indicates that POM has important functions in neural development(83).

---

[*] Portions of this chapter are reprinted with kind permission from: Protein O-Mannosyltransferases affect sensory axon wiring and dynamic chirality of body posture in the *Drosophila* embryo by Baker, R[*].,Nakamura, N[*]., Chandel, I[*]., *et al.,* Journal of neuroscience, 2018, 38(7):1850 –1865. [*]equal contribution.

Recent studies have revealed that POM is present on many glycoproteins that can function in the nervous system, including cadherins, plexins, and receptor protein tyrosine phosphatase ζ(31, 84). Experiments in mouse models indicated that POM is required for integrity of the pial basement membrane and neuronal migration(52, 85). However, most studies have concentrated on POM-mediated regulation of Dg activity in muscles, while POM functions in the nervous system remain poorly understood. Previous studies demonstrated that *Drosophila* POMT1 and POMT2 [rotated abdomen (*rt*) and twisted (*tw*), respectively] show strong synergistic genetic interactions(74, 86, 87). Mutations in *rt, tw*, and *Dg* result in muscle developmental defects, abnormal synaptic transmission, and age-dependent muscle degeneration(75-78), the phenotypes also associated with human dystroglycanopathies(83). However, the pathogenic mechanisms in *Drosophila pomt* mutants are poorly understood. Interestingly, *rt* and *tw* mutants show misalignment of adult abdominal segments that causes the clockwise "abdomen rotation" phenotype, a unique example of a developmental defect associated with abnormal chirality(74, 86). Previous studies in the lab described a novel POMT embryonic phenotype associated with body rotation that is reminiscent of the abdomen rotation in adults. This embryonic phenotype was rescued by expressing POMT1/2 in neurons, including a class of multidendritic sensory neurons. The embryonic rotation phenotype arises during peristaltic muscle contractions. *Pomt* mutants also exhibit uncoordinated muscle contractions, which are regulated by different types of sensory neurons. Here, I present a novel function of POMT1/2 in regulating the morphology of the same multidendritic sensory neurons, without affecting general axon morphologies

or the axon projections of other sensory neurons such as chordotonal organs. I show, in collaboration with others, that a peripheral nervous system defect which abolishes most sensory neuronal function exhibits embryonic posture defect similar to POMT mutants. I present evidence that POMT1 is expressed in the ER of muscles, sensory neurons and epidermis. Rescue results and RNAi experiments indicate that the axon regulatory function of POMT1/2 is cell autonomous. I also discovered perdurance in POMT1 function of regulating axon branching. This finding is in accordance with previous studies done in the lab related to POMT associated posture defects. I further dissected the regulatory function of POMT1/2 by detailed analyses of single axons using Flp-out and MARCM (Mosaic analysis of cell repressible marker) techniques to obtain higher anatomical resolution of the axonal phenotype. Moreover, I show that Dystroglycan may not be fully responsible for the embryonic body rotation phenotype seen in POMT mutants.

Materials and methods

Drosophila stocks and crosses. The mutant alleles for *rt* and *tw* were previously described, as follows: tw^{1} is a hypomorphic allele; rt^{2}, rt^{P}, and rt^{571} are strong hypomorphic alleles that are close to amorphs(74, 86). $sens^{E2}$ is a loss-of-function allele(88) and Dg^{086} is a null allele(89). UAS-tw transgene was previously described(74). Other mutant and transgenic strains were obtained from the Bloomington Drosophila Stock Center at Indiana University. Unless indicated otherwise, embryos of either sex were included in all analyses, as our experiments, as well as studies by other groups, revealed no evidence of sex-specific phenotypes of POMT mutants.

Fluorescent staining and microscopy. First instar larvae expressing tdTomato or tdGFP in the Ppk pattern(90) in a wild-type, *tw*, or *rt* mutant background, were collected. The CNS (brain lobes together with the ventral ganglion) was dissected, fixed in PBS with 4% paraformaldehyde, and stained with rabbit anti-dsRed (Clontech) in a 1:1000 dilution or mouse anti-GFP antibody (8H11 DSHB) in a 1:100 dilution. Mouse anti-Fasciclin II (FasII) and anti-Repo antibodies[1D4 and 8D12 from Developmental Studies Hybridoma Bank (DSHB),respectively] were used in a 1:5 and 1:10 dilution, respectively. Alexa Fluor 488 or 546-conjugated goat anti-rabbit or anti-mouse antibodies were used as a secondary antibody in a 1:250 dilution. For RT expression, rabbit anti-GFP in 1:800 dilution was used. Stained samples were mounted on slides and imaged using the Zeiss Axioplan 2 Microscope using 40X magnification objective. To minimize potential errors, control and experimental samples were stained using the same master-mix of antibodies and imaged with the same settings for camera, illumination, and microscope. Commissural branch thickness was measured in stacks of optical sections with 1μm step size using ImageJ for every branch in a given ventral nerve cord and averaged, and the collective average from a given genotype reported. Images were analyzed blindly without genotype information. Longitudinal tracts were scored by averaging the brightness of the spaces between commissural branches for a background brightness, and tracts were scored as "absent" when the brightness of the region where the tract was expected to be was <10% above background, as measured by ImageJ. Embryos were dechorionated, fixed, and dissected manually from the vitelline membrane according to published protocols(91). They were stained with Alexa Fluor

488-conjugated phalloidin (Invitrogen) using 1:200 dilution. Digital images were obtained using a Zeiss Axioplan 2 fluorescent microscope with the ApoTome module for optical sectioning. AxioVision and ImageJ software were used for 3D reconstruction and Z-projections of fluorescent samples.

Flp-out and MARCM analysis of individual axons. A Flp-out approach for labeling individual class IV dendritic arborization (da) neurons was performed using previously described strategy with some modifications(92). Briefly, males of yw hsFlp; +; rt P/ T(2;3)TSTL14, SM5: TM6B, Tb1 were crossed to 10XUAS>(FRT stop) >GFP-Myr; rt^{2} ppkGal4/TM3-KrGFP females. F1 progeny was collected as embryos for 17–20 h and given a heat shock at 34°C for 12 min to induce the expression of Flp recombinase. Then these embryos were allowed to develop until third instar at 25°C, and brains of yw hsFlp/10XUAS> (FRT stop) >GFP-Myr; rt^{P}/rt^{2} ppkGal4 larvae were dissected, fixed, and incubated with primary mouse anti-GFP antibody (8H11, DSHB) at 1:100 dilution, followed by incubation with secondary goat anti-mouse Alexa Fluor 488 (Invitrogen) antibody diluted 1:250. For wild-type control, the same genotype, but without *rt* mutation, was analyzed. A MARCM approach for labeling individual mutant class IV dendritic arborization (da) neurons was performed using previously described strategy with some modifications(93). Briefly, males of yw hsFLP; UAS-GFP/+; FRT2A rt^{P} /TM3-KrGFP were crossed with yw; ppkGAL4/+; tub-GAL80, FRT2A/TM3-KrGFP females. F1 progeny was collected as embryos on freshly yeasted grape agar plate for 2 hours. Developing eggs were kept at 25^{o}C and given a heat shock at 37^{o}C for 1hr, 4-5 hours after the end of the egg laying period. Then these embryos were allowed to

develop until third instar stage at 25 ^{o}C and brains of yw hsFLP/+; ppkgal4/UAS-GFP; FRT2A, tub-GAL80/FRT2A, rt^{P} were dissected, fixed and stained with primary mouse anti-GFP antibody (8H11, DSHB) at 1:100 dilution. For wildtype control, same genotypes, but without *rt* mutation were used. Stained brains were mounted in Vectashield (Vector Laboratories) and imaged using a Zeiss Axio Imager Fluorescence Microscope with ApoTome module for optical sectioning.

Experimental design and statistical analysis. Experiments were performed at least three times. N refers to the number of embryos or larvae of particular genotypes or the number of individual axons with particular morphology. Statistical analyses were performed by one-way ANOVA with Tukey's HSD post hoc comparisons for significance. For bar graphs and box plots, data for each bar or box in the graph were analyzed as a separate column. In all figures, 1 and 2 asterisks represent p values of <0.05 and 0.01, respectively; NS indicates that no significant differences were found (p >0.05). Details on statistical analysis are included in figure legends and text.

Results

POMT mutant embryos accumulate misalignment in body segments after muscle contractions begin

Previous studies of *rt* and *tw* mutants have mostly concentrated on adult and larval stages, while the effect of POMT mutations on embryonic development has not been well characterized(77, 86, 87). With the rationale that potential phenotypes of POMT mutants at early developmental stages could shed light more directly on pathological mechanisms associated with POM defects, we decided to focus on embryonic stages. We

analyzed *rt* and *tw* mutant embryos and discovered that they have a prominent body posture defect manifested as a whole-body left-handed torsion (rotation of more anterior segments, relative to more posterior ones, in counterclockwise direction, as viewed from the posterior), which is reminiscent of the adult abdomen rotation phenotype. This "embryonic torsion" phenotype becomes pronounced at stage 17, the last stage of embryonic development(Fig. 7A). No posture defects or any conspicuous muscle abnormalities were observed in stage 16 embryos. Since the somatic musculature and epidermis are already formed at stage 16, these data suggested that the torsion phenotype may originate from abnormal muscle contractions rather than from a developmental defect of musculature or abnormal epidermal morphology. This scenario is also consistent with the fact that the torsion phenotype becomes prominent soon after the embryos initiate coordinated muscle contractions(94, 95). Abnormal coordination of muscle contractions and the failure to maintain body posture may be caused by defects in function of muscle and/or neurons, including PNS (peripheral nervous system) cells that were shown to be important for the generation of coordinated waves of muscle contractions. To shed light on the cell-specific requirement of POMT activity for normal body posture, we applied a rescue strategy using UAS-GAL4-driven expression of a transgenic *tw* construct in *tw* mutants. We found that a pan-neuronal driver (ELAV-Gal4) and a driver specific for class IV da sensory neurons (Ppk-Gal4) were each able to significantly rescue the embryo torsion phenotype. On the other hand, three different muscle specific drivers (DMEF2-GAL4, MHC-GAL4, and How-GAL4); could not mediate the rescue of body torsion(Fig 7B). These results suggested that *tw* is required in

neurons, and specifically in class IV da sensory neurons. These neurons are a type of sensory neurons which possess multiple dendrites and are present in the epidermal cells(93). Based on the morphology of the dendrites, they are divided into four categories, Class I-IV. Each of these neurons send their axons to the ventral nerve cord, a part of *Drosophila* CNS, forming a sensory feedback circuit(92). Therefore, we hypothesized that POMTs function in the PNS to ensure a proper feedback from these cells to maintain normal body posture. To test this, we examined embryos with significantly depleted PNS function caused by a defect in senseless (*sens*). Mutations in *sens* result in the loss of peripheral sensory neurons by stage 16 through cell-specific apoptosis, thus impairing feedback from the PNS to the CNS in *sens* mutants. We found that ~80% of embryos show body torsion, with left-handed and right-handed torsion defects being detected at approximately the same frequencies (Fig 7C and 7D). These data also supported our hypothesis that PNS cells participate in generating coordinated muscle contractions, which is essential for the maintenance of body posture.

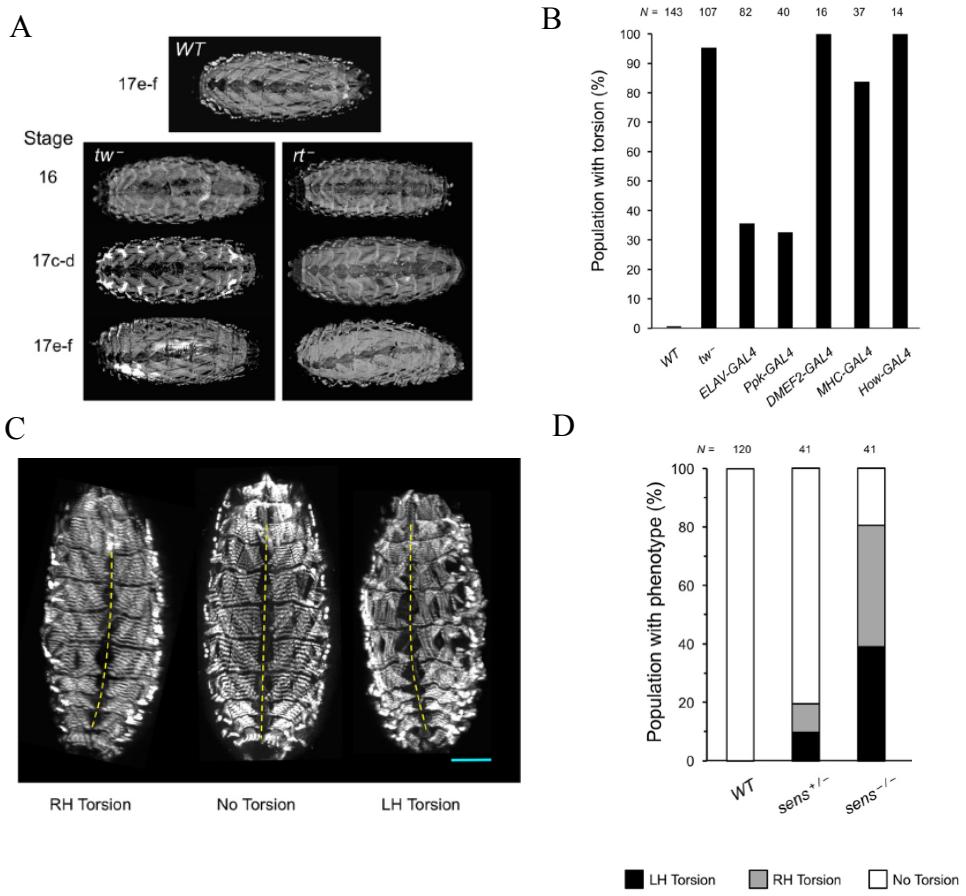

Figure 7. POMTs are required in peripheral sensory neurons for the maintenance of body posture. A, POMT mutants show body torsion phenotype. Top, Wild-type embryos have no torsion at any stage (stage 17e–f is shown).Bottom, *tw* and *rt* mutants show no torsion at stage 16 and usually no torsion at stages 17a– d. By stages 17e–f, nearly 100% of mutant embryos show left-handed torsion. **B,** Rescue of embryonic torsion by transgenic expression of UAS-*tw* construct in *tw* mutants using cell-specific drivers. Expression in all neurons (ELAV-GAL4) or in class IV da neurons (Ppk-GAL4) can substantially rescue torsion, while muscle-specific expression using DMEF2-GAL4, MHC-GAL4, and How-GAL4 cannot rescue the torsion phenotype. Genotypes are designated as follows: WT, wild-type. tw$^-$, tw1/ tw1(or tw1/Y). ELAV-GAL4, tw1/ tw1(or tw1/Y); UAS-*tw*/ELAV-GAL4. Ppk-GAL4, tw1/ tw1(or tw1/Y); UAS-tw/+;Ppk-GAL4 /+. DMEF2-GAL4,tw1/ tw1(or tw1/Y); UAS-tw/+; DMEF2-GAL4/+. MHC-GAL4, tw1/ tw1(or tw1/Y); UAS-tw/+; MHC-GAL4/+. How-GAL4, tw1/ tw1(or tw1/Y); UAS-tw/How-GAL4. **C,** Examples of sens mutants with left-handed (LH) or right-handed (RH) body torsion, or without body torsion phenotype. **D,** Proportions of embryos with left-handed torsion, right-handed torsion, and no detectable torsion among WT, sens$^-$, tw$^-$. Data obtained in collaboration with Dr. Nakamura (A&B) and Dr. Baker (C&D)(96).

POMTs are required for patterning of axonal projections of sensory neurons

To elucidate possible cellular mechanisms underlying the requirement of POMTs for PNS function, I examined POMT mutants for possible defects of PNS functional morphology. Since our rescue and genetic interaction experiments suggested that the function of POMTs could be required in class IV da sensory neurons, I focused on the analysis of these cells in POMT mutants. Class IV da cells develop a characteristic laminar pattern of axonal projections in the ventral ganglion(92). I labeled these projections using a Ppk-tdTom reporter or a Ppk-Gal4- driven UAS-tdGFP marker(90) and analyzed their morphology once embryos hatched from the shell (the first instar stage). I found that the axonal projections show significant abnormalities in *tw* and *rt* mutants, including thickened commissural branches and, in the case of *rt* mutants, missing or severely depleted longitudinal tracts (Fig 8A). The axon phenotype of *tw* mutants was milder on average, which is consistent with the fact that the tw^{1} mutant allele used in these experiments is a hypomorph. Transgenic expression of *tw* or *rt* induced specifically in class IV da cells could rescue defects of axonal projections in *tw* or *rt* mutants, respectively, which confirmed the specificity of the phenotypes and also suggested that POMTs function cell autonomously to pattern axonal projections of sensory neurons (Fig 8B-E).

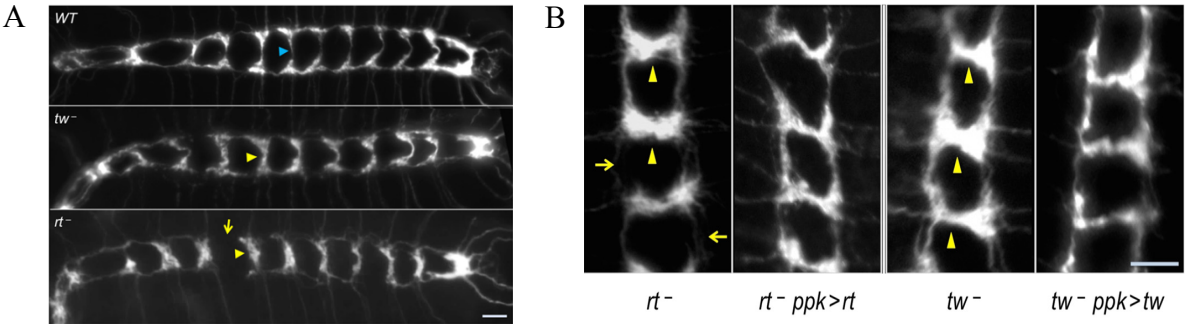

Figure 8. POMTs affect the function of peripheral sensory neurons. A, POMT mutants have abnormal axonal projections of class IV da sensory neurons in the ventral ganglion. The laminar pattern of axonal projections shows abnormally thickened commissural tracts in *rt* and *tw* mutants (yellow arrowheads, compared with tracts indicated by blue arrowheads in WT control), and missing longitudinal tract in *rt* mutants (arrow). Anterior is to the left, Scale bar 10μm. B, Transgenic expression of POMTs in class IV da neurons can rescue the phenotype of axonal projections. Anterior is up. Representative images of the same region of the laminar pattern (neuromeres a1–3 that are more frequently affected in POMT mutants) are shown for mutant and rescue genotypes. The phenotypes of thickened commissural branches (arrowheads) and depleted longitudinal tracts (arrows) are rescued by transgenic expression of POMTs in class IV da neurons. Number of animals analyzed for each genotype: WT, 14; tw^{-}, 15; tw^{-}, ppk>tw (rescue), 14. (C-E), Quantification of axon width in WT, tw^{-}, rt^{-}, and rescue genotypes. In all panels, error bars indicate SEM. **p<0.01; ns, not significantly different. WT, wild type. tw^{-}, tw^{1}/tw^{1}(or tw^{1}/Y). tw^{-}; ppk>tw, tw^{1}/tw^{1}(or tw^{1}/Y); Ppk-GAL4/+;UAS-tw/+. rt^{-}, rt^{2}/rt^{2}. rt^{-}, ppk>rt, rt^{2} Ppk- GAL4/rt2 UAS-rt.

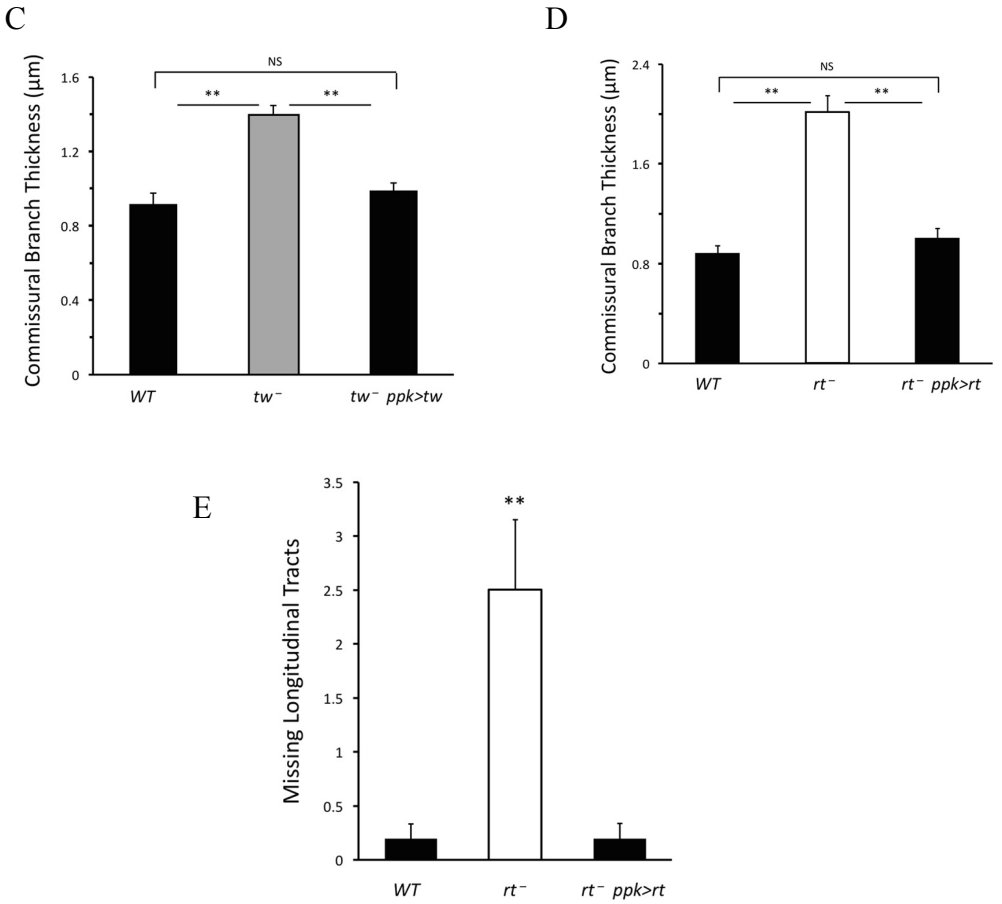

Figure 8. Continued.

POMTs do not affect general axon pathfinding or development of nervous system

To characterize the nervous system phenotype in more detail, I used markers for glial cells and major axonal tracts in the ventral ganglion. Immunostaining with Repo antibody that specifically labels the majority of glial cells(97) revealed no significant difference between wild-type and *rt* mutants, which suggests that glia development is not affected in POMT mutants(Fig. 9A). To rule out possible abnormalities in midline glia development, I labeled WT and *rt* mutant brains with anti-wrapper antibody, a protein expressed specifically in midline glia(98), and found no morphological defects in midline glia development (Fig. 9B). To check for possible abnormalities in axon

guidance, I examined immunostaining for FasII that labels all major long axon tracts in the ventral ganglion(99). These tracts are affected by mutations in genes involved in major axon guidance pathways (e.g., defects in the Slit/Robo pathway cause abnormal midline crossing)(100); Plexin and Semaphorin mutants show disorganized morphology of selected tracts(101, 102), while mutations in Netrins and frazzled affect tract continuity(103). I found no obvious abnormalities of long axon tracts in *rt* mutants (Fig. 9C and D). The FasII-positive tracts also provided a useful reference for examining the dorsoventral position of sensory projections in the ventral ganglion. Analysis of optical sections stained for FasII revealed that class IV sensory axons project properly to the ventral region of the ganglion in *rt* mutants (Fig. 9E). Together, these results suggest that axon guidance is not generally affected by POMT mutations.

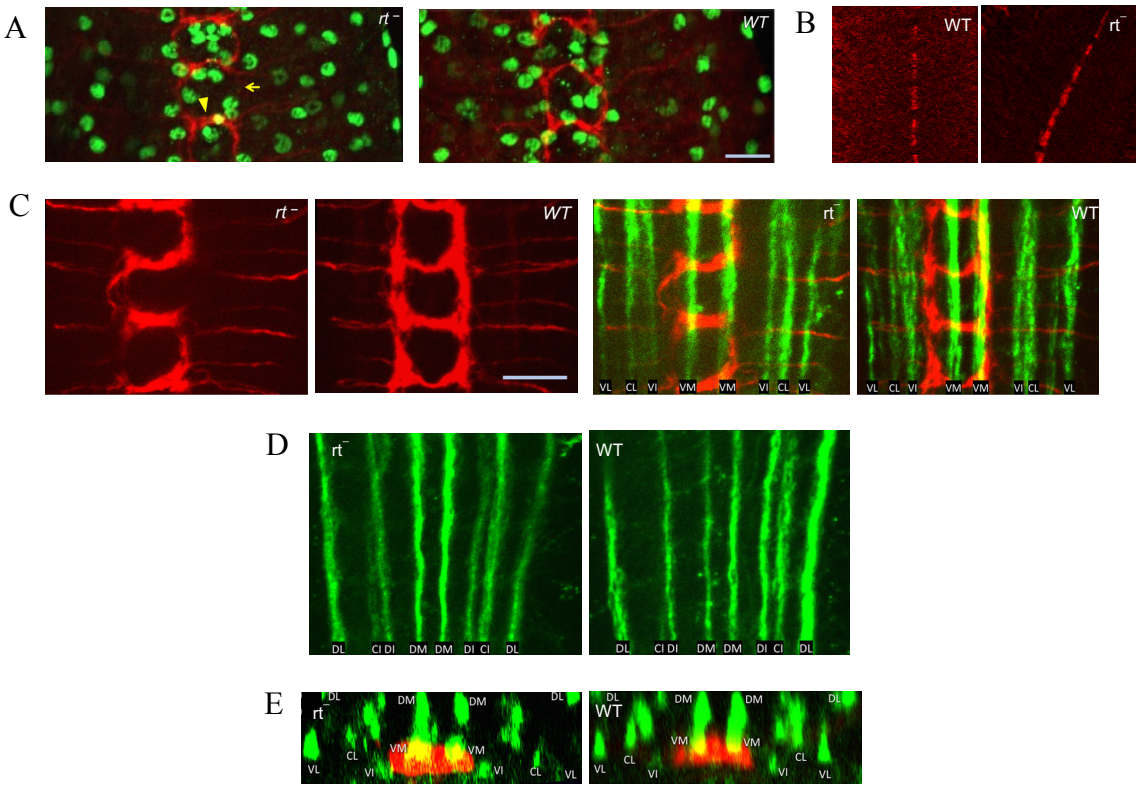

Figure 9. POMT mutations do not generally affect glia development and axon pathfinding, while being associated with defects in patterning of sensory axon termini. A, Immunostaining with anti-Repo antibody that specifically labels glial cells (green) revealed no significant defects in the distribution and number of glial cells in *rt* mutants (22.1± 0.9 and 23.7± 0.8 glial cells per hemisegment in *rt* and WT control, respectively; t test, p>0.2). **B,** Immunostaining with anti-wrapper antibody that secfically labels midline glia (red) revealed no significant difference in morphology of midline glia. **C,** Class IV sensory axons (red) in *rt* mutants and wild-type control, respectively (left), overlay of the axon staining shown above with the staining of long axonal tracts (FasII, green) in the ventral part of the ganglion (right). The same region of the ventral ganglion corresponding to neuromeres a1–3 is shown for both genotypes. **D,** FasII immunostaining of long axonal tracts in dorsal part of the ganglion in *rt* and wild-type, respectively. **E,** Z-projections reconstructed from stacks of horizontal optical sections through the ventral ganglion show similar dorsoventral lamination of class IV axon termini (red) in *rt* and wild-type, respectively, based on their location relative to FasII tracts (green). The commissural branch (red) of neuromere a2 is shown for both genotypes. Images in **A-D** represent projections of stacks of optical sections through ventral and dorsal regions of the ventral ganglion, respectively. *rt*, rt ^{2}/rt^{2}. Scale bar, 20 μm.

POMTs do not affect axon patterning of other sensory neurons

To further rule out the involvement of POMTs in regulating axon morphology of other sensory neurons and interneurons that are speculated to be important for regulating rhythmic muscle contractions and locomotion(104-106), I expressed GFP in these neurons and analyzed their respective morphologies in WT and POMT mutants. The chordotonal (Ch) organ, an internal stretch receptor located in the subepidermal layer, is one of the major sensory organs in the peripheral nervous system of *Drosophila melanogaster* (105). Ch organs are proprioceptive components that underlie touch sensitivity, locomotion, and peristaltic contraction by providing sensory feedback to the locomotor circuit in larvae(107). I expressed GFP in Ch organ and analyzed their axon termini in the ventral ganglia, using 8-73-Gal4 that drives expression specifically in the Ch organ. I did not find any defects in the axon morphology of Chordotonal organs in POMT mutants (Fig. 10A&B). I further used a more ubiquitous driver G14-Gal4 which is expressed more broadly in the peripheral nervous system (PNS) cells, muscle and epidermal cells, and analyzed the axons of the PNS neurons in the ventral ganglia (79). I again, did not see any defects in the morphology of axons in POMT mutants as compared to WT (Fig. 10C&D). These results suggest that POMTs are specifically required for maintaining axon connectivity of Class IV multidendritic (da) sensory neurons.

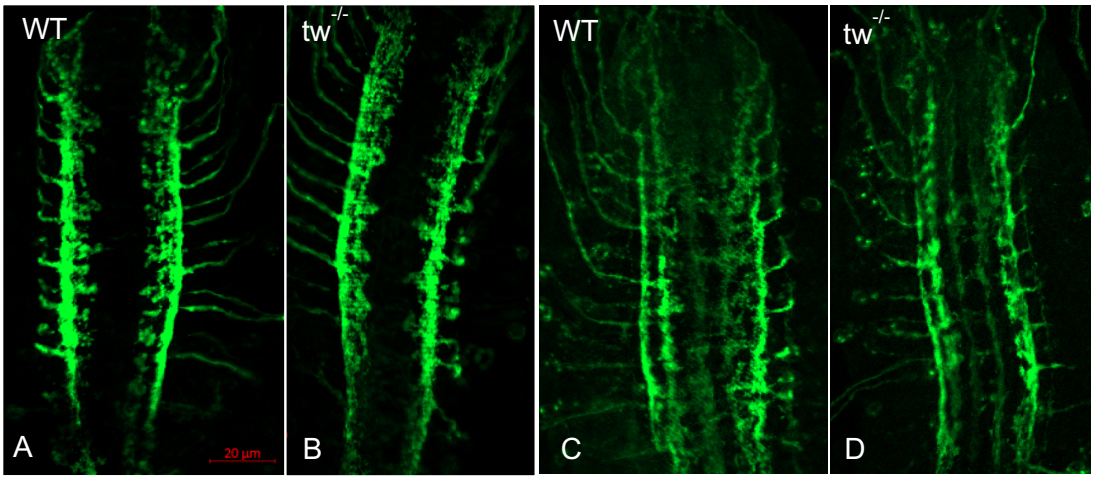

Figure 10. POMT mutations do not affect other sensory axon projections. A-B, Chordotonal organ axon projection (green) using 8-73Gal4 in WT and *tw* mutants. **C-D,** G14 gal4 projection pattern (green) in WT and *tw* mutants. Ventral nerve cord is shown, posterior is up in all panels. Scale bar is 20µm (indicated). $tw^{-/-}$, tw^{1}/tw^{1}.

POMTs are required to regulate termini branching of Class IV da sensory axons

I further investigated in greater detail the phenotype of sensory projections by labeling individual class IV axons using the Flp-out technique (Fig. 11A). These experiments revealed that the morphology of sensory axon termini in *rt* mutants is different from that in wild-type controls. In agreement with a previous report(108), I found that individual axon termini in wild-type ventral nerve cords fall into two distinct categories: the axons that branch along longitudinal tracts of the laminar pattern without crossing the midline ("branching only"); and the axons that both branch longitudinally and cross the midline ("branching and crossing"). However, in *rt* mutants, in addition to these two types of axons, I observed a substantial proportion of axons that cross the midline without branching (Fig. 11B). This type of axon was not present in wild-type ventral nerve cords.

The “crossing-only” axons appear to develop at the expense of branching and crossing axons, as the proportion of branching-only axons was about the same in mutants and controls (20% and 19% in *rt* mutants and wild-type, respectively) (Fig. 11C). These data are consistent with the phenotype of the overall laminar pattern of sensory axon projections in POMT mutants that shows thickening of commissural tracts and depletion of longitudinal connections (Fig. 8). However, other possible abnormalities of axon termini, such as defects in fasciculation or branch distribution, may also contribute to the phenotype of the laminar pattern, but they could not be revealed in my Flp-out experiments because the laminar pattern is already established at the larval stage I am analyzing it. For fasciculation defects or branching distribution defects, axons should be examined much earlier during embryonic stage, when the axon tracts are being formed. Further studies using multiple markers will be required for more detailed analysis of individual sensory axon termini in POMT mutants. Nevertheless, together, my results strongly support the hypothesis that POMTs are specifically required for proper patterning of class IV sensory axon termini, but protein O-mannosylation is not involved in general axon guidance or overall development of the nervous system.

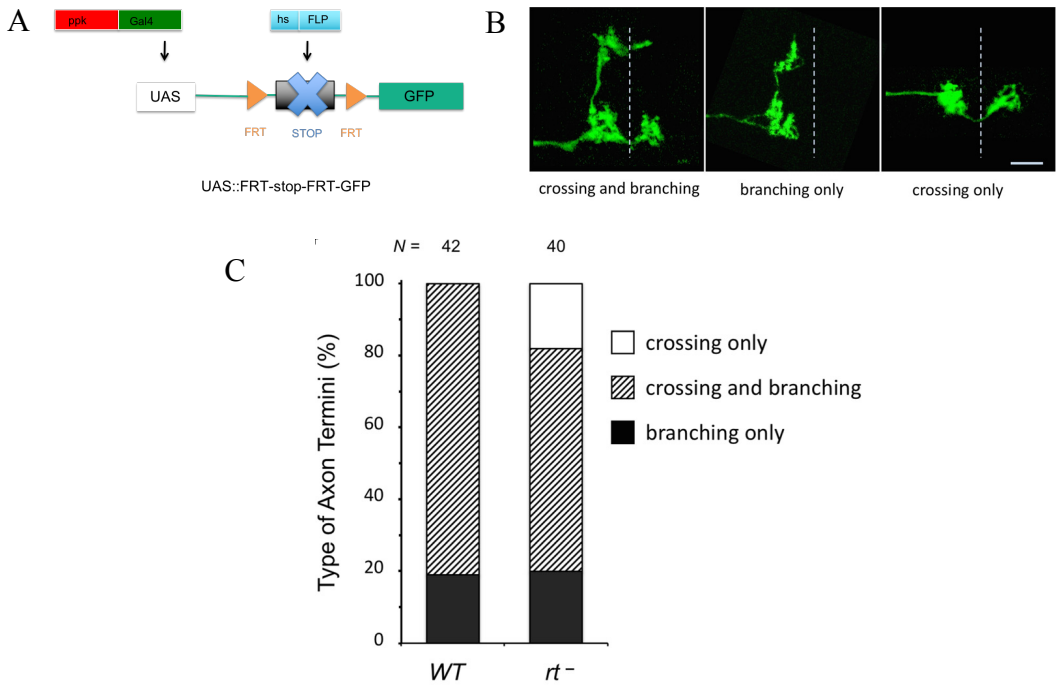

Figure 11. POMTs are required for Class IV axons to branch properly. A, Flp-out strategy, GFP from UAS::FRT-stop-FRT-GFP construct is expressed only in cells that express both Flippase (FLP, under heat shock promoter, hs) and Gal4. Flp recombinase removes the stop codon between FRT sites, thus driving GFP expression. **B,** Examples of individual class IV sensory axons with "crossing and branching," "branching only," and "crossing only" types of morphology, relative to the midline (dashed line). **C,** Quantification of types of class IV sensory axons revealed by Flp-out clones in wild-type and *rt* mutants. N, Number of individual axons analyzed. Scale bar 20μm.

POMTs are required cell autonomously to regulate Class IV sensory axon termini

To elucidate cell autonomous effect of POMTs on axon patterning and to assess other possible abnormalities of axon termini, such as defects in fasciculation or branch distribution, I employed the MARCM (mosaic analysis with a repressible cell marker) system to generate individual POMT mutant sensory neurons in POMT heterozygotes. MARCM utilizes the hsFlp-FRT system along with a Gal80 repressor protein, which is under the control of a ubiquitous promoter and represses Gal4 activity (ppk-Gal4, in my case), preventing the expression of a reporter construct (eg. UAS-CD8::GFP, repressible

marker (Fig. 11A). I placed FRT sites proximal to POMT mutation in one chromosome arm and proximal to GAL80 repressor in the homologous chromosome arm. Heat shock induced mitotic recombination generates homozygous mutant clones that have lost the repressive Gal80 and thus are labeled by the expression of GFP. All other surrounding cells are heterozygous and unlabeled (Fig. 12A). To my surprise, I did not detect the abnormal "crossing only" axons or any other defects in the axons analyzed in POMT mutants (Fig. 12B&C). This result can possibly be explained by the perdurance of the maternally provided POMT function (mRNA, and/or RT/TW protein, or O-mannosylated product of RT/TW activity) during early stages (Stage 5) of *Drosophila* embryo. Since the time of mutant generation (heat shock) in MARCM technique is also early (Stage 8), maternally provided POMT function is sufficient to carry out branching in sensory axons. This is consistent with previous results from lab indicating perdurance of POMT function in alignment of adult abdominal segments wherein a pulse of *tw* expression during late larval-early prepupal stages, can result in long lasting function (79).

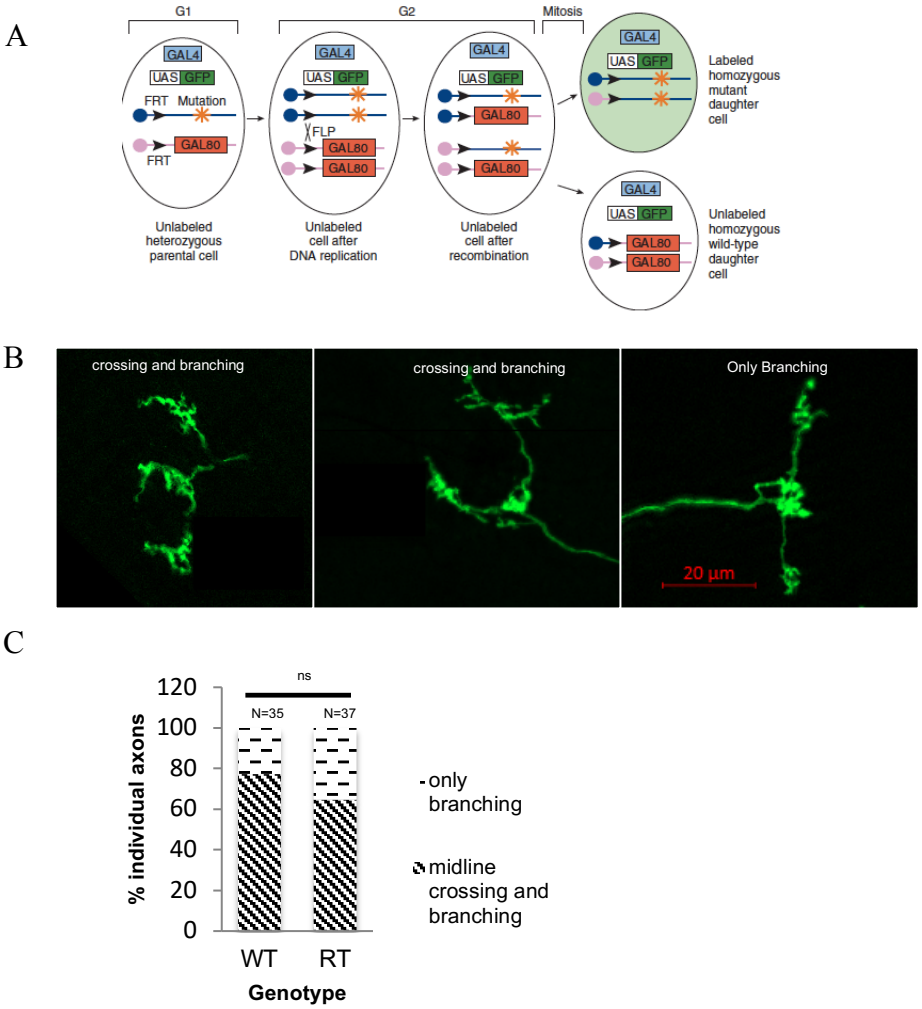

Figure 12. MARCM analysis of WT and POMT mutants. A, In the MARCM system, a transgene encoding the repressor (GAL80) of marker gene expression is placed distal to the FRT site on the homologous chromosome arm from the mutant gene. Site-specific mitotic recombination at FRT sites (black arrowheads) gives rise to two daughter cells, each of which is homozygous for the chromosome arm distal to the FRT sites. Ubiquitous expression of GAL80 represses GAL4-dependent expression of a UAS–marker (GFP) gene. Loss of GAL80 expression in homozygous mutant cells results in specific expression of GFP(109). B, Representative examples of individual Class IV md-da axons (green) with the morphology of "crossing and branching" and "branching only" as generated by mosaic analysis of cell repressible marker (MARCM) are shown here. Scale bar 20µm (indicated). C, Quantification of types of class IV sensory axons as revealed by MARCM clones in WT and *rt* mutants, N is number of individual axons analyzed, Chi square test was performed for statistical significance, ns, not significant; p >0.2.

Since the MARCM results were inconclusive, I used RNAi to ensure that the POMT function of regulating branching in sensory axons is cell autonomous as seen by rescue results. I found that POMTs are required cell autonomously to regulate morphology of Class IV sensory axons (Fig. 13A&B).

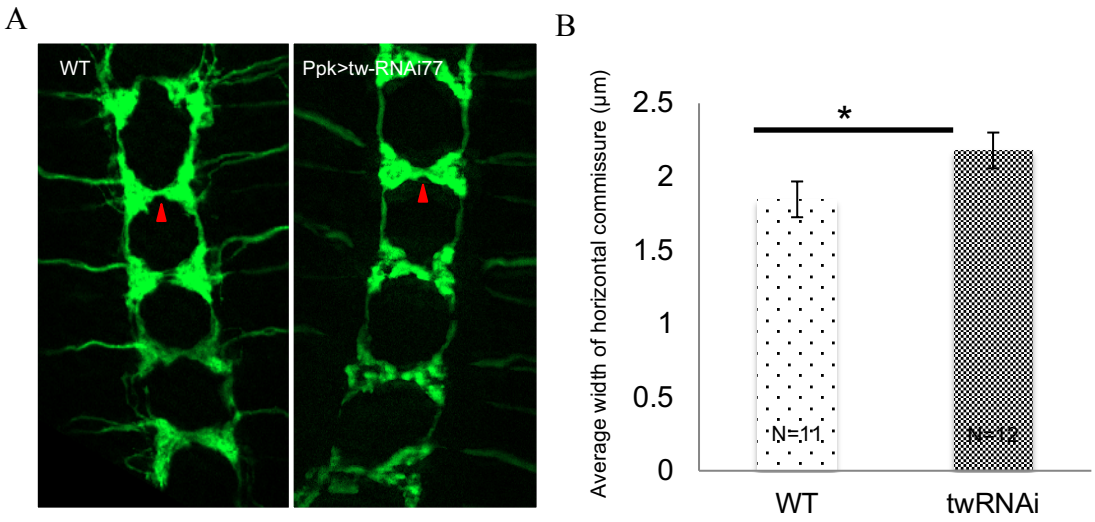

Figure 13. POMTs are required cell autonomously to regulate axon patterning. A, Expression of RNAi construct for *tw* in Class IV multidendritic neurons causes terminal branching defects. Representative images of laminar pattern for most affected neuromeres A1-A4 are shown. Posterior is up, Scale bar 20µm. **B,** Quantification of commissural axon width in WT and twRNAi, error bars indicate SEM, N is number of brains analyzed, *p<0.05, Student's t test was performed for statistical significance. WT, ppkGAL4/+;ppkGFP/+; twRNAi, ppkGAL4/+;twRNAi77/ppkGFP.

POMTs are expressed ubiquitously in several tissues

We have previously used in situ hybridization to show that POMT transcripts exhibit prominent expression from as early as stage 14 of *Drosophila* embryo through late embryogenesis (74). Interestingly, *rt* mRNA is present at stage 5 suggesting maternal contribution of the transcript. The transcript expression was prominently seen in epidermal cells, hindgut, fore gut regions and in the developing trachea (role of POMTs in gut and tracheal cells is not yet known), but not in somatic muscle cells(74). However, the protein expression pattern of POMTs has not been determined yet. To determine the expression pattern I utilized the TransgeneOme pipeline wherein several *Drosophila* genes were endogenously labeled with superfolder GFP and fly lines with each endogenously tagged gene were created(110). I obtained a RT-GFP tagged line to study its protein expression pattern. By immunostaining, I found RT to be expressed in muscles, epidermis and neurons in the brain (Fig. 14).

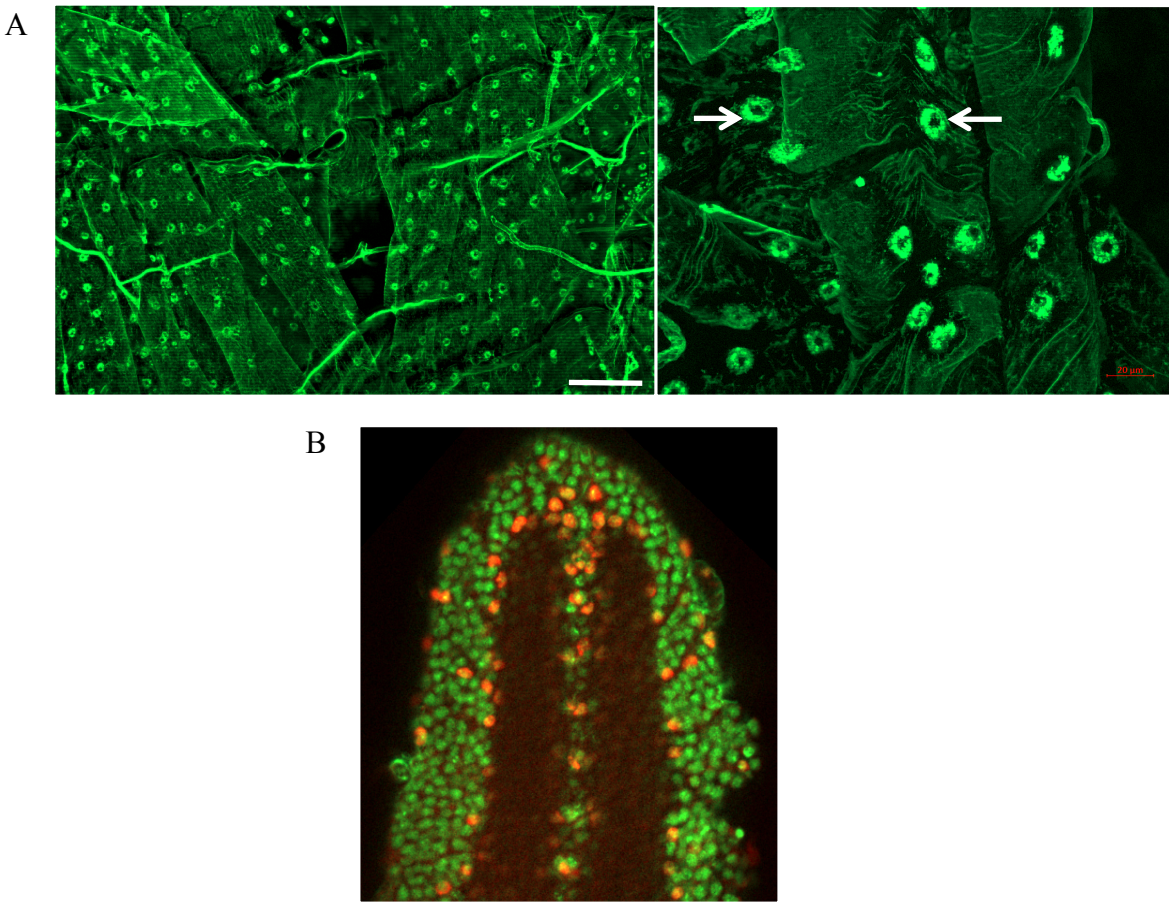

Figure 14. Expression pattern of RT. A, Genomic tagging of RT (green) shows expression in muscles, epidermis and possibly sensory neurons at 5X (left) and 40X(right) magnifications. White arrows denote RT expression in the ER. Third instar larval fillet is shown in both images. Scale bar 100μm (left) and 20μm (right). **B,** RT expression (green) in neurons of the ventral nerve cord of first instar larval brain, glial cells stained with anti-repo are shown (red). Scale bar 20μm.

Dystroglycan mutants do not have the torsion phenotype

Dg (Dystroglycan) is the best characterized target of protein O-mannosylation. POMT-mediated glycosylation of Dg is important for its functional interactions with ECM ligands(18, 26). While O-mannosylation was found on many other mammalian glycoproteins(84), Dg is so far the only known O-mannosylated protein in *Drosophila*.

To test whether the torsion phenotype of POMT mutants is caused by a defect in Dg activity, I analyzed first instar *Dg* mutant larvae. While nearly all first instar POMT mutant larvae showed conspicuous body torsion, I did not detect torsion phenotype in *Dg* mutants (Fig. 15). These results suggest that the torsion phenotype of POMT mutants is not caused by the loss of Dg activity and that some other yet unknown functional substrates of POMTs play a role in the pathogenic mechanisms underlying this phenotype.

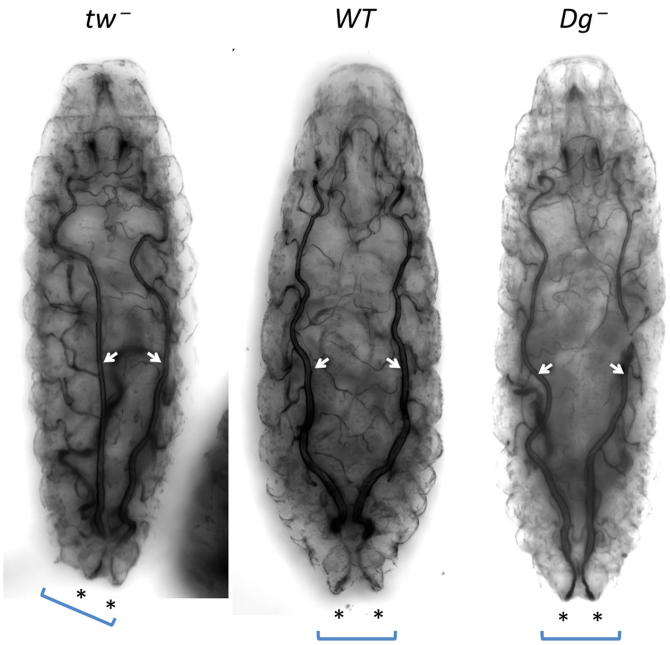

Figure 15. Genetic inactivation of Dg does not result in body posture abnormality. While *tw* mutants show conspicuous body torsion resulting in displacement of dorsal tracheal trunks (arrows) and a rotated position of the last segment (bracket) with posterior spiracles (asterisks), *Dg* mutants show no torsion and are indistinguishable from wild-type control (WT). Representative images of fixed first instar larvae obtained with transmitted light illumination. *Dg*$^{-}$, Dg086/Dg086; *tw*$^{-}$, tw^{1}/tw^{1}(or tw^{1}/Y); WT, wild-type control with matching genetic background (Canton-S). More than 20 larvae were analyzed for each genotype.

Discussion

Here I have described a novel axonal phenotype in POMT mutants and investigated its mechanism using genetic tools. I have shown that POMT mutations specifically affect patterning of axon termini in a cell autonomous manner, while axon guidance and the ventral ganglion development are not generally affected. These neurons are a type of sensory neurons which possess multiple dendrites and are present in the epidermal cells(93). Based on the morphology of the dendrites, they are divided into four categories, Class I-IV. Each of these neurons send their axons to the ventral nerve cord (VNC), a part of *Drosophila* CNS, forming a sensory feedback circuit (Fig. 16). They're polymodal with a function in proprioception and mechanosensation and have an involvement in the regulation of peristaltic larval locomotion(104, 105, 111, 112).

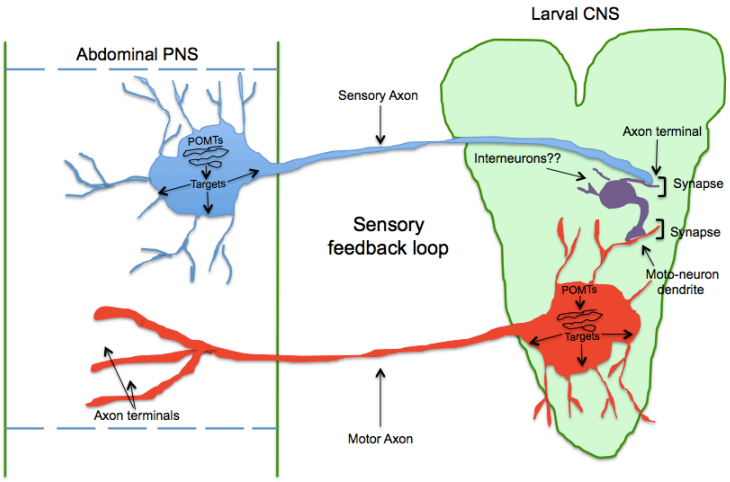

Figure 16. Sensory feedback circuit. Class IV multidendritic neurons reside in larval epidermal cells comprising the PNS and send axons to VNC, a part of CNS. In the CNS they make connections with other neurons which make further connections with other neurons eventually leading to motor neurons that send their axons to the muscles, thus forming a circuit.

Two main orthogonal systems that position sensory axons along dorsoventral and mediolateral axes rely on Semaphorin/Plexin and Slit/Robo signaling, respectively, while connectivity across the midline also depends on the Netrin/Frazzled pathway(113). I discovered that POMT mutants have sensory axons properly positioned along the dorsoventral axis, suggesting that POMTs may affect primarily mediolateral and/or midline-crossing and branching cues. However, axon guidance is not generally abnormal in POMT mutants, and defects are probably limited to the patterning of Class IV axon termini. Proper patterning of axon termini is important for correct circuit assembly (Fig. 16); however, this mechanism remains poorly understood and probably involves the cooperation of canonical cues with additional modulators such as cadherins, RPTPs, and other adhesion and signaling molecules(103, 108, 114). In POMT mutants, sensory neurons apparently generate an aberrant signal to the CNS due to improper circuit assembly, which results in an abnormal pattern of muscle contraction waves and the torsion phenotype (Fig. 17). The proper pattern of muscle contraction waves presumably requires a PNS-mediated feedback that relays information on body posture to the CNS. Several lines of evidence provide support for this mechanism. First, our data suggest that the torsion phenotype is not caused by gross defects of muscle morphology. Although I cannot completely exclude the possibility that muscles may have some fine morphological defects or/and abnormal physiology, our analyses suggested that embryonic muscles, rather than being misaligned during development, are formed properly in POMT mutants. I have also shown that POMTs are expressed in muscles during developmental stages indicating a role of POMTs in muscles. Also, the torsion

phenotype arises only during peristaltic muscle contractions and is essentially fully penetrant. Occasional muscle defects were reported in POMT mutants, but these defects are present at low frequency and are not bilaterally biased and thus it was previously concluded that they are unlikely to cause the misalignment of body segments(86). This is consistent with our results, which furthermore indicated that the torsion phenotype is developmentally transient, as the phenotype becomes undetectable at later larval stages. This presumably happens because the torsion becomes fixed as the cuticle hardens during late embryogenesis, but the phenotype disappears once the cuticle is shed upon transition to the second instar. Second, the torsion arises due to alteration in the pattern of contraction waves, while the effects of individual waves on posture are not altered in POMT mutants. These data suggest that individual muscles contract normally and that the torsion is caused primarily by a neurological abnormality affecting wave patterns. Third, our analyses of *sens* mutants highlighted the role of PNS cells in producing the torsion phenotype. A defect in the specification of PNS neurons alone could cause muscle contraction and posture phenotypes similar to those in POMT mutants. Third, POMT mutations specifically affect patterning of Class IV sensory axon termini, suggesting that aberrant connectivity between sensory and CNS neurons underlies the defect of sensory feedback. Finally, genetic rescue and RNAi knockdown revealed that POMT activity restored in class IV da sensory neurons in POMT mutants was sufficient to rescue the torsion phenotype and both the abnormality of contractions and the defect in axonal projections, suggesting that these neurons play an important role in POMT-mediated control of contractions and body posture.

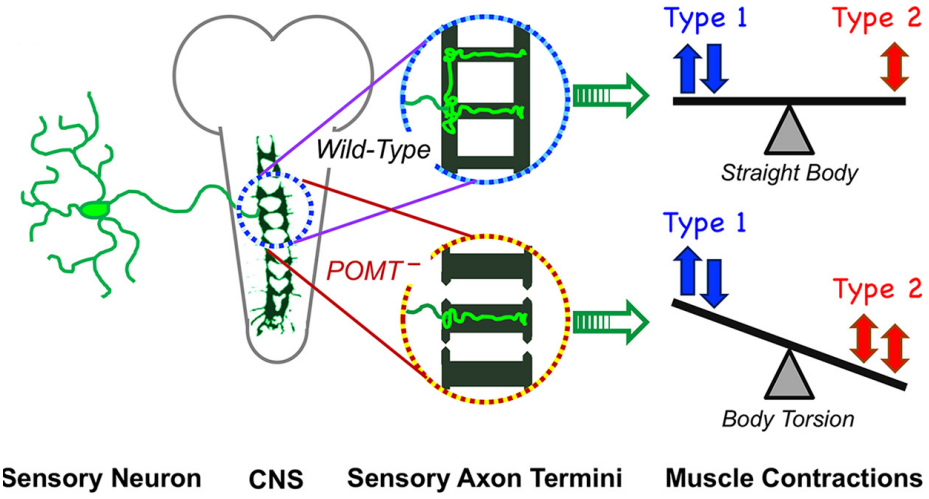

Figure 17. Control of body posture by sensory feedback. To maintain straight posture, sensory neurons send feedback to the CNS to control the pattern of alternating type 1–type 2 waves. In POMT mutants, sensory axon termini are abnormal, which affects sensory circuit assembly, causing aberrant feedback from sensory neurons. This compromises the control of the wave pattern and results in an excessive proportion of type 2 waves, which leads to body torsion.

Furthermore, I found that *Dg* (Dystroglycan) mutants do not have body torsion, suggesting that the torsion phenotype of POMT mutants is not caused by the loss of Dg activity and other POMT target(s) could affect sensory axon patterning. Which proteins can be functionally relevant POMT targets remains to be elucidated.

Remarkable conservation of POMTs in animals suggests an intriguing possibility that their role in facilitating neural connectivity to control muscle contractions may be conserved in vertebrates. Interestingly, the downregulation of POMK, a kinase involved in biosynthesis of vertebrate O-mannosyl glycans, causes abnormality in coordinated muscle contractions in zebrafish embryos, while clinical features of syndromes associated with POM defects commonly include abnormal muscle contractions(115, 116). Further studies should shed light on evolutionary conservation of the role of

POMTs in regulating muscle contractions and axonal connectivity, which can potentially elucidate pathogenic mechanisms of diseases caused by POM abnormalities.

CHAPTER III

RECEPTOR PROTEIN TYROSINE PHOSPHATASES (RPTPS) ARE A NOVEL SUBSTRATE OF POMT1/2 DEPENDENT O-MANNOSYLATION IN *DROSOPHILA*

Introduction

Neuronal wiring is crucial for development of the nervous system in all animals. Several factors play an important role in establishing the circuitry, which controls physiological functions in organisms. In the previous chapter, I described the enzyme complex Protein O-mannosyltransferase 1 and 2 (POMT1/2), as an important regulator in establishing a sensory circuit that controls coordinated muscle contractions and body posture in *Drosophila*. POMT1/2 add mannose sugar to the Oxygen atom of Ser/Thr residues of proteins in the ER. Deficiencies in POMT1/2 lead to congenital muscular dystrophies (CMDs) in humans(6, 44). Congenital muscular dystrophy (CMD) is a group of debilitating neuromuscular disorders present at birth or early infancy. Patients with CMDs caused by protein O-mannosylation (POM) defects exhibit striking neurological abnormalities(6). Although substantial research has been done to understand the role of POM in muscles and neuromuscular junctions, little is known about its role in the brain. *Drosophila* is an excellent model system to study neurological abnormalities caused by POM defects due to evolutionarily conserved genes of the POM pathway, simpler glycosylation patterns and efficient genetic approaches. We have previously described that *pomt1/2* mutant embryos display abnormalities in their body posture and muscle contractions and were rescued by expressing POMT1/2 in neurons including a subtype

of sensory neurons(96). In the previous chapter, I have demonstrated that *pomt1/2* mutant embryos show morphological defects in the same sensory axons terminating in the brain. This defect affects neuronal communication that controls body posture. Therefore, we established that POMT1/2 play a regulatory role in sensory neuronal connectivity and thus, body posture. Multidendritic sensory neurons present in the epidermis control heat, pain and locomotion responses in *Drosophila* embryos and larvae(105). Multidendritic sensory neurons are divided into four subtypes (Class I-IV) based on their dendritic morphology. They send axons to the ventral nerve cord (VNC) where axons make connections with other first order neurons establishing a circuit that regulates muscle contractions and body posture in *Drosophila.* Class IV axons were defective in the VNC of *pomt1/2* mutants. The *Drosophila* VNC is analogous to the mammalian spinal cord(114) hence neurological roles of POM are likely conserved and will further our understanding of CMDs.

Despite POM's importance and implication in human disease substrate proteins that are modified by POMT1/2 are largely unknown. So far, only one well-studied substrate, Dystroglycan, a cell adhesion molecule is known. Dystroglycan's extracellular domain is O-mannosylated in mammals and *Drosophila*(30). Recently, 2 new substrates for POMT1/2 were identified from human cell lines; both of those proteins have *Drosophila* homologues but are not well characterized (7, 16). I have previously demonstrated that Dystroglycan alone does not account for the posture defects seen in *Drosophila* embryos (Fig. 15), indicating the functional relevance of other substrates. Therefore, I hypothesized that, proteins important in making axon connections during development

might be functionally relevant targets of POMT1/2. Interestingly, Receptor protein tyrosine phosphatase 69D, a trans membrane signal transduction phosphatase, was identified in a forward genetic screen as a regulator of multidendritic sensory axon connections in *Drosophila* VNC(92). RPTPs have large extracellular domains containing multiple immunoglobulin (Ig) and/or fibronectin type III (FNIII) repeats, reminiscent of cell adhesion molecules (CAMs)(117). Similar RPTPs are expressed on vertebrate growth cones. One such vertebrate, RPTPζ, was found to be O-mannosylated(31). *Drosophila* has 6 well-studied RPTPs of redundant functions(118). RPTPs have enormous roles in the nervous system ranging from axon guidance, synapse formation, neural tissue morphogenesis and cell-adhesion dependent signaling(117). Due to their elaborate extracellular domain, cell adhesion molecule like features and well-characterized roles in axon guidance, I posited that RPTPs are good, functionally relevant candidates of POMT1/2 modification.

Here, I demonstrate that Dystroglycan alone is not responsible for multidendritic axon defects seen in *pomt1/2* mutants. Using various mutant and RNAi strategies, I demonstrate that *pomt1/2* and *rptps* interact synergistically to regulate multidendritic axon connectivity in the VNC. In collaboration with experts in mass spectrometry (Dr. Lance Wells, CCRC, Athens, GA), I show that RPTP69D, one of the RPTPs implicated in regulating laminar pattern of Class IV sensory axons is indeed O-mannosylated by POMT1/2 and also N-glycosylated on its extracellular domain in *Drosophila*. *Rptp69d* also exhibits strong genetic interactions with *pomt1/2* to regulate axon morphology of Class IV axons. I further present genetic and biochemical evidence that O-

mannosylation of RPTP69D is not required for its correct localization to the axonal membrane, rather O-mannosylation of RPTP69D by POMT1/2 may protect it from proteolysis, thus protecting its function. My results uncover a novel substrate of POMT1/2 and a possible molecular mechanism of how O-mannosylation might affect the function of axon guidance molecules such as RPTPs. These functions might be evolutionarily conserved and give mechanistic insights into understanding CMDs better.

Materials and Methods

Drosophila stocks and crosses. The mutant alleles for *rt* and *tw* were previously described, as follows: tw^{1} is a hypomorphic allele; rt^{2}, rt^{P}, are strong hypomorphic alleles that are close to amorphs(74, 86). Dg^{248} has been previously described(119) and Dg^{086} is a null allele(89). *UAS-tw* transgene was previously described(74). $Ptp69D^{1}$(null allele) and $PTP69D^{20}$(hypomorph) have been previously described(120, 121) respectively. $Ptp69D^{dn}$ is previously described (122), *UAS-Ptp69D*-RNAi is described previously (123). Lar^{E55}, $Ptp99A^{1}$, $Ptp52f^{18.3}$, $Ptp4E^{1}$ and $Ptp10D^{1}$ were previously described,(124-128) respectively. All other mutant and transgenic strains(RNAi lines and *UAS-69D-Myc*) were obtained from the Bloomington Drosophila Stock Center at Indiana University. Unless indicated otherwise, flies/larvae of either sex were included in all analyses, as our experiments, as well as studies by other groups, revealed no evidence of sex-specific phenotypes of POMT mutants.

Fluorescent staining and microscopy. First instar and late 3rd instar larvae expressing tdGFP in the Ppk pattern(90) in a wild-type, *tw*, or *rt, rptp* mutant, background, were collected. The CNS (brain lobes together with the ventral ganglion) was dissected, fixed

in PBS with 4% paraformaldehyde, and stained with mouse anti-GFP antibody (8H11 DSHB) in a 1:20 dilution. Alexa Fluor 488 conjugated anti-mouse antibodies were used as a secondary antibody in a 1:250 dilution. Stained samples were mounted on slides and imaged using the Zeiss Axioplan M2 Microscope using 40X magnification objective. To minimize potential errors, control and experimental samples were stained using the same master-mix of antibodies and imaged with the same settings for camera, illumination, and microscope. Commissural branch thickness was measured in stacks of optical sections with 0.6μm step size using ImageJ or ZEN for every branch in a given ventral nerve cord and averaged, and the collective average from a given genotype reported. The tracts were scored as "present" when the brightness of the region where the tract was expected to be was >10% above background, as measured by ImageJ or ZEN.

Ex69D construct

The Ex69D construct was generated by in frame fusion of cDNA encoding the first 687 amino acids of RPTP69D with the fragment encoding 3xFLAG tag (sigma) using standard molecular biology techniques. The Ex69D protein encoding by the construct lacks the transmembrane domain and the proteolytic cleavage site and is predicted to be secreted.

In vivo expression and purification of Ex69D

Ex69D was cloned into pUAST vector for in vivo expression and transgenic Drosophila strains were created by P-element mediated germline transformation. In vivo expression of UAS-Ex69D was induced by UAS-Gal4 system. The specificity of Ex69D detection by western blot was confirmed using negative control samples without Ex69D

expression ("WT mock"). Ex69D was expressed in vivo in the following genetic backgrounds : *rt*$^{-}$, *rt*^{P}/*rt*^{2} ; *rt*+ *tw*+, UAS-rt, UAS-tw/Act5C-GAL4; WT, Canton S, w- (designated as MH2J). Ex69D was purified from 350-500 adult flies (1-2 day old)with anti-FLAG M2 agarose (Sigma). Briefly, flies were lysed in lysis buffer (50mM Tris-HCl, pH 7.5, 200mM NaCl, 0.5% Triton X100) including cocktail of protease inhibitors (complete, Roche) and 1X PMSF and briefly sonicated. After centrifugation at 18000g, for 20 min at 4oC the supernatant was added to 10µl of FLAG beads and incubated overnight at 4oC on nutation. Beads were washed and resuspended in Lysis buffer of decreased Triton X-100 concentration (0.05%) and then sent for mass spectrometry directly.

Mass spectrometry

All samples were digested with Trypsin, then were treated with PNGase F and subsequently with PNGase A, to remove all N-glycans. MS/MS was collected with sHCD and CID-NL_MS3 (Hex). All mass spectrometry was done at Dr. Lance Wells lab in CCRC (complex carbohydrate research center), Georgia.

Western blot analyses

Analysis was performed according to standard protocols. Briefly, tissue lysates were prepared from late 3rd instar and run on 8% SDS-PAGE gel. Separated proteins were transferred to nitrocellulose membranes. Mouse anti-FLAG M2 primary (Sigma) antibody and rabbit anti-mouse HRP-conjugated secondary (Jackson Laboratories) antibodies were used for detection by chemiluminescence (SuperSignal, Thermo Scientific). Blots were imaged using Amersham Imager 600.

Experimental design and statistical analysis. Experiments were performed at least three times. Statistical analyses were performed by one-way ANOVA with Tukey's HSD post hoc comparisons for significance using IBM SPSS version 26 software. For box plots, data for each box in the graph were analyzed as a separate column. In all figures, 1 and 2 asterisks represent p values of <0.05 and 0.01, respectively; NS indicates that no significant differences were found (p >0.05). Details on statistical analysis are included in figure legends and text.

Results

Dystroglycan does not account for the axonal defect seen in POMT1/2 mutants

Since Dystroglycan (Dg) is the well-studied substrate of POMT1/2 in both *Drosophila* and mammals and is crucial for axon guidance of photoreceptor axons, I hypothesized that it may be crucial for establishing axon connectivity of Class IV axons in the VNC. To test this hypothesis, I studied mutants of *Dg* alone and in combination with POMT2 mutants (*tw*). Interestingly, *Dg* mutants alone show a slight effect on the laminar pattern of Class IV axons (Fig. 18A), but they fail to phenocopy the defects in POMT1/2 mutants such as seen in *rt* mutants (Fig. 18B). Next, I decided to test if combining *Dg* mutants with a hypomorphic POMT mutant might enhance the slight defects seen in both mutants. Hypomorphic POMT mutant (*tw*) and *Dg* mutants together did not worsen the phenotype of Class IV axons, indicating the importance of other relevant substrates (Fig. 18A&B).

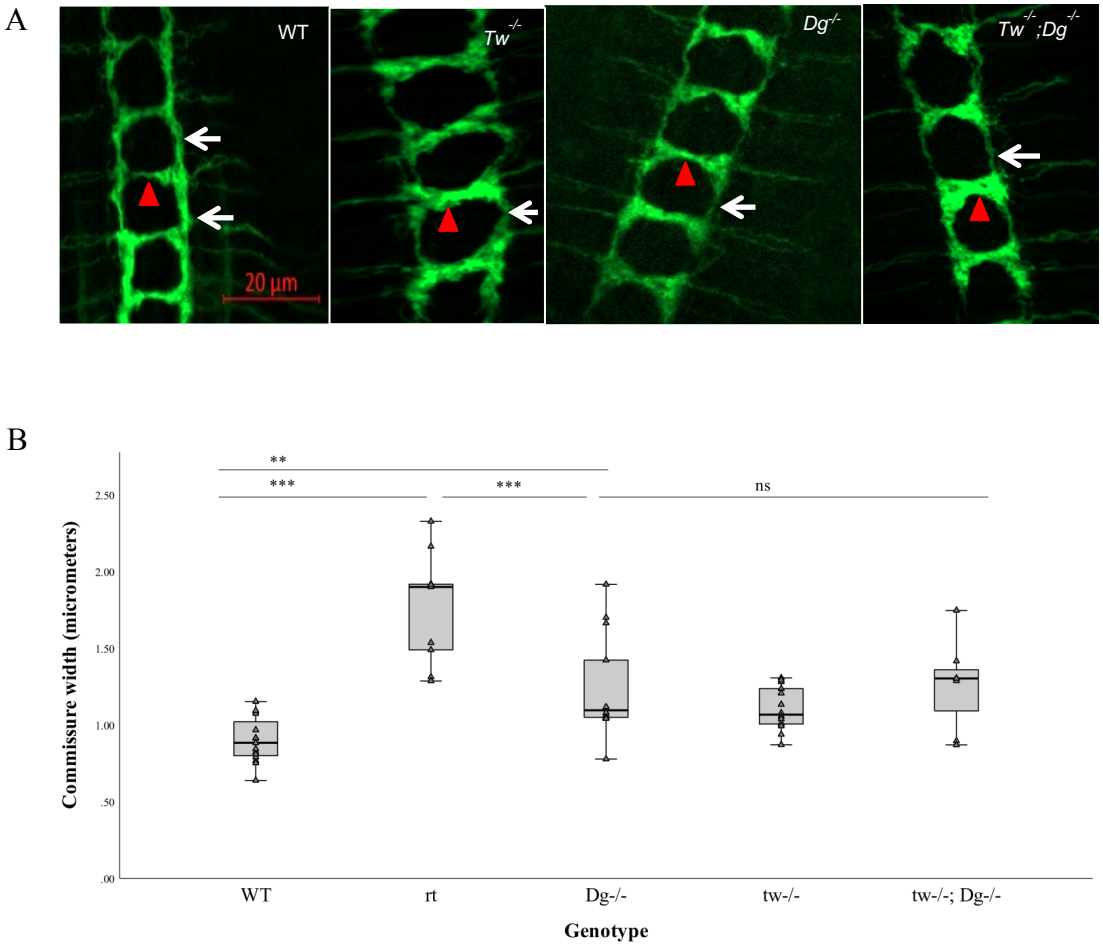

Figure 18. Dystroglycan does not phenocopy POMT1/2 defects in Class IV axons. **A,** Dystroglycan mutants show mild terminal branching defects in Class IV multidendritic axons (green) which do not appear to worsen on combining with *tw* mutants. Arrows indicate longitudinal axon branches, red arrowheads indicate commissural axons. Scale bar is 20µm (indicated). Most affected neuromeres(A1-A5 segments) of 1st instar brains are shown in all panels, posterior is up. **B**, Quantification of commissural axon width in all genotypes as indicated. In all panels, error bars indicate SEM, **,$p<0.01$;ns, not significant. Grey rectangles represent interquartile range and horizontal line inside them represents the median. Number of brains (N) analyzed is 7-15 for each genotype. Statistical analysis done using One way ANOVA with Tukey's HSD post hoc test. WT, wild type; $tw^{-/-}$, tw^{1} /Y or tw^{1}/tw^{1}; $rt^{-/-}$,rt^{2}/rt^{2}; $Dg^{-/-}$, Dg^{248}/Dg^{086} ; $tw^{-/-}$; $Dg^{-/-}$, tw^{1}/Y;Dg^{248}/Dg^{086}.

Receptor protein tyrosine phosphatases show synergistic genetic interactions with POMT1/2

To evaluate substrates of POMT1/2 that function in regulating laminar pattern of Class IV axons in the VNC of *Drosophila*, I studied genetic interactions of *POMTs* with functionally relevant candidate genes. To this end, I started with a receptor protein tyrosine phosphatase 69D (*rptp69d*), which was previously identified in a forward genetic screen as an important regulator of Class IV axon morphology(92). *Rptp69d* has no known vertebrate orthologues, however a RPTPζ, with similar extracellular domain structure, was shown to be O-mannosylated in mammalian neurons and glia(31). I combined two different mutant alleles of *rptp69d*, one with the deletion of a large gene region encoding the extracellular domain ($Ptp69d^{1}$) and another with a point mutation inactivating one of the two intracellular catalytic phosphatase domains ($Ptp69d^{20}$) (Fig. 19A) with a hypomophic *POMT* mutant (tw^{1}). Specifically, I combined single copy of $Ptp69d^{20}$ and a heteroallelic combination of $Ptp69d^{1}$ and $Ptp69d^{20}$, with *tw*. I did not observe any significant genetic interactions with these combinations (Fig. 19B&C). The absence of interactions between $Ptp69d^{1/20}$ and *tw* probably indicate that the $Ptp69d^{1/20}$ heteroalleleic combination is a too weak hypomorphic mutant. Indeed, $Ptp69d^{1/20}$ does not show the axon wiring defects (Fig 19C). In order to analyze a stronger loss-of-function *Ptp69D* mutant, I attempted to use $Ptp69d^{1}$ homozygotes (121). However, $Ptp69d^{1/1}$ turned out to be lethal at late embryonic stages. As an alternative approach, I decided to use the overexpression of a dominant negative form of RPTP69D ($Ptp69d^{dn}$) that lacks the intracellular, catalytic domain and is known to efficiently antagonize

RPTP69D functions, presumably by titrating out RPTP69D ligands. The overexpression *Ptp69d*^{dn} in Class IV axons resulted in severe defects in laminar pattern of sensory axons that phenocopied *rt*$^{-/-}$ mutants (Fig. 19D&E). The commissural axons appear to abnormally cross the midline and are therefore thicker than WT and longitudinal axons are thinner. Combining the overexpression of the dominant negative *ptp69d* with *tw*^{1} did not show significantly different phenotype from *PTP69D*^{dn} alone, suggesting that *PTPs* are epistatic to *POMTs*. (Fig. 19D&E). As an alternative approach, I decided to knockdown *Ptp69d* in Class IV axons, using RNAi. On combining *Ptp69d*-RNAi, with *tw* mutant, I observed a strong, highly penetrant, phenotype, with thicker commissure axons that appear to abnormally cross the midline (Fig. 19F&G). Taken together, these data suggested that that RPTP69D might be a novel, functionally relevant substrate of POMT1/2.

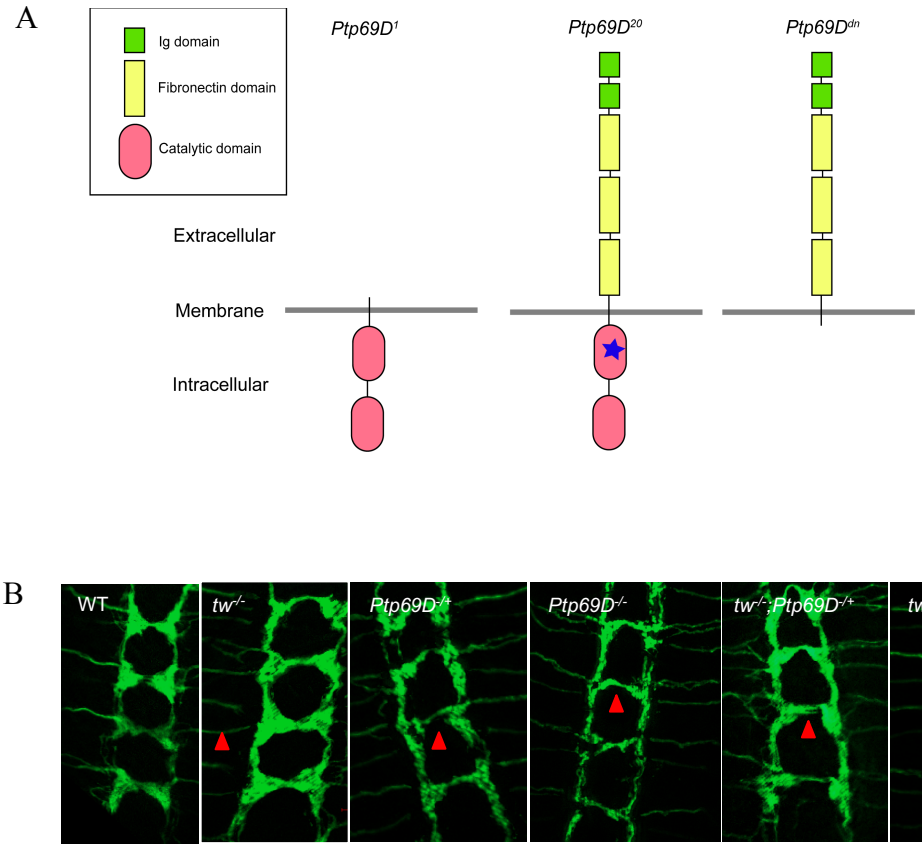

Figure 19. RPTP69D is a potential substrate of POMT1/2. **A,** Cartoon illustrating the different PTP69D mutant alleles used in the study. Blue star indicates a point mutation. **B,** Genetic interaction study using different single and double mutants of POMT and RPTP69D as indicated. **C,** Quantification of commissural axon width for the genetic interaction study. Circles depict outliers. N (number of brains analyzed) is 7-16.**D,** *Ptp69D^{dn}* shows defects similar to POMT1/2. **E,** Quantification of commissural axon width for the dominant negative phenotype and comparisons to POMT mutants are shown. N is 12-17. **F,** POMTs interact genetically with RNAi knockdown of RPTP69D. **G,** Quantification of commissural axon width for POMT-RPTP69DRNAi interactions is shown. N is 6-11. For all representative images, Class IV axons (green) of most affected neuromeres(A1-A4)in 3rd instar larval brains are shown, red arrowheads indicate commissural axons, white arrows indicate longitudinal axons. Posterior is up. Scale bar 20µm. For all quantifications, error bars depict SEM. **,$p<0.01$; ns, not significant. One way ANOVA with Tukey's HSD post hoc test was performed for statistical significance. WT, wild type; tw$^{-/-}$, tw^{1} /Y or tw^{1}/tw^{1}; rt$^{-/-}$,rt^{2}/rt^{P}; ptp69D$^{-/+}$,ptp69D$^{20/+}$; ptp69D$^{-/-}$, ptp69D^{1}/ptp69D^{20}. tw$^{-/-}$;ptp69D$^{-/+}$, tw^{1}/Y;ptp69D$^{20/+}$. tw$^{-/-}$; ptp69D$^{-/-}$,tw^{1}/Y;ptp69D^{1}/ptp69D^{20}. tw$^{-/-}$;ppk>ptp69d^{dn}, tw^{1}/Y;ppk>ptp69D^{dn}. tw$^{-/-}$;Ppk>Ptp69D-RNAi, tw^{1}/Y;ppk>ptp9d-RNAi.

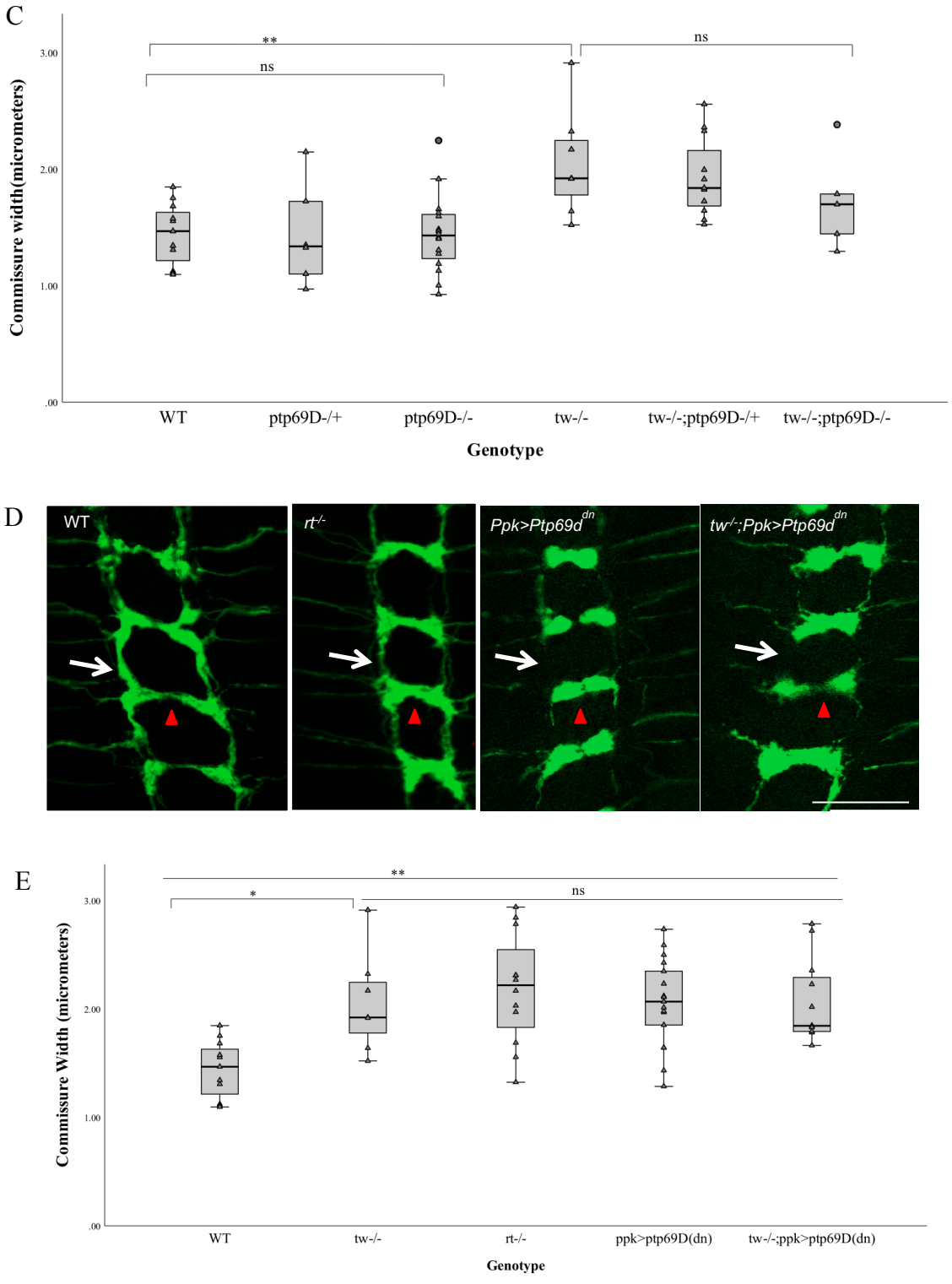

Figure 19. Continued.

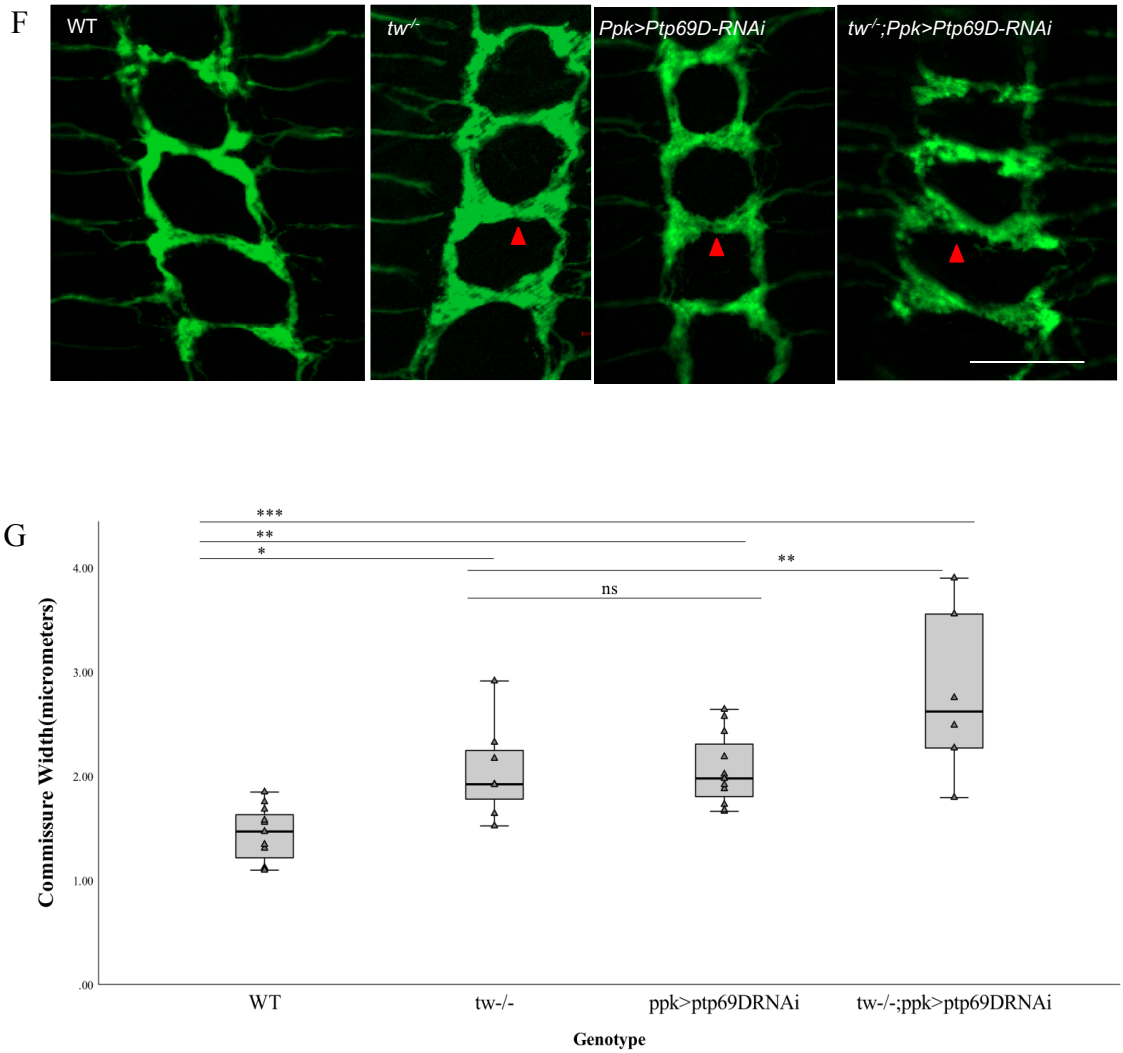

Figure 19. Continued.

Drosophila has 6 characterized RPTPs with partially redundant functions in controlling CNS axon and motor axon morphologies(120, 127). Since $Ptp69d^{dn}$ exhibits a severe phenotype in Class IV axons and is thought to antagonize the function of other RPTPs, I decided to test if other RPTPs can contribute to sensory axon wiring.

To test the involvement of other RPTPs in regulating Class IV axon morphology, I again used genetic interaction as a tool to identify potential players. Specifically, I combined a single copy of Lar^{E55}, $Ptp99A^{1}$ or $Ptp52F^{18.3}$ mutant alleles with *tw* and added $Ptp10D^{1}$ mutant in a hemizygous combination with $tw^{-/-}$; $Ptp69D^{1}$/+. In addition, I also studied double mutants of $Ptp4E^{1}$ and $Ptp10D^{1}$. Interestingly, I observed an improvement in *tw* phenotype when tw^{1} was combined with single copy Lar^{E55}, mutant, however it was not statistically significant. Since, Lar^{E55} is a deletion of the extracellular domain of LAR, it might indicate a negative regulation of extracellular domain function by POMT1/2. I also observed a mild increase in the severity of *tw* phenotype when combined with $Ptp52F^{18.3}$ mutant (Fig. 20A&B). $Ptp52F^{18.3}$ is a point mutation (Ser to Pro) in the fifth fibronectin domain of the extracellular region(126). Other combinations of *Ptp* mutants ($Ptp99A^{1}$, $Ptp4E^{1}$, $Ptp10D^{1}$) with *tw*, did not yield strong genetic interactions (Fig. 20C&D).

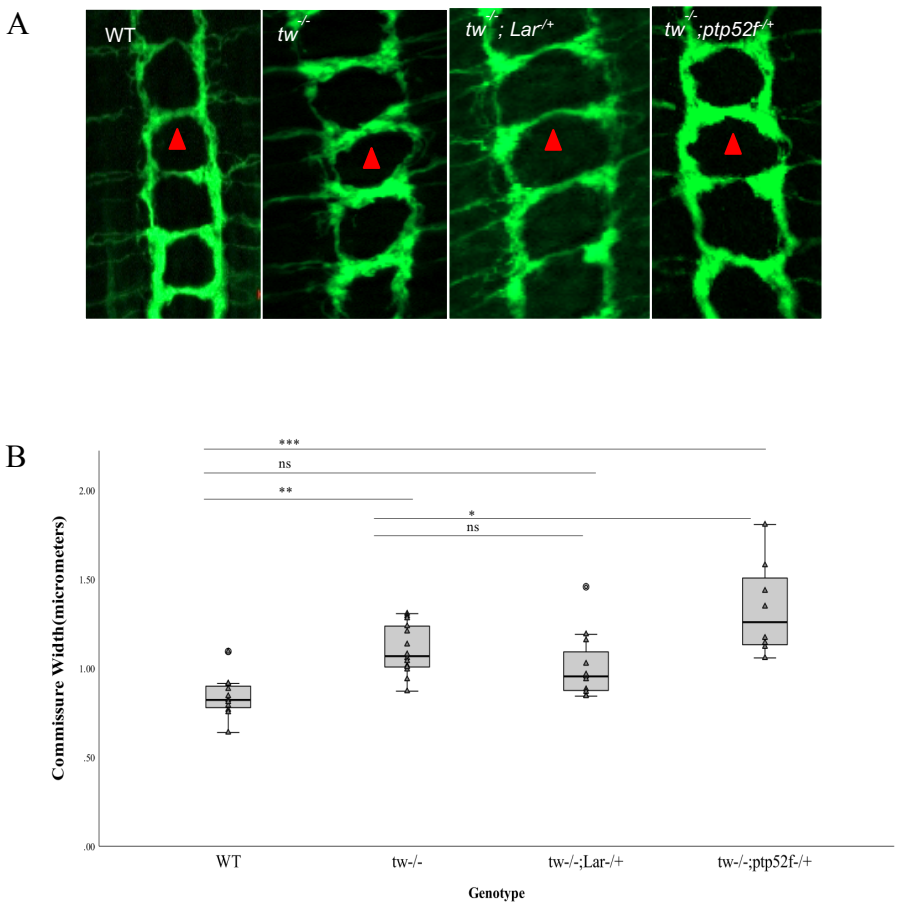

Figure 20. POMT1/2 affect the function of other RPTPs . A, POMTs show genetic interactions with *Lar* and *Ptp52F* to regulate Class IV axon (green) morphology. **B,** Quantification of commissure axon width for genetic interactions of Lar and 52F with POMTs are shown. N is 8-14 **C**, POMTs did not show significant genetic interactions with single copy mutants of other PTPs. **D**, Quantification of commissure axon width for genetic interactions of PTP99A with POMT are shown. N is 7-13. E, Quantification of commissure axon width for PTP4E and PTP10D double mutants are shown. N is 7-11. F, Quantification of commissure axon width for genetic interactions of PTP10D and PTP69D with POMT are shown. N is 7-11. For all representative images, Class IV axons (green) of most affected neuromeres(A1-A4)in 1st(**A**) and 3rd instar larval brains (**C**) are shown, red arrowheads indicate commissural axons. Posterior is up. Scale bar 20µm. For all quantifications, error bars depict SEM. **,$p<0.01$; ns, not significant;***,$p<0.001$;*,$p<0.05$. One way ANOVA with Tukey's HSD post hoc test was performed for statistical significance. WT, wild type; $tw^{-/-}$, tw^{1} /Y or tw^{1}/tw^{1};tw-/-;$Lar^{-/+}$,tw^{1}/tw^{1} or tw^{1}/Y;Lar^{E55}/+; $tw^{-/-}$;$ptp52f^{-/+}$, tw^{1}/tw^{1} or tw1/Y;$Ptp52F^{18.3}$/+; $tw^{-/-}$; $ptp99A^{-/+}$, tw^{1}/Y;$Ptp99A^{1}$/+; $Ptp4E^{1}$,$ptp10D^{1}$, $Ptp4E^{1}$,$ptp10D^{1}$/Y; $tw^{-/-}$,$ptp10D^{1}$; $ptp69D^{1}$/+, tw^{1}, ptp10D/Y;$ptp69D^{1}$/+.

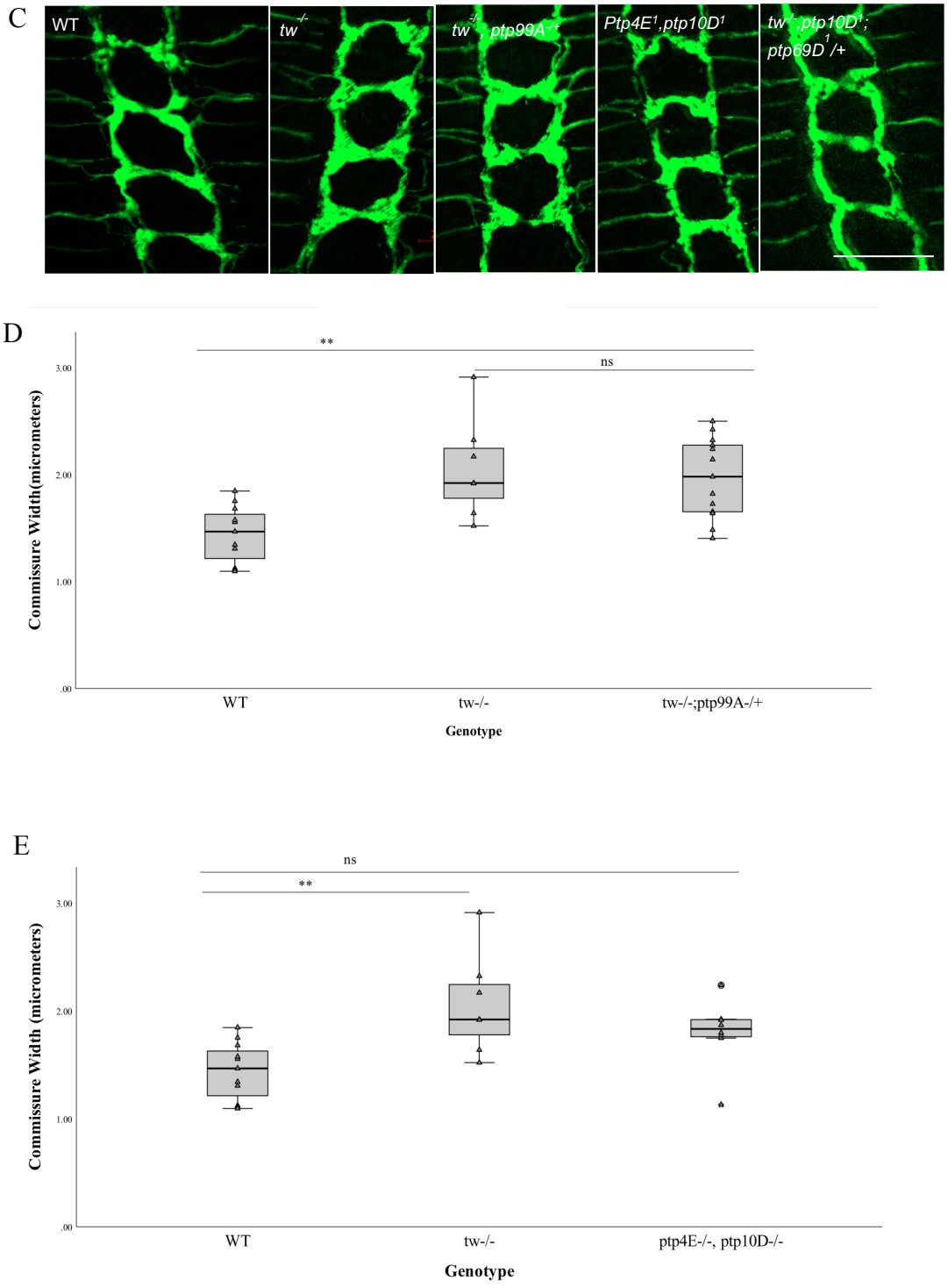

Figure 20. Continued.

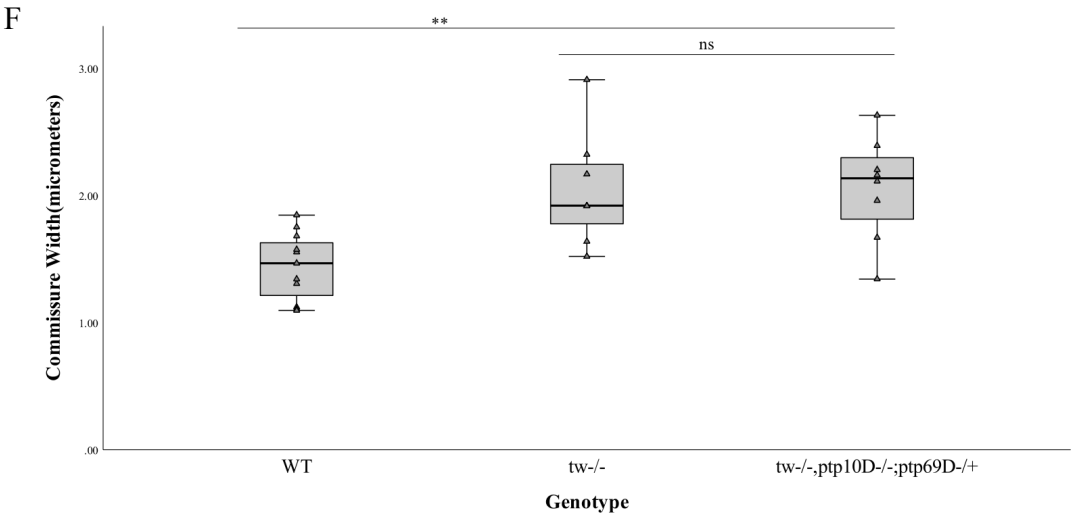

Figure 20. Continued.

To test the possibility that one copy of these *Ptp* mutant alleles may not downregulate *Ptp* activities sufficiently enough to show genetic interactions, I used RNAi-mediated knockdown as a strategy to downregulate these genes. Interestingly, downregulation of *Ptp99A*, *Ptp4E* by RNAi in *tw mutants*, showed strong, synergistic, highly penetrant phenotype in Class IV axon morphology (Fig. 21A,B). *Ptp10D*-RNAi combined with *tw* showed missing T3 thoracic commissure in all brains, but no change in overall thickness of other commissures (Fig. 21E). RNAi of *Ptp4E* when combined with *tw* showed novel defects in Class IV axons along with thicker commissures in some segments, that appear to abnormally cross the midline. The novel defects were highly penetrant and not observed with RNAi of *Ptp4E* alone(Fig. 21H). This indicates that POMT1/2 may be involved in the regulation of several RPTPs, or maybe all of them. Unfortunately, RNAi of *Ptp52F* could not be studied due to unhealthiness of the RNAi line.

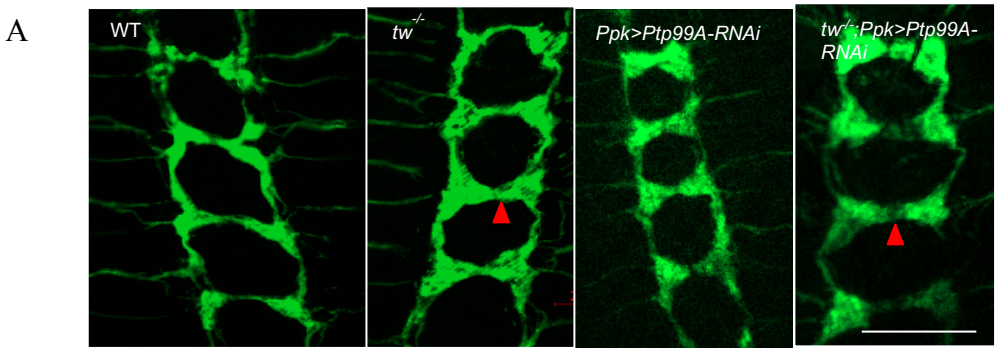

Figure 21. POMTs affect the function of RPTPs. A, POMTs show genetic interactions with *Ptp99A* to regulate Class IV axon (green) morphology. **B,** Quantification of commissure connection width for analyzing genetic interactions of Ptp99A with POMTs. N=5-11. **C,** POMTs do not show strong genetic interactions with Lar. **D**, Quantification of commissure connection width in genotypes with Lar and POMT mutant alleles. are shown. N=5-11 **E,** POMTs do not show interactions with Ptp10D with respect to thicker commissures, but yellow arrowheads show missing thoracic commissures. **F,** Quantification of commissure width of genotypes with Ptp10D and POMT mutant alleles . N=2-11. **G,** POMTs do not show strong genetic interactions with respect to thicker commissures, but other novel defects are seen in **H**, yellow arrowheads show missing commissures, orange arrowheads show thicker or missing longitudinal axons, blue arrowhead shows a commissure crossing the midline at a wrong point. **I,** Quantification of commissure width in genotypes with Ptp4E and POMT mutant alleles. N=5-11. For all representative images, Class IV axons (green) of most affected neuromeres(A1-A4) 3rd instar larval brains are shown, red arrowheads indicate commissural axons. Posterior is up. Scale bar 20μm. For all quantifications, error bars depict SEM. **,$p<0.01$; ns, not significant;***,$p<0.001$;*,$p<0.05$. One way ANOVA with Tukey's HSD post hoc test was performed for statistical significance. WT, wild type; $tw^{-/-}$, tw^{1} /Y or tw^{1}/tw^{1}; $tw^{-/-}$;Ppk>Ptp99A-RNAi, tw^{1}/Y;ppk>ptp99A-rnai. $tw^{-/-}$;Ppk>Lar-RNAi, tw^{1}/Y;ppk>Lar-rnai. $tw^{-/-}$;Ppk>Ptp10D-RNAi, tw^{1}/Y;ppk>ptp10Drnai. $tw^{-/-}$;Ppk>Ptp4E-RNAi, tw^{1}/Y;ppk>ptp4Ernai. Ppk>Ptp99A-RNAi, tw/+;ppk>ptp99A-rnai. Ppk>ptp10D-RNAi, tw/+;ppk>ptp10D-rnai. Ppk>ptp4E-RNAi ,tw/+;ppk>ptp4E-rnai.

B

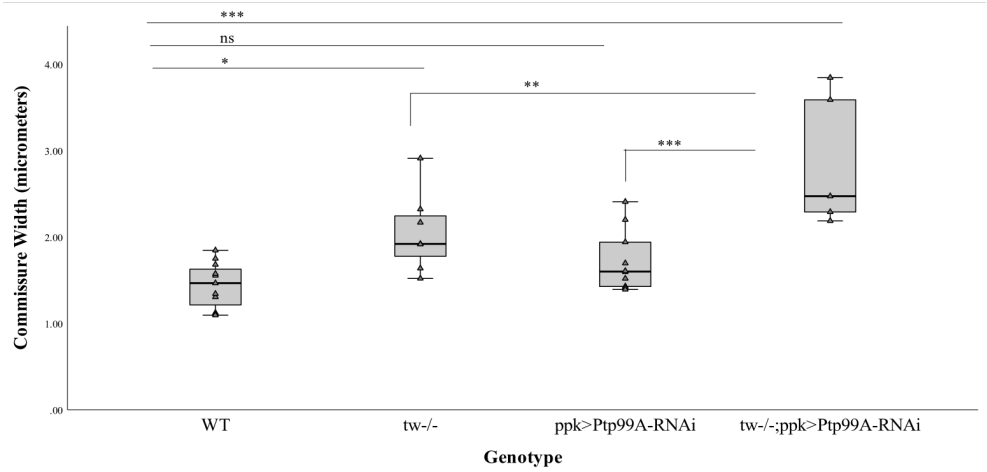

C

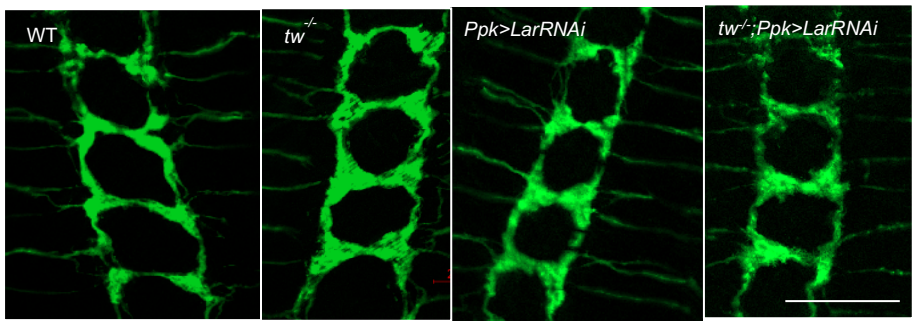

D

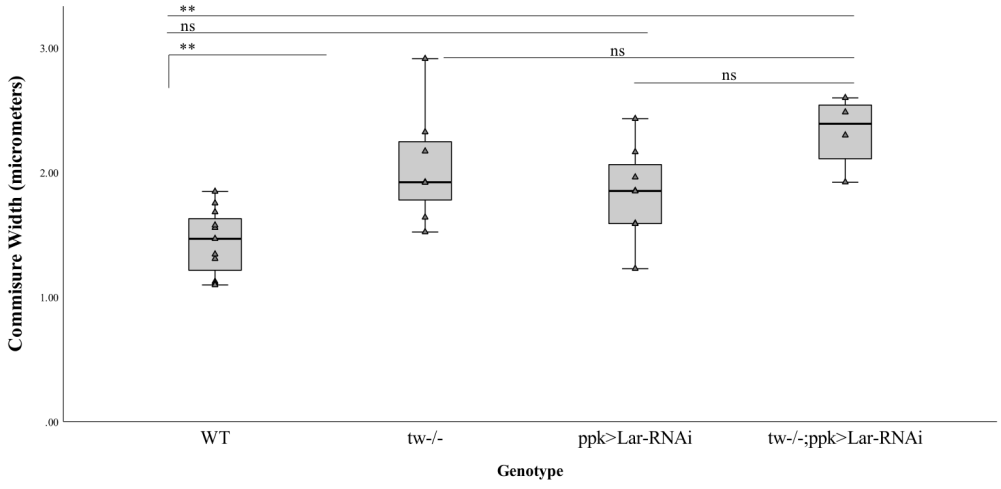

Figure 21. Continued.

E

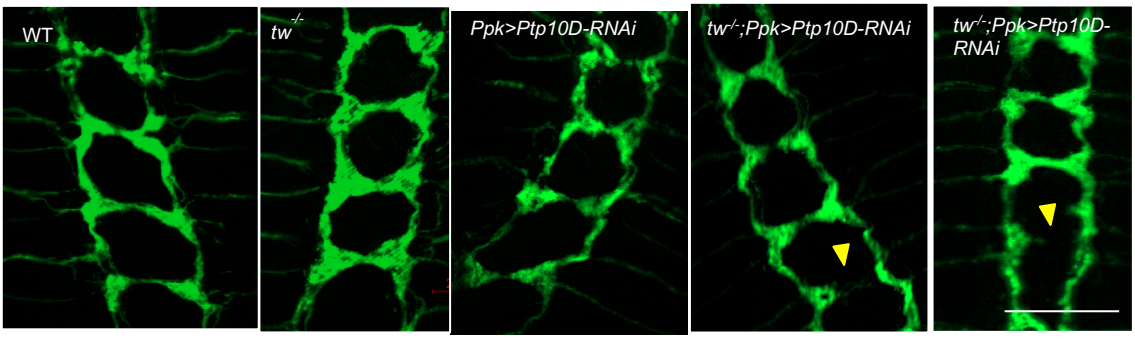

F

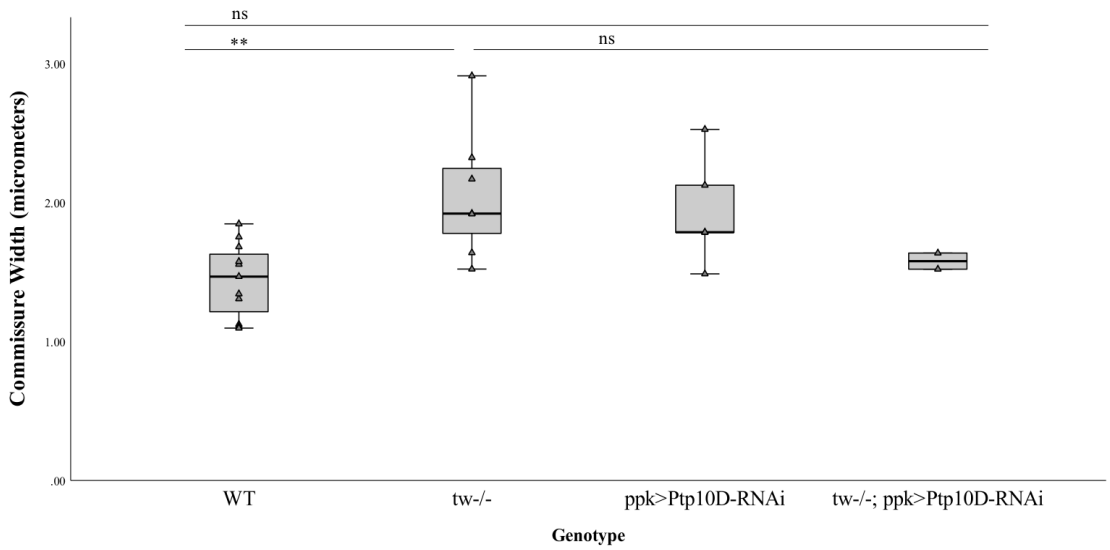

G

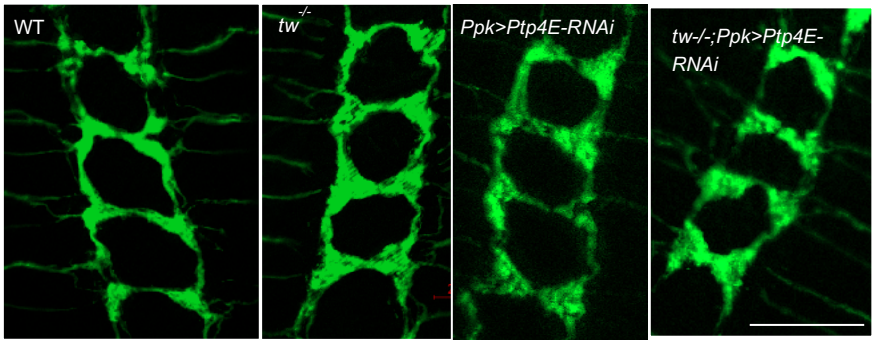

Figure 21. Continued.

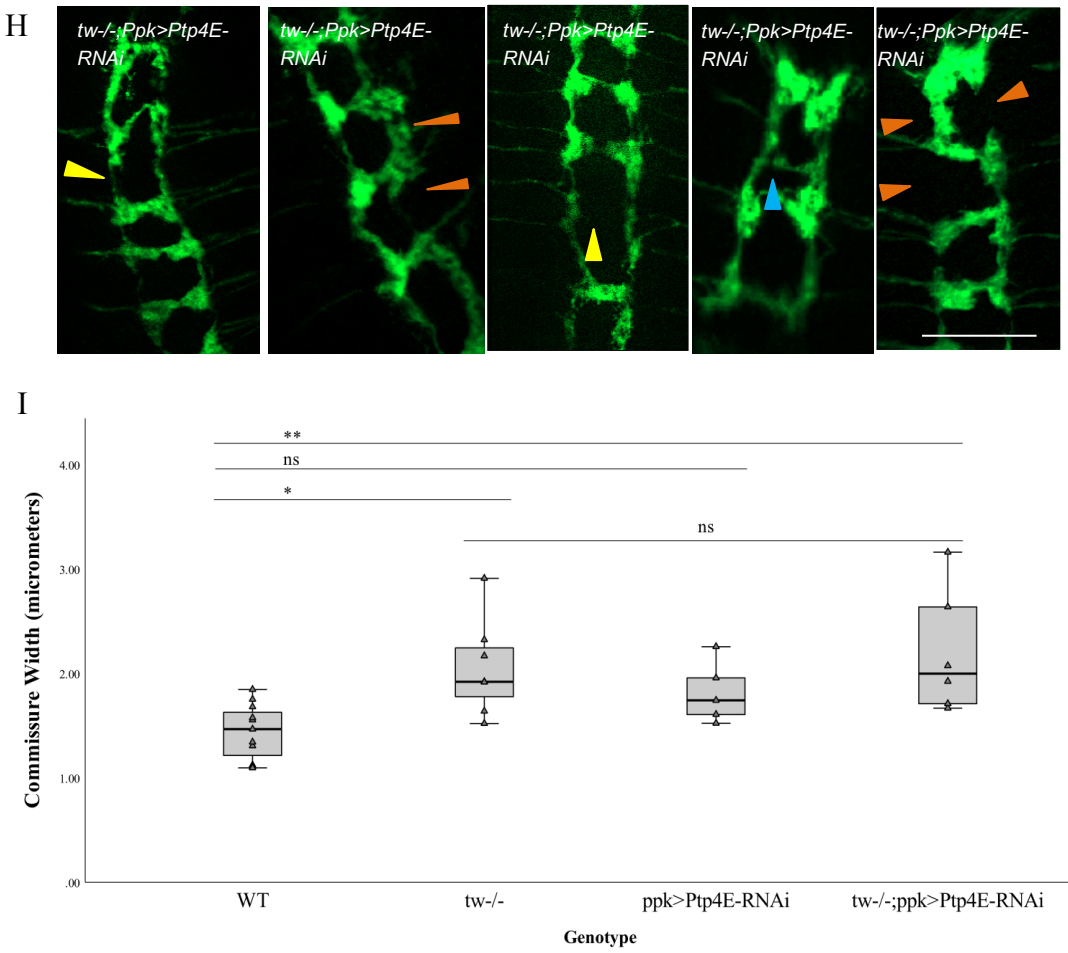

Figure 21. Continued.

RPTP69D is O-mannosylated by POMT1/2

To further elucidate the relationship between PTPs and POMTs, I tested the possibility that RPTPs can be direct molecular targets of POMT-mediated O-mannosylation. I cloned the extracellular domain of RPTP69D tagged with a 3XFlag tag (Ex69D), in a fly expression vector for expression and purification approaches to isolate RPTP69D for mass spectrometry analyses. I selected RPTP69D as a potential candidate due to (i) the fact that its downregulation phenocopies POMT1/2 defects (Fig. 19D&E), (ii) genetic

interactions with POMT1/2 in regulating Class IV axon connectivity (Fig. 19F&G) and producing adult abdominal rotation (R. Baker, D. Lyalin, unpublished data obtained in the lab). I introduced the expression construct Ex69D into WT, *pomt1/2* mutant and *pomt1/2* overexpression backgrounds in flies and ectopically expressed it in vivo using Gal4-UAS system. I used a ubiquitous driver Actin-Gal4 to drive expression of Ex69D in all cells, purified the protein from adult flies (Fig. 22A), and sent out the purified protein to Dr. Wells laboratory (UGA, Athens, GA) for mass spectrometric analyses. These experiments revealed that RPTP69D is O-mannosylated on several Ser/Thr sites across the extracellular domain(Fig. 22B,C&D). All O-mannose were single, not extended as is expected in *Drosophila.* The extracellular domain was also found to be extensively N-glycosylated on Asn residues. Interestingly, the O-mannose sites are majorly concentrated towards the membrane proximal region (MPR). The MPR harbors a cleavage site which separates the protein into two halves after proteolytic processing. The O-mannose sites were similar in WT and *pomt1/2* overexpression, with an additional O-mannosylated residue (T515) in *pomt1/2* overexpression (Table 1). The Ex69D-3FLAG protein purified from *pomt1/2* mutants did not have any O-mannose modifications suggesting that the O-mannose is added to PTP69D by POMT1/2. The absence of O-mannosylated peptides from mass spectra was not due to low protein coverage (Table 2) or insufficient amount of material purified from POMT1/2 mutants. This conclusion was further supported by the observation that PTP69D was similarly N-glycosylated in all three genetic backgrounds that were analyzed.

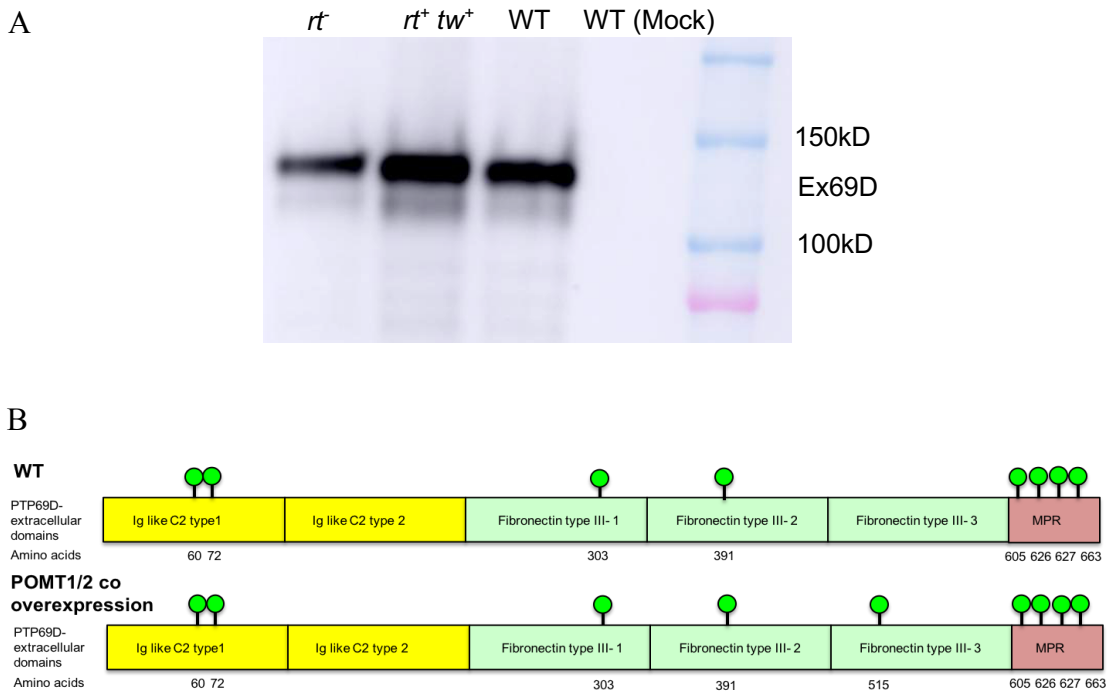

Figure 22. RPTP69D is O-mannosylated by POMT1/2. A, Western blot showing the expression of tagged extracellular domain of RPTP69D-3Flag (110 kD) from WT, POMT1/2 overexpression and mutant adult flies. Mock sample included only anti-Flag beads. **B,** Schematic showing the O-mannose (green circles) sites mapped to the extracellular domain. MPR indicates membrane proximal regions, note T515 only in POMT1/2 overexpression. No O-mannose was found on Ex69D purified from POMT1/2 mutant. **C,** Representative MS^2 and MS^3 (**D**) peaks indicating O-mannosylation on Ser626. Red arrows indicate neutral loss of O-mannose. *rt*-, ActGal4/+;UAS-Ex69D,rt^P/rt^2 ; *rt*+,*tw*+, ActGal4/UAS-Rt,tw;UAS-Ex69D/+; WT, ActGal4/+;UAS-Ex69D/+

C

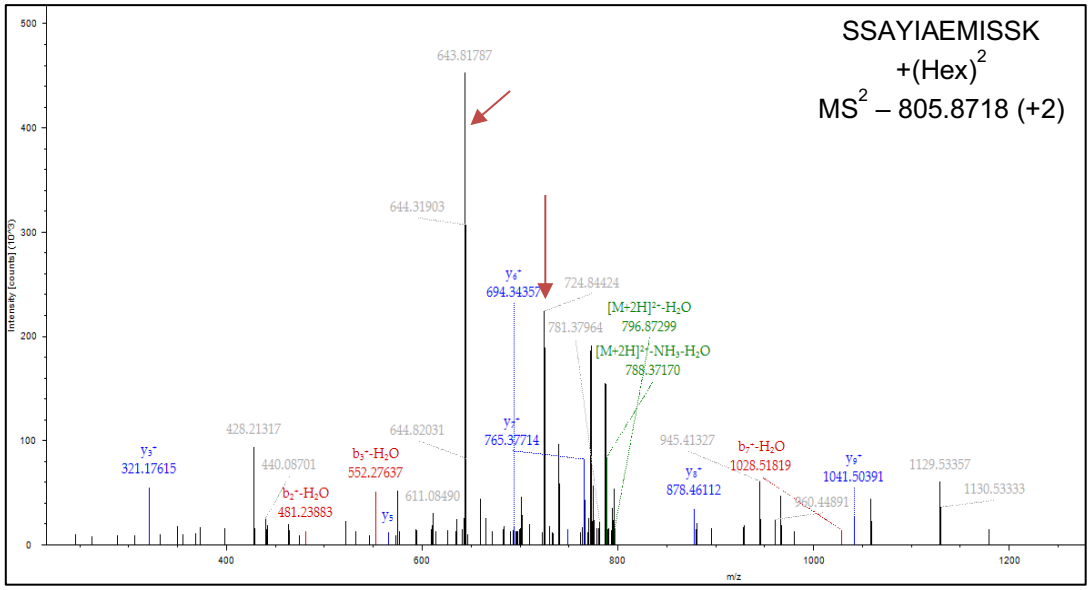

D

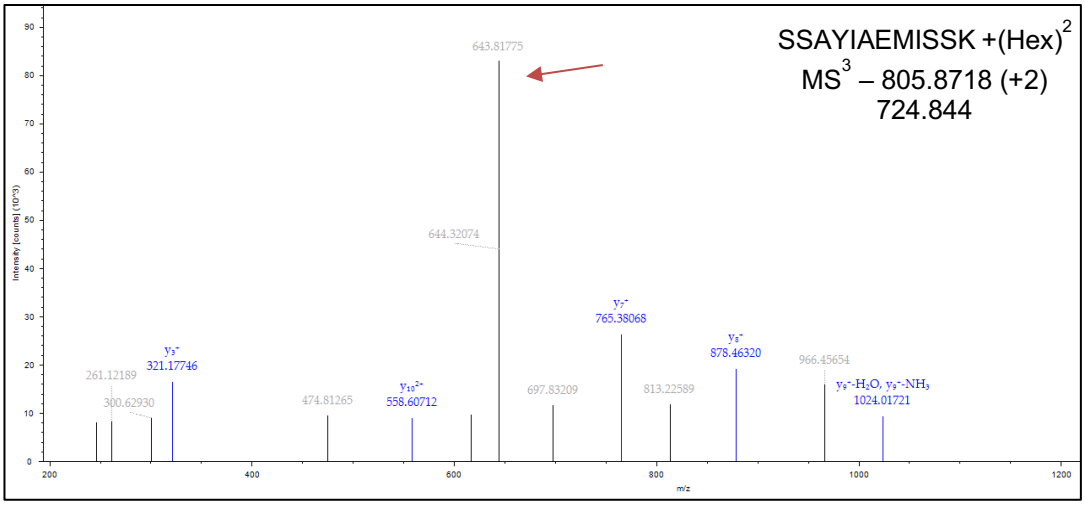

Figure 22. Continued.

WT			POMT1/2 overexpression		
O-linked sites	**Protein sequence**	**Precursor mass accuracy**	**O-linked sites**	**Protein sequence**	**Precursor mass accuracy**
T60	LGNQTINK	16.71 PPM	T60	LGNQTINK	16.71 PPM
T72	TEPLK	5.93 PPM	T72	TEPLK	5.93 PPM
T303	PNTTYFLR	5.93 PPM	T303	PNTTYFLR	5.93 PPM
S391	VIEEAIYQQNSR	2.42 PPM	S391	VIEEAIYQQNSR	2.42 PPM
T605	LNIATYQEVHSDNVTR	2.95 PPM	T605	LNIATYQEVHSDNVTR	2.95 PPM
T663	CLEGTPFLR	2.22 PPM	T663	CLEGTPFLR	2.22 PPM
S626/627	SSAYIAEMISSK	3.02 PPM	T515	TLYESVSPNTNYTVTVSAITR	-4.66 PPM
			S626/627	SSAYIAEMISSK	3.02 PPM

Table 1. O-mannose sites on RPTP69D. Mass spectrometry reveals the Ser/Thr residues potentially O-mannosylated from WT and *pomt1/2* overexpression background. Note that T515 and S626/627 are O-mannosylated only in *pomt1/2* overexpression. Red denotes the O-mannosylated residues in the sequence.

	Coverage	|log prob|	PSMs	Uniq Peps	Modified Peps
WT 1	375.72	423	69	31	65.6
WT 2	526.3	773	85	50	70.6
OE 1	407.31	442	75	41	61.7
OE 2	545.35	743	90	53	63.3
Mutant	466.93	622	71	36	67.1

Table 2. Protein coverage for all indicated samples of Ex69D. Protein metrics for all samples is shown. WT1, 2 and OE 1, 2 indicate biological replicates of Ex69D from WT and POMT1/2 overexpression. Coverage indicates the percentage of the protein sequence covered by identified peptides. PSM's indicate the number of peptide spectrum matches. The number of PSM's is the total number of identified peptide spectra matched for the protein. The PSM value may be higher than the number of peptides identified for high-scoring proteins because peptides may be identified repeatedly. Unique Peptides (Uniq Peps) are the number of peptide sequences that are unique to a protein group. These are the peptides that are common to the proteins of a protein group, and which do not occur in the proteins of any other group.

POMT1/2 potentially protect RPTP69D from proteolysis

Single O-mannose in yeast is known to be required for chaperone binding and prevent aggregation of the protein in the ER(38). Aggregated protein is unable to exit the secretory pathway and hence localize properly, gets stuck in the ER and is directed for degradation. To probe the effect of O-mannosylation on RPTP69D localization, I studied how endogenous RPTP69D localizes in *pomt1/2* mutants. I used anti-PTP69D antibodies to detect it in the axons of ventral nerve cord. Although a complex expression pattern was seen, I did not detect any obvious problems in its localization in axons (Fig. 23A). Next, I decided to stress the system by overexpressing *Rptp69D* in Class IV axons in *pomt1/2* mutants and study any effect of O-mannosylation on localization of an increased amount of PTP69D protein. I again did not observe any defect in localization of overexpressed PTP69D in *pomt1/2* mutants (Fig. 23B). These results indicate that O-mannosylation is not crucial for localization of RPTP69D.

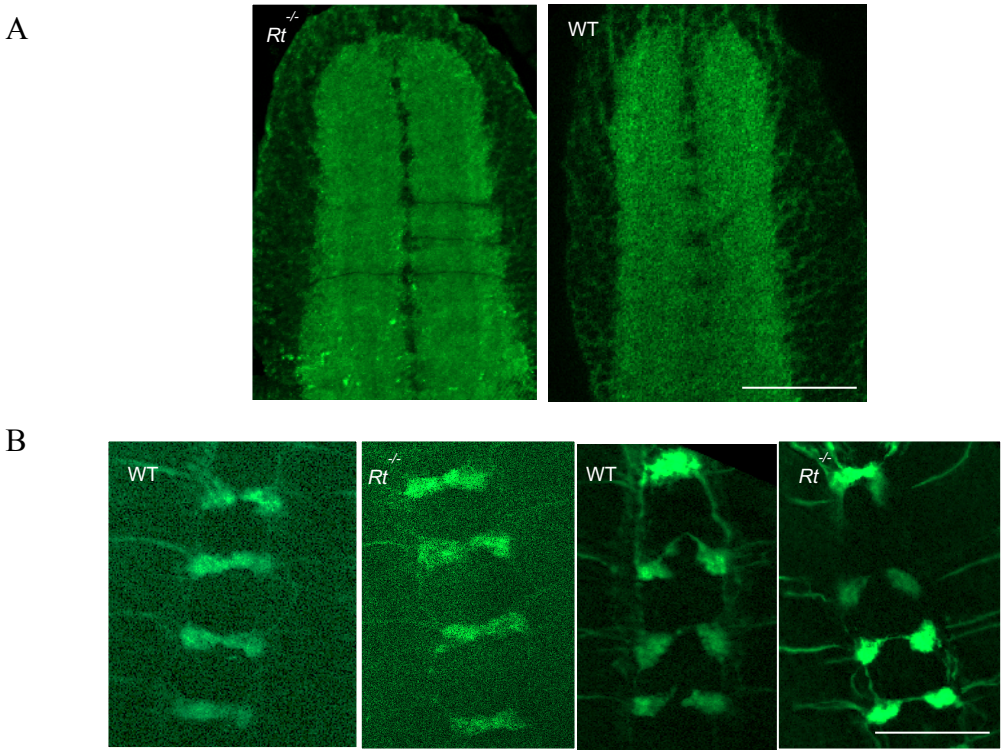

Figure 23. POMT1/2 do not affect localization of RPTP69D. A, Endogenous localization of Ptp69D (green) in the neuropil of 1st instar brain, immunostained with anti-ptp69D antibody (3F11). **B**, Overexpressed RPTP69D-Myc (green), localizes properly in the Class IV axons of 3rd instar brains, immunostained with anti-Myc antibodies. Scale bar is 20μm, posterior is up in all images. WT, wildtype; $Rt^{-/-}$, rt^2/rt^2 in (A) and rt^2/rt^Pin (B).

O-glycosylation has been shown to regulate cleavage of proteins and peptides(129-131). Since RPTP69D extracellular domain is cleaved at a membrane proximal site(132) and O-mannose seems to concentrate in the MPR, I decided to test if O-mannosylation has an effect on this juxtamembrane cleavage. To this end, I prepared lysates of overexpressed Ptp69D from WT and *pomt1/2* mutants and probed it with anti-PTP69D antibody (3F11), specific to the MPR of the extracellular domain. Proteolytic processing of RPTP69D generates 2 cleaved products, one extracellular half of 110kD and another

intracellular half of 90kD (Fig. 24A). To my surprise, I did not detect any obvious problems with regards to cleavage as the extracellular domain ran as a cleaved 110kD product on SDS-PAGE in both mutants and WT. However, a small fraction of RPTP69D (200kD) that does not get proteolytically processed appears to be smaller in *pomt1/2* mutants (Fig. 24B). This suggests that POMT1/2 may protect the unprocessed, full length form from unnecessary proteolysis. Whether this unnecessary proteolysis occurs at the C-terminal or N-terminal of the full length RPTP69D remains to be seen. The functional relevance of the RPTP69D cleavage and the unprocessed form is currently unknown, but that phenomenon likely reflects an additional level of RPTP regulation. Further studies will need to explore this novel hypothesis.

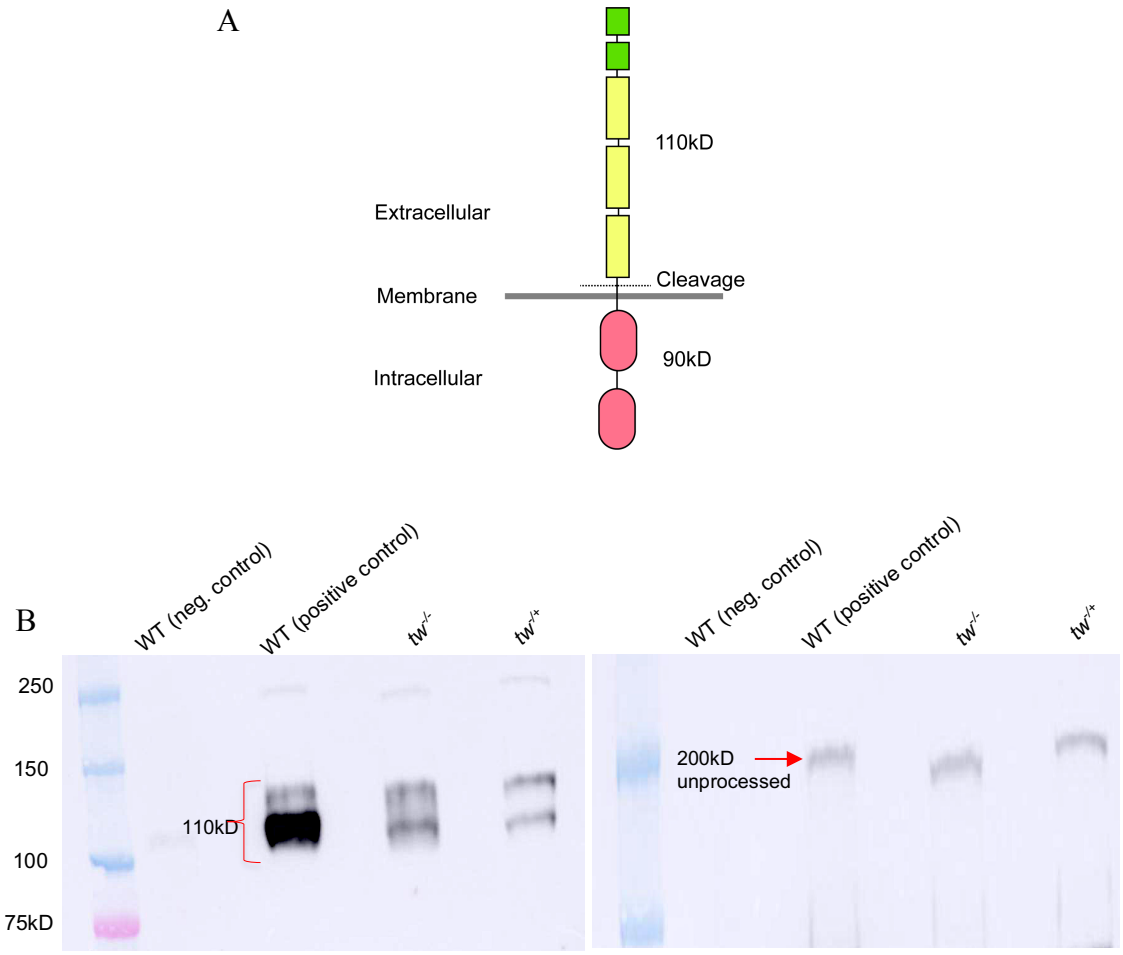

Figure 24. POMT1/2 protect RPTP69D from proteolysis. A, Schematic showing the two cleaved halves generated after proteolytic processing. **B,** The cleaved extracellular domain is shown at 110kD, two bands are likely different glycosylated forms in all lanes. The full length unprocessed forms runs at ~ 250kD and is notably smaller in POMT mutant (3rd lane, *tw*$^{-/-}$). Anti-ptp69D antibody (3F11) is used to probe the extracellular domain in all lanes. WT (negative control), Canton-S; WT(positive control), ActGal4/+;Ptp69D-Myc/+; *tw*$^{-/-}$, tw^{1}/Y;G14-Gal4/+;Ptp69D-Myc/+. *tw*$^{-/+}$, tw^{1}/+;G14-gal4/+;Ptp69D-Myc/+.

Discussion

Most studies on O-mannosylation substrates have focused on identifying modified proteins without any details on the functional relevance of the sugar on them(7, 13, 14, 16, 35). Here, I report a novel substrate of POMT1/2, along with mechanistic insight into how O-mannose might affect the function of RPTP69D. I demonstrate that POMT1/2 show synergistic, genetic interactions with *rptps*, in regulating the morphology of Class IV axons. I also demonstrate that RPTP69D phenocopies POMT1/2 in the effect on Class IV sensory axon wiring in the ventral ganglion. My experiments further demonstrate that RPTP69D is indeed O-mannosylated by POMT1/2 on its extracellular domain. I also explore the possibility of O-mannose affecting the localization of RPTP69D to the axon membrane under normal or stressed circumstances, and demonstrate that O-mannosylation might not be crucial for its localization. I further found that the full length, unprocessed RPTP69D, in *pomt1/2* mutants, is truncated at its N or C terminal, suggesting that O-mannosylation may be involved in a proteolysis-protection mechanism.

Several lines of evidence support the conclusions of my studies. First, single O-glycosylation has recently emerged as a major regulator of proteolytic processing. Proteolytic processing is an essential and ubiquitous post translational modification affecting secreted proteins and failure to regulate this process often leads to diseases(129). Second, RPTP69D is a Type IIa RPTP and there is massive evidence for proteolytic processing of Type IIa RPTPs at a membrane proximal site(133, 134). Third, RPTP69D was identified as a regulator of mediolateral positioning of Class IV axons in

a forward genetic screen, a defect similar to *pomt1/2* (92, 96), indicating they function in the same pathway. Lastly, a different type of mammalian RPTP was shown to be O-mannosylated in neurons and glia, however the enzymes responsible for this O-mannosylation remain unknown(31, 69).

RPTPs (receptor protein tyrosine phosphatases) are important mediators of signal transduction at the plasma membrane featuring in events as diverse as cell growth and proliferation (tumor suppressors), neural development (axon guidance molecules) and the immune response(135). While the structure of the cytoplasmic, catalytic domains of RPTPs is conserved across RPTP subfamilies, the extracellular domains are highly divergent, consisting of a wide variety of different structural domains. Based on extracellular domain organization, RPTPs are classified into 7 types(136). Here, I focus on RPTP69D that belongs to the Type IIa subfamily of RPTPs. The type IIa RPTPs are the best characterized family of RPTPs that are classified as cell adhesion molecule(CAM)-like proteins as they contain Immunoglubulin (Ig) domains similar to CAMs. In general, most RPTP family members are still classified as orphan receptors, with no extracellular ligands known to date. The type IIa RPTPs are, however, remarkable in that a large collection of protein ligands have been proposed to interact with them, particularly in the context of the nervous system(135).

The type IIa RPTP family members share a common domain architecture: an extracellular domain containing upto 3 Ig domains and upto 9 fibronectin domains, a single transmembrane helix and tandem intracellular phosphatase domains. *Drosophila* has 2 type IIa RPTPs, DLAR and PTP69D and vertebrates have 3 (RPTPσ, RPTPδ,

LAR). These receptors are produced as proproteins and processed intracellularly, at a dibasic amino acid site, by a subtilisin like endoprotease and subsequently expressed on the cell surface as 2 noncovalently bonded subunits(133, 134). However, there is a small fraction that is not processed in this manner, indicating diverse forms of type IIa RPTPs exist in the cell. Variations of type IIa RPTPs are also generated by alternative splicing, in particular within the extracellular domain which yields multiple isoforms(137, 138). This indicates several levels of complexity that exist to produce various forms of RPTPs with possibly different functions. It is attractive to speculate that O-mannosylation might fine tune the process of proteolysis of type IIa RPTPs. The decreased size of full-length RPTP69D in POMT mutants suggests that the loss of O-mannosylation makes the RPTP69D protein sensitive to cleavage by some proteases. This proteolysis most likely occurs at the N terminus, in the Ig-1 domain, 30-35 amino acids after the signal peptide. Since, RPTP69D is able to exit the ER, the signal peptide cleavage is not affected in POMT1/2 mutants.

The Ig-1 domain is extremely important for ligand binding to type IIa RPTPs(139, 140). Ig 1-2 domains form a V-shaped structure to effectively bind ligands such as HSPGs (Heparan sulphate proteoglycans) and CSPGs (chondroitin sulphate proteoglycans), the function that appears to be conserved in *Drosophila* (135). Proteoglycans are extracellular matrix components composed of a core protein module to which a variable number of glycosaminoglycan (GAG) chains are covalently attached(141). GAGs are linear polymers of repeating disaccharide units(141). Further GAG diversity is generated by sulphation at defined positions, giving HSPGs and CSPGs a strong negative

charge(141). Ig-1 β strands contain basic amino acids that create an extended positively charged surface required for ligand binding. Specifically, 4 Lysine residues, K67, K68, K70, K71 and 2 arginine residues, R96 and R99, make up the positively charged surface in PTPσ(140). Similar positive charged surface has been demonstrated for DLAR (*Drosophila* LAR)(140).

RPTP69D also contains lysine and arginine residues, K63, R67, K69 and R71, on the Ig-1 domain that might make up for a similar positively charged surface essential for ligand binding. More importantly, closely placed basic residues also act as a site for proteolytic cleavage by endoproteases. Interestingly, O-mannose is located on T60 and T72, around the basic amino acids. Also, the juxtamembrane cleavage site for RPTP69D located in the MPR (membrane proximal region) is predicted to be RDKR(121) and O-mannose is concentrated around this basic site as well. Therefore, I hypothesize that proteases target the N- terminal region at the Ig-1 domain basic surface in the absence of O-mannose, leading to a loss of the positively charged surface and hence ligand binding. Further studies will be needed to test this theory. However, why do the proteases not inadvertently cleave the MPR basic site of unprocessed RPTP69D, in absence of O-mannose, is an outstanding question. The differences in structure of the 2 regions (Ig domain and MPR) might have something to do with it. Although conceivable, it is unlikely that the truncation in *pomt1/2* mutants occurs at the intracellular C-terminus. No predicted proteolytic sites are present in the second phosphatase domain located at the C-terminus, and it is unclear how the O-mannose on the other side of the membrane could affect that hypothetical processing. Nevertheless, my study provides evidence that O-

mannosylation might underlie an additional level of fine tuning to produce different isoforms of RPTP69D.

The functional relevance of proteolytic processing at MPR is yet to be elucidated, however an appealing model proposes that binding and release of associated extracellular domains may help regulate adhesivity of certain cell-cell contacts(136). It might help in decoupling the phosphatase activity from regulation via ligand binding to Ig domains and it might help the released RPTP fragment to compete with the remaining intact receptors for binding to extracellular ligands(135).

Here, I have shown that RPTP69D is O-mannosylated, however, I do not rule out the possibility that other RPTPs might also be O-mannosylated and may regulate Class IV axon morphology, especially the ones that show genetic interactions (Ptp99A,Ptp52f, Lar). Ptp10D and Ptp4E also seem to be quite important for regulating Class IV axon morphology, however their phenotypes are quite different from POMT1/2 associated defects. Further studies are needed to carefully analyze the importance of O-mannosylation on the other RPTPs.

CHAPTER IV

LIVE IMAGING AND ANALYSIS OF MUSCLE CONTRACTIONS IN *DROSOPHILA* EMBRYO*

Introduction

Peristaltic muscle contraction is a rhythmic motor behavior similar to walking and swimming in humans (94, 95, 142). Embryonic muscle contractions seen in *Drosophila* late stage embryos represent an example of such a behavior. *Drosophila* is an excellent model organism to study various developmental processes because embryonic development in *Drosophila* is well characterized, relatively short and easy to monitor. The overall goal of our method is to carefully record and analyze the wave like pattern of contraction and relaxation of embryonic muscles. We used a simple, non-invasive approach that offers a detailed visualization, recording and analysis of muscle contractions. This method can also be potentially used to study other *in vivo* processes, such as embryonic rolling seen in late stage embryos just prior to hatching. In previous studies, embryonic muscle contractions were mostly analyzed in terms of frequency and direction(95, 142). In order to estimate the relative extent of contractions as they progress along the body axis in the anterior or posterior direction, we have used embryos expressing GFP specifically in muscles. This analysis provides a more quantitative way

* Portions of this chapter are reprinted with kind permission from: Chandel, I., Baker, R., Nakamura, N., Panin, V. Live imaging and analysis of muscle contractions in *Drosophila* embryo. *J. Vis. Exp* (149), 2019.

to analyze muscle contractions and to reveal how body posture in embryos is maintained during series of peristaltic waves of muscle contractions.

Peristaltic muscle contractions are controlled by central pattern generator (CPG) circuits and communications between neurons of the peripheral nervous system (PNS), the central nervous system (CNS), and muscles(105, 143). Failure to produce normal peristaltic muscle contractions can lead to defects such as failure to hatch(142), abnormal larval locomotion(104) and can be indicative of neurological abnormalities. Live imaging of peristaltic waves of muscle contraction and detailed analysis of contraction phenotypes can help uncover pathogenic mechanisms associated with genetic defects affecting muscles and neural circuits involved in locomotion. We recently used that approach to investigate mechanisms that result in body posture torsion phenotype of ***p***rotein ***O m***annosyl***t***ransferase (POMT) mutants(96).

Protein O-mannosylation (POM) is a special type of posttranslational modification, where a mannose sugar is added to serine or threonine residues of secretory pathway proteins(74, 144). Genetic defects in POM cause congenital muscular dystrophies (CMD) in humans(6, 44, 145). We investigated the causative mechanisms of these diseases using *Drosophila* as a model system. We found that embryos with mutations in *Drosophila* protein O-mannosyltransferase genes *POMT1* and *POMT2* (a.k.a. rotated abdomen *(rt*) and twisted (*tw*) show a displacement ("rotation") of body segments, which results in an abnormal body posture(96). Interestingly, this defect coincided with the developmental stage when peristaltic muscle contractions become prominent(96).

Since abnormal body posture in POM mutant embryos arises when musculature and epidermis are already formed and peristaltic waves of coordinated muscle contractions have started, we hypothesized that abnormal body posture could be a result of abnormal muscle contractions rather than a defect in muscle or/and epidermis morphology(96). CMDs can be associated with abnormal muscle contractions and posture defects(115), and thus the analysis of the posture phenotype in *Drosophila POMT* mutants may elucidate pathological mechanisms associated with muscular dystrophies. In order to investigate the relationship between the body posture phenotype of *Drosophila POMT* mutants and possible abnormalities in peristaltic waves of muscle contractions, we decided to analyze muscle contractions in detail using a live imaging approach.

Our analysis of peristaltic contraction waves in *Drosophila* embryos revealed two distinct contraction modes, designated as type 1 and type 2 waves. Type 1 wave is a simple wave propagating from anterior to posterior or vice versa. Type 2 wave is a biphasic wave that initiates at the anterior end, propagates halfway in posterior direction, momentarily halts, forming a temporal static contraction, and then, during its second phase, is swept by a peristaltic contraction that propagates forward from the posterior end. Wild-type embryos normally generate a serious of contractions that consists of approximately 75% type 1 and 25% type 2 waves. In contrast, *POMT* mutant embryos generate type 1 and type 2 waves at approximately equal relative frequencies.

Our approach can provide detailed information for quantitative analysis of muscle contractions and embryo rolling(96). This approach could be also adapted for analyses of other behaviors involving muscle contractions, such as hatching and crawling.

Protocol for live imaging and analysis of muscle contractions in *Drosophila* embryo

1. Collection of late stage embryos

1.1 Prepare a fly cage by making approximately 50 holes in a 100 mL capacity tri-corner plastic beaker using a hot 25 gauge needle.

1.2 Prepare 60 mm X 15mm Petri dishes with apple juice-agar (3% agar and 30% apple juice).

1.3 Prepare fresh yeast paste by mixing dry yeast granules and water. Spread the yeast paste onto the apple agar plates to increase egg laying.

1.4 Anaesthetize about 50–60 flies (use approximately equal numbers of males and females) on CO_2 and put them in the fly cage. Note: Using increased proportion of females (up to ~2:1 ratio of females: males) may help increase amount of laid eggs for some genotypes.

1.5 Attach an apple juice-agar Petri dish with yeast paste to the fly cage tightly and seal it with modeling clay. Make sure it is sealed at all corners.

1.6 Wait until flies wake up from anesthesia and then invert the cage such that the Petri dish is now at the bottom. Put the cage into an incubator with controlled temperature (25 ^{o}C) and humidity (60%).

1.7 Allow flies to lay eggs for 2–3 hours, replace the apple plate with a fresh one, and let the plate with eggs age for 19–20 hours in an incubator.

Note: Prior to the above step, flies must be synchronized to facilitate collection of stage 17e-f (19–21 hrs AEL) embryos. This can be achieved by transferring flies to a cage with a fresh yeast apple juice-agar plate 3–4 times for 12 hours (once every 3–4 hours).

Keeping flies at controlled circadian light environment (LD cycle) can also help with collecting a synchronized population of embryos, but this was not essential in our experiments.

2. Collection of Embryos

2.1 Carefully pick embryos with a wet paintbrush and place them in a collecting glass dish filled with 1X PBS.

2.2 Select the embryos that have their tracheae filled with air. Air-filled tracheae indicate that embryos reached Stage 17, and their peristaltic muscle contractions should have begun. Tracheae become clearly visible when they are filled with air, which can serve as a marker for Stage 17.

2.3 Place an apple juice agar slab on a glass slide and carefully transfer embryos from PBS to the slab. Line up the embryos with their ventral side up.

Note: Dorsal and ventral sides of embryos can be distinguished by the position of dorsal appendages on the eggshell.

2.4 Make a rectangular wax boundary on another glass slide using a wax pen.

2.5 Place a double-sided sticky tape within that boundary and gently pick up the embryos by lowering this slide on the agar slab. Apply gentle pressure to ensure that embryos stick to the tape well, with their dorsal side up. If necessary, embryos still can be rolled on the tape to correct their orientation. Do all manipulations while monitoring embryos under a dissection microscope.

2.6 Cover embryos with 1X PBS for live imaging of muscle contractions.

Note: Some procedures described above are related to basic *Drosophila* techniques used in many studies. More detailed description of common *Drosophila* techniques can be found elsewhere(146).

3. Recording of embryos

3.1 Perform live imaging of mounted embryos on an epifluorescence microscope with a time lapse function and a digital camera with suitable emission filters using a 10X water immersion objective lens.

Note: Here we used embryos expressing GFP in muscles. Other fluorescent markers with suitable excitation light and emission filter sets can also be used (e.g., for tdTomato detection, one can use Chroma ET-561 filter set for excitation and emission around optimal 554 nm and 581 nm, respectively).

3.2 Perform live video recording of embryos using a suitable software for about 1–2 hours with an acquisition rate of 4 frames/s.

Note: To analyze rolling of the developing embryo within its shell, embryos without expression of fluorescent markers can be used. To this end, regular transmitted light illumination without spectral filters is applied to visualize embryo motion within the shell.

4. Analysis of the recordings

4.1 Export the recorded video directly into Image J for further analyses (e.g. as AVI files).

4.2 In ImageJ, crop the video recordings to the size of individual embryos by drawing a box around each embryo and then clicking on “Image” -> “Crop”. This greatly reduces the size of video files without affecting its resolution and facilitates their analysis.

4.3 Rotate cropped images to achieve vertical position of the embryo midline relative to the screen, by clicking on “image → “transform” → “rotate”.

Note: Selecting “preview” during this process will provide guidance for rotation, showing gridlines to ensure vertical position of the midline.

4a. Quantitative analysis of embryo rolling

Note: For distance analyses, first confirm that your images include scale information. Image scale can be added by selecting “Analyze” → “Set Scale”, and then entering a conversion of pixels to distances, e.g., micrometers.

1. Mark the position of one or both tracheae in the first frame of the video at a point midway between posterior and anterior ends. Click on “Analyze” → “Tools” → “ROI manager” and record this position as “slice number-y coordinate-x coordinate” by drawing a box of approx. 7.7 μm (width x height) around it and, typing “t” on the keyboard. Ensure that when typing “t” a region of interest is selected on the video. Alternatively, select the “Add (t)” tab on the ROI manager to record the position of trachea instead of type command because the type commands only work for videos in grayscale.

Note: The region of interest can vary in shape or size depending on the embryonic region or developmental event being studied.

2. Mark the position of the same area of the trachea after peristaltic contractions of interest. Measure the distance from the pre-contraction position to the post-contraction position by drawing a line connecting the centers of each box and typing “m” on the keyboard.

3. Correlate the distance and direction of each rolling event with the direction of muscle contraction propagation in at least 8 embryos for statistically significant differences.

4b. Quantitative analysis of embryonic muscle contractions

1. Use embryos expressing fluorescent markers in muscles (e.g., we used transgenic flies expressing a fusion construct of Myosin Heavy Chain promoter and GFP called MHC-GFP(143)) to analyze muscle contraction parameters such as contraction amplitude.

2. Use the recording of fluorescent readout and draw a region of interest (e.g., a box of ~15×45μm H x W) centered on the muscles (which are clearly visible due to the presence of fluorescent marker) of particular body segments and, select “Add (t)” tab on the ROI manager to record the position of the ROI. Click on “ROI manager” → “Measure” to record the average fluorescent intensity of each region of interest selected.

3. Move the box to other body segments of interest and click on “Add (t)” in the ROI manager to record their positions. This will give regions of interest of identical size in all body segments to be analyzed. Select ROI in at least one posterior, one medial, and one anterior segment, e.g., A7, A4, and T2, respectively.

4. In the ROI manager, select all regions of interest recorded as “slice number-y coordinate-x coordinate” (e.g., by selecting while holding “ctrl”) and click on “More” → “Multi measure” to measure the mean fluorescent intensity of each region of interest for

all frames of the video, and report each measurement in a table. Each region of interest is a column of the table, and each frame is a row. Transfer the table for further analyses to Excel or another spreadsheet program.

5. Plot a graph with frame number on the x-axis and mean fluorescent intensity on the y-axis. Frame number can be converted to time using the frame rate of the video (e.g., 4 frames/s, Fig 25a.).

6. Determine muscle contraction amplitude by estimating the increase in normalized GFP fluorescence intensity relative to the baseline. Muscle contractions increase the GFP intensity as they bring more GFP into the vicinity of the focal area as more muscles get pulled in during these contractions(96). Establish a baseline fluorescence as the average intensity between contraction waves. Normalize GFP intensity to the baseline by dividing every ROI intensity value by the baseline intensity.

Note: (1) Each profile has a different baseline fluorescence, as there may be different GFP expression levels in different muscle segments. (2) One potential complication is that the GFP fluorescence may change over time due to photo bleaching. This can be resolved by monitoring changes in fluorescence baseline and using a sufficient sample size for wave analyses (we normally use sets of 10 fluorescent waves and confirm that the baseline is approximately constant by taking an average of only those peak minima as baseline that have decreased in fluorescence by 10% or less relative to the initial minima peak.). A pulse-LED illumination may be also applied to mitigate that problem(147).

7. Compare muscle contractions on left and right sides of the embryo by analyzing peak intensities on both sides of the embryo for same segments. Use contraction amplitude and time of peak intensities to conclude on differences in extent and timing of peristaltic muscle contraction waves propagating along both sides of the embryo.

8. Compare normalized intensity of GFP at different segments (e.g., at anterior, medial and posterior regions) during muscle contraction wave propagation to examine changes in the contraction as the wave propagates. This analysis also determines the direction of the wave, that is whether it propagates toward anterior or posterior regions of the embryo.

Results

We have developed a live imaging approach for quantitative analyses of peristaltic waves of muscle contractions in Drosophila embryos. Our analysis of pattern of muscle contractions uncovered two main types of muscle contractions. We designated a peristaltic contraction as a type 1 wave if its profile has a peak that arises at the posterior region first, followed by peaks at middle and anterior regions (forward wave) or a profile in which the peak first arises at anterior segments and then propagates toward posterior regions (backward wave) (Fig. 26a). We also observed another type of waves that we designated as Type 2. Type 2 wave starts at one end of the embryo, proceeds toward the middle regions, and then returns to its origin as a sweeping wave re-initiated at the opposite end (Fig. 26b). *POMT* mutant embryos show abnormal relative frequency of

type 1/ type 2 wave generation (Fig. 27), which results in body posture abnormality, the body torsion (or “rotation”) phenotype (Fig. 28).

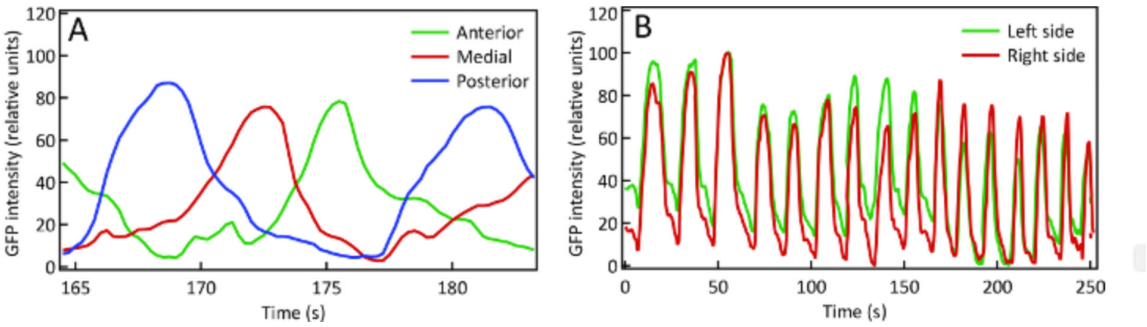

Figure 25. Muscle contraction amplitude. A, Muscle contraction amplitude monitored over time as normalized GFP intensity at different embryo segments (anterior, middle and posterior) peaks during 165–178 s time period (arbitrary time axis) represent a simple forward wave (type 1). GFP intensity is plotted against (Y- axis) time (X-axis) for different body segments of the embryo. **B,** There is no difference in the amplitude (depicted as GFP intensity) and time of muscle contractions on right and left sides of the embryo. GFP intensity (Y- axis) plotted against time for left and right sides of the same segment of a contracting embryo. Frame rate is 4 frames/sec for both graphs.

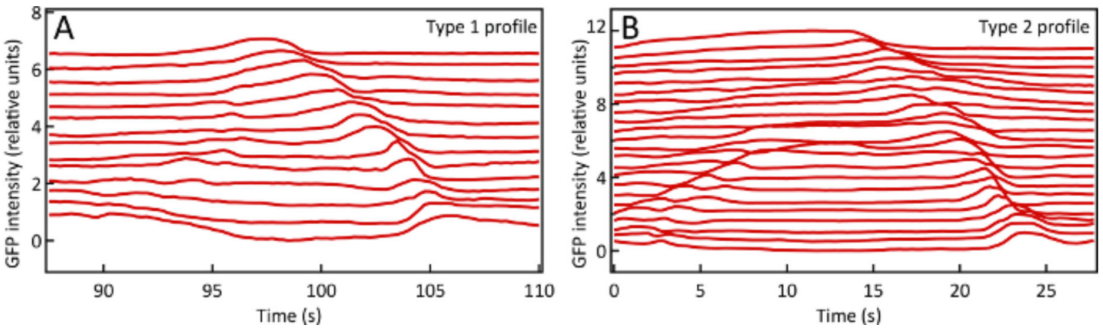

Figure 26. Type 1 and Type 2 peristaltic muscle contraction wave profiles. Type 1 (panel A) and Type 2 (panel B) muscle contraction profiles generated using GFP intensity as a measure of contraction amplitude. **A**, Type 1 wave profile in which individual lines represent normalized GFP intensities of particular body segments over time, while the peaks indicate contraction events. Type 1 wave is a single wave generated at the anterior or posterior end of the embryo that continues propagation towards the opposite end. **B**, Type 2 wave profile that shows an example of a biphasic contraction wave, plotted in the same way as in A. In Type 2 waves, the wave propagates to the middle of the embryo during the first phase and then returns to the origin as a peristaltic contraction reinitiated at the opposite end. Each wave line represents normalized GFP intensity detected in successive body segments of an embryo, and peaks correspond to muscle contraction. Slant appearance of the peaks illustrates that muscle contractions propagate along successive segments, from anterior to posterior, or vice versa, and thus peaks occur in a consecutive manner in successive body segments.

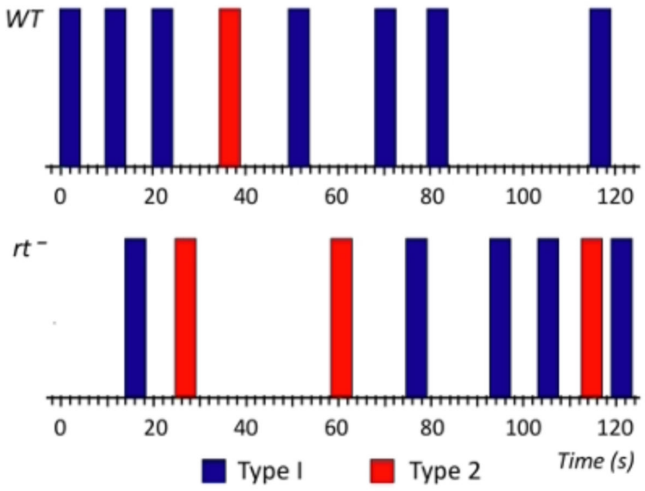

Figure 27. Series of contraction waves generated by wild-type and POMT mutant embryos. Graphs of contraction wave series in WT and POMT mutant embryos. The graphs illustrate that Type 2 contraction waves are generated at increased relative frequency in POMT mutants, as compared to WT embryo. Series of waves in WT embryo (top graph) depicts the contractions. Blue and red bars depict Type 1 and Type 2 waves, respectively.

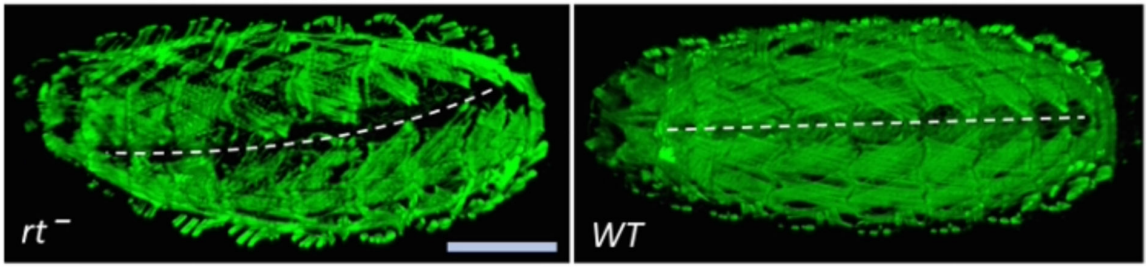

Figure 28. Fixed and stained POMT mutant (*rt*⁻) and WT embryos. Muscles are visualized by staining with fluorescein-conjugated phalloidin to highlight embryo body posture. Curved dashed line (tracing the position of midline) illustrates the body posture phenotype of POMT mutant. Note the rotation in body segments of the POMT mutant embryo, highlighted by a dashed line. Anterior is to the left, dorsal is up. Scale bar is 100 μm. (Image was kindly provided by Dr. Nakamura, (148))

Discussion

Our method provides a quantitative way to analyze important embryo behaviors during development, such as peristaltic muscle contraction waves, including wave periodicity, amplitude and pattern, as well as wave effect on embryo rolling and posture. This can be useful in analyses of different mutants to study the role of specific genes in regulating these and other behaviors during embryonic development. We have used changes in muscle-specific GFP marker intensity to analyze muscle contraction amplitude, frequency and direction of contraction wave propagation in embryos. These changes in GFP signal reflect the extent of contractions, as contracting body segments bring more GFP into an ROI and the vicinity of the focal area. This approach significantly simplifies analyses and gives a better visual representation of the pattern of peristaltic contraction waves.

In our experiments, we used genotypes with muscle-specific transgenic expression of GFP to visualize and study in detail muscle contractions during embryonic development. Other studies used a similar approach to analyze larval motion such as crawling and bending(143, 149). A similar technique to study coordinated muscle contractions was previously applied for sandwich preparation of embryos, which is a more invasive approach that may affect embryo behaviors and development (94). In contrast, our method is completely non-invasive and the embryos are unperturbed during assays. Our protocol doesn't require the embryos to be dechorionated or *devitellinized*, and live embryos of interest can be recovered after assays and propagated for further analyses.

Our method can potentially be developed further for a high content analysis (HCA)-based screening to isolate and analyze mutations that affect embryonic muscle contractions and other behaviors and developmental processes. This strategy, for instance, can be used to simultaneously record muscle contractions of many embryos and for assessing their response to various stimuli, drugs, or environmental changes.

CHAPTER V

SUMMARY AND CONCLUSIONS

My research is focused on understanding the role of O-mannosyl glycans in neural development using *Drosophila* as a model system to help us better understand the pathogenic mechanisms of neurological abnormalities seen in patients with defective O-mannosylation pathway. O-mannosylation is an O-glycosylation where O-mannose is added to Ser/Thr residues of proteins. My focus has been on the canonical O-mannosylation pathway which involves the O-mannosyltransferases POMT1/2. Defects in POMT1/2 cause several congenital muscular dystrophies (CMDs) in humans that are associated with nervous system problems. POMT1/2 dependent O-mannosylation is important for neuronal migration, synapse maintenance and stability, neuronal wiring, cell-extracellular matrix interactions and cell-cell contact.

Recently, a new pathway of O-mannosylation involving the genes TMTC1-4 (**t**ransmembrane O-**m**annosyltransferases **t**argeting **c**adherins 1-4) was discovered(7). They specifically O-mannosylate Ser/Thr residues on cadherins, a type of cell adhesion molecules(7). Another yet unknown O-mannosylation pathway exists that specifically targets plexins, membrane bound or secreted receptors classically expressed on axons. POMT1/2 dependent O-mannosylation is so far studied in detail only on Dystroglycan (DG), in humans and *Drosophila*(30). Both pathways, POMT1/2 and TMTC1-4 are implicated in several diseases in humans such as, Walker-Warburg syndrome (CMD), cobbletstone lissencephaly and hearing loss, respectively(13), indicating the importance of studying O-mannosylation.

Walker Warburg syndrome(WWS) is a severe form of muscular dystrophy associated with hypotonia, muscle weakness, several brain abnormalities and mental retardation(44). The extended O-mannosyl glycan chains on Dg are linked to some of the clinical phenotypes in WWS patients, especially the muscle associated defects(44). The neural abnormalities are much less studied, although there are a few studies showing hypoglycosylation of Dg is associated with breaches of basement membrane in the brain(85) and axon guidance defects in mammals(68). The complexity of O-mannosylation pathways in higher vertebrates makes it harder to analyze the role of O-mannosyl glycans in neural development. In my PhD project, I decided to use *Drosophila* as a model to understand the neurological defects associated with loss of POMT1/2 dependent O-mannosylation.

Similar to vertebrates, *Drosophila* also has two O-mannosyltransferase genes, encoding DmPOMT1 (*rt*) and DmPOMT2 (*tw*) which work as non-redundant components of enzymatic complex in the ER to O-mannosylate substrate proteins. Both genes are evolutionarily conserved, along with their substrate Dystroglycan. Therefore, *Drosophila* is a well-established model system to study the functions of O-mannosyl glycans(79). In my dissertation, I have established a new role of O-mannosyl glycans in the nervous system and a new substrate, with a possible mechanism of how O-mannose might affect the substrate's function.

Previous studies in the lab had shown that *rt* and *tw* mutant embryos have an abnormal body posture which begins to develop at a later stage when musculature and neural circuitry is established(96). It also came to light that a group of multidendritic sensory

neurons are somehow involved in regulating the abnormal body posture(96). This is where my work comes into picture. My work is divided into two parts. In the first part, I describe how sensory neurons might regulate body posture. In collaboration with Dr. Ryan Baker, I found that a general loss of sensory neurons causes a similar body posture defect in embryos as seen in *rt/tw* mutant embryos. This indicates the importance of rhythmic muscle contractions and their control by peripheral sensory neurons in maintaining body posture. Interestingly, body posture defects are also a characteristic feature of CMDs(115). This suggests that communication between muscles and neurons might be defective in CMD patients.

Next, I independently explored how sensory neurons may be defective that they're unable to relay information from muscles to neurons, in *rt/tw* mutants. Interestingly, abnormal body posture was found to be associated with a group of sensory neurons, Class IV multidendritic (da) neurons. Transgenic expression of *rt/tw* in da neurons of the mutants partially rescued the rotated embryo defect. *Rt* mutants are known to have morphologically defective neuromuscular junctions(NMJs) with lesser glutamate receptors present on synaptic membranes (75). The function of NMJs is important for communication between muscles and neurons and may in part explain the abnormal body posture seen in *rt/tw* mutants. Therefore, I was eager to investigate if Class IV da neurons are morphologically defective too. To test this, I studied the axons that Class IV da neurons (located in epidermal cells) send to the brain and found them to be defective in *rt/tw* mutants. Specifically, I found that commissural axons are unable to branch correctly at the terminal point in the brain. I further found that *rt/tw* work cell

autonomously to regulate this branching. I found that other major CNS axon morphologies in the brain are not regulated by *rt/tw*. I also found that other sensory axons (such as axons of chordotonal neurons) are not significantly affected in *rt/tw* mutants. Glial cells are important regulators of axon guidance and pathfinding as they secrete several factors that help axons navigate their environment and make stopping or branching decisions. I found that glial cell development remains intact in *rt/tw* mutants. Axon morphology is an important factor in maintaining communication between neurons and other cells such as muscles. Morphology of axons dictates how they will connect with other neurons in a circuit for fast, point-to-point transfer of information. Defective morphology of sensory axon connections indicates incorrect and/or inefficient communication between the sensory neurons and CNS neurons, eventually leading to defects in muscle contractions. Uncoordinated muscle contractions are also seen in *rt/tw* mutants, and this phenotype is also rescued by transgenic expression of *rt/tw* in Class IV sensory neurons.

Thus, the first part of my work reveals a novel role of O-mannose in regulating axon morphology and muscle contractions thus regulating body posture. This mechanism might be evolutionarily conserved and help us better understand muscular dystrophies. In the second part of my work, I have investigated which substrates of *rt/tw* dependent O-mannosylation are responsible for causing the defects in Class IV axon connectivity. The only well studied substrate of POMTs in *Drosophila* and humans is Dystroglycan (Dg). Dg has important functions in regulating photoreceptor axon guidance in *Drosophila*(76). However, upon analyses of *Dg* mutants, I found that Dg does not fully

account for the Class IV axon defect seen in *rt/tw* mutant brains. I have also shown that Dg mutants do not show posture defects in embryos similar to *rt/tw* mutants. This indicates the importance of uncovering new functionally relevant substrates of RT/TW. Recently, 2 new substrates of POMT1/2 were identified in human cell lines, KIAA1549 and SUCO (**SU**N-domain **c**ontaining **o**ssification factor). Both of these proteins are not well studied in humans(7). One of them SUCO, has a direct ortholog in *Drosophila* (CG31678) which is also uncharacterized. Interestingly, *receptor protein tyrosine phosphatase 69D (Ptp69D)* was identified along with other genes as a candidate regulator of Class IV axon morphology, in a forward genetic screen(92). Moreover, RPTP69D was of particular interest because one of its mammalian homologues, RPTPζ, was found to be O-mannosylated in the nervous system (31, 69). However, whether RPTPζ is a substrate of POMT1/2 remains unknown, and no functional studies on the role of *Ptp69D* in sensory neurons were previously carried out. Therefore, I decided to analyze RPTPs in detail as possible relevant targets of O-mannosylation that potentially play roles in the regulation of sensory axon connectivity in Drosophila.

To test whether RPTPs are functionally relevant substrates of RT/TW, I studied genetic interactions between *POMT1/2* and *RPTP*s. *Rptp69D* phenocopied POMT1/2 defects in Class IV axons and *RPTP69D*-RNAi showed synergistic genetic interactions with *POMT1/2*. Single copy mutation in extracellular domain of *Lar* also showed some effect on *POMT1/2* mutant phenotype, however it was an antagonistic interaction and its quantification did not show statistical significance. Lar belongs to the same subfamily of

RPTPs as 69D, Type IIa(124, 136). *Lar* mutant seemed to suppress *tw* phenotype suggesting a possibility of a negative regulation of Lar function by POMT1/2. *PTP99A*-RNAi and *PTP52F* mutant also showed synergistic interactions with *POMT1/2*. *PTP4E* and *PTP10D* RNAi showed synergistic interactions with *POMT1/2* in regulating Class IV axon morphology however their phenotypes were different from *POMT1/2* mutants alone. This suggests a distinct function of PTP4E and 10D in regulating Class IV axon morphology and that POMTs affect this distinct function, however the corresponding phenotype is possibly masked in *POMT* mutants due to partial redundancy of RPTPs.

In collaborative experiments with mass spectrometry experts, I also found that RPTP69D is indeed O-mannosylated by POMT1/2 on its extracellular domain and that this O-mannosylation might be important for protection from proteolysis and the integrity of the extracellular domain. The extracellular Ig-1,2 domains are known to be important for ligand binding and therefore for transducing signal inside the axons to make stopping or branching decisions. Thus, the potential proteolytic cleavage of the N-terminal Ig domains may directly affect signaling and adhesion properties of RPTP69D. Further studies will be required to test this important hypothesis.

Taken together, the results of the second part of my work uncovered a novel class of functionally relevant substrates of POMTs and suggests a possible mechanism of how O-mannosylation may affect RPTP69D function. This greatly improves our understanding of how O-mannose modifications can function in neural development.

Further studies are required to understand if other RPTPs are also O-mannosylated and how non-elongated O-mannosyl glycans affect their function. In humans, is O-mannose on RPTPζ is extended with other sugars, suggesting a more complex regulation of O-mannosylation and perhaps different functions of the extended glycans. However, the TMTC1-4 directed O-mannosylation on cadherins is also non-extended, suggesting a possibility that non-extended O-mannose plays similar functional roles on different substrates. It would be interesting to reveal how non-extended O-mannose on Cadherins and plexins affect their function.

REFERENCES

1. Rosenthal A, Nordin J. Enzymes that hydrolyze fungal cell wall polysaccharides. The carbonhydrate constitution of mycodextranse, an endo-alpha (1 yields 4)-D-glucanase from Pencillium melinii. Journal of Biological Chemistry. 1975;250(14):5295-303.

2. Raizada MK, Schutzbach JS, Ankel H. Cryptococcus laurentii cell envelope glycoprotein. Evidence for separate oligosaccharide side chains of different composition and structure. Journal of Biological Chemistry. 1975;250(9):3310-5.

3. Nakajima T, Ballou CE. Structure of the linkage region between the polysaccharide and protein parts of Saccharomyces cerevisiae mannan. Journal of Biological Chemistry. 1974;249(23):7685-94.

4. Jukka Finne TK, Rene K. Margolis, and Richard U. Margolis. Novel Mannitol-containing Oligosaccharides Obtained by Mild Alkaline Borohydride Treatment of a Chondroitin Sulfate Proteoglycan from Brain*. Journal of biological chemistry. 1979;254(October 25):10295-300,.

5. Dobson CM, Hempel SJ, Stalnaker SH, Stuart R, Wells L. O-Mannosylation and human disease. Cell Mol Life Sci. 2013;70(16):2849-57. doi: 10.1007/s00018-012-1193-0. PubMed PMID: 23115008; PMCID: PMC3984002.

6. Beltran-Valero de Bernabe D, Currier S, Steinbrecher A, Celli J, van Beusekom E, van der Zwaag B, Kayserili H, Merlini L, Chitayat D, Dobyns WB, Cormand B, Lehesjoki AE, Cruces J, Voit T, Walsh CA, van Bokhoven H, Brunner HG. Mutations in the O-mannosyltransferase gene POMT1 give rise to the severe neuronal migration disorder Walker-Warburg syndrome. Am J Hum Genet. 2002;71(5):1033-43. doi: 10.1086/342975. PubMed PMID: 12369018; PMCID: PMC419999.

7. Larsen ISB, Narimatsu Y, Joshi HJ, Siukstaite L, Harrison OJ, Brasch J, Goodman KM, Hansen L, Shapiro L, Honig B, Vakhrushev SY, Clausen H, Halim A. Discovery of an O-mannosylation pathway selectively serving cadherins and protocadherins. Proc Natl Acad Sci U S A. 2017;114(42):11163-8. doi: 10.1073/pnas.1708319114. PubMed PMID: 28973932; PMCID: PMC5651762.

8. Sentandreu R, Northcote D. The structure of a glycopeptide isolated from the yeast cell wall. Biochemical Journal. 1968;109(3):419-32.

9. Manya H, Chiba A, Yoshida A, Wang X, Chiba Y, Jigami Y, Margolis RU, Endo T. Demonstration of mammalian protein O-mannosyltransferase activity: coexpression

of POMT1 and POMT2 required for enzymatic activity. Proc Natl Acad Sci U S A. 2004;101(2):500-5. doi: 10.1073/pnas.0307228101. PubMed PMID: 14699049; PMCID: PMC327176.

10. Manya H, Chiba A, Margolis RU, Endo T. Molecular cloning and characterization of rat Pomt1 and Pomt2. Glycobiology. 2006;16(9):863-73.

11. Neubert P, Strahl S. Protein O-mannosylation in the early secretory pathway. Current opinion in cell biology. 2016;41:100-8.

12. Bai L, Kovach A, You Q, Kenny A, Li H. Structure of the eukaryotic protein O-mannosyltransferase Pmt1− Pmt2 complex. Nature structural & molecular biology. 2019;26(8):704-11.

13. Larsen ISB, Narimatsu Y, Clausen H, Joshi HJ, Halim A. Multiple distinct O-Mannosylation pathways in eukaryotes. Current opinion in structural biology. 2019;56:171-8.

14. Neubert P, Halim A, Zauser M, Essig A, Joshi HJ, Zatorska E, Larsen ISB, Loibl M, Castells-Ballester J, Aebi M. Mapping the O-mannose glycoproteome in Saccharomyces cerevisiae. Molecular & Cellular Proteomics. 2016;15(4):1323-37.

15. Faulkner C, Ellis HP, Shaw A, Penman C, Palmer A, Wragg C, Greenslade M, Haynes HR, Williams H, Lowis S. BRAF fusion analysis in pilocytic astrocytomas: KIAA1549-BRAF 15-9 fusions are more frequent in the midline than within the cerebellum. Journal of neuropathology and experimental neurology. 2015;74(9):867-72.

16. Larsen ISB, Narimatsu Y, Joshi HJ, Yang Z, Harrison OJ, Brasch J, Shapiro L, Honig B, Vakhrushev SY, Clausen H, Halim A. Mammalian O-mannosylation of cadherins and plexins is independent of protein O-mannosyltransferases 1 and 2. J Biol Chem. 2017;292(27):11586-98. doi: 10.1074/jbc.M117.794487. PubMed PMID: 28512129; PMCID: PMC5500819.

17. Chiba A, Matsumura K, Yamada H, Inazu T, Shimizu T, Kusunoki S, Kanazawa I, Kobata A, Endo T. Structures of sialylated O-linked oligosaccharides of bovine peripheral nerve α-dystroglycan The role of a novel O-mannosyl-type oligosaccharide in the binding of α-dystroglycan with laminin. Journal of Biological Chemistry. 1997;272(4):2156-62.

18. Barresi R, Campbell KP. Dystroglycan: from biosynthesis to pathogenesis of human disease. Journal of cell science. 2006;119(2):199-207.

19. Sheikh MO, Halmo SM, Wells L. Recent advancements in understanding mammalian O-mannosylation. Glycobiology. 2017;27(9):806-19. doi: 10.1093/glycob/cwx062. PubMed PMID: 28810660; PMCID: PMC6082599.

20. Stalnaker SH, Stuart R, Wells L. Mammalian O-mannosylation: unsolved questions of structure/function. Curr Opin Struct Biol. 2011;21(5):603-9. doi: 10.1016/j.sbi.2011.09.001. PubMed PMID: 21945038; PMCID: PMC3356693.

21. McDearmon EL, Combs AC, Sekiguchi K, Fujiwara H, Ervasti JM. Brain α-dystroglycan displays unique glycoepitopes and preferential binding to laminin-10/11. FEBS letters. 2006;580(14):3381-5.

22. Smalheiser NR, Haslam SM, Sutton-Smith M, Morris HR, Dell A. Structural analysis of sequences O-linked to mannose reveals a novel Lewis X structure in cranin (dystroglycan) purified from sheep brain. Journal of Biological Chemistry. 1998;273(37):23698-703.

23. Endo T. Glycobiology of α-dystroglycan and muscular dystrophy. The Journal of Biochemistry. 2015;157(1):1-12.

24. Morita I, Kakuda S, Takeuchi Y, Itoh S, Kawasaki N, Kizuka Y, Kawasaki T, Oka S. HNK-1 glyco-epitope regulates the stability of the glutamate receptor subunit GluR2 on the neuronal cell surface. Journal of Biological Chemistry. 2009;284(44):30209-17.

25. Sheikh MO, Venzke D, Anderson ME, Yoshida-Moriguchi T, Glushka JN, Nairn AV, Galizzi M, Moremen KW, Campbell KP, Wells L. HNK-1 Sulfotransferase modulates α-dystroglycan glycosylation by 3-O-sulfation of glucuronic acid on matriglycan. Glycobiology. 2020.

26. Yoshida-Moriguchi T, Campbell KP. Matriglycan: a novel polysaccharide that links dystroglycan to the basement membrane. Glycobiology. 2015;25(7):702-13.

27. Inamori K-i, Yoshida-Moriguchi T, Hara Y, Anderson ME, Yu L, Campbell KP. Dystroglycan function requires xylosyl-and glucuronyltransferase activities of LARGE. Science. 2012;335(6064):93-6.

28. Stalnaker SH, Aoki K, Lim J-M, Porterfield M, Liu M, Satz JS, Buskirk S, Xiong Y, Zhang P, Campbell KP. Glycomic analyses of mouse models of congenital muscular dystrophy. Journal of Biological Chemistry. 2011;286(24):21180-90.

29. Stalnaker SH, Hashmi S, Lim J-M, Aoki K, Porterfield M, Gutierrez-Sanchez G, Wheeler J, Ervasti JM, Bergmann C, Tiemeyer M. Site mapping and characterization of

O-glycan structures on α-dystroglycan isolated from rabbit skeletal muscle. Journal of Biological Chemistry. 2010;285(32):24882-91.

30. Nakamura N, Stalnaker SH, Lyalin D, Lavrova O, Wells L, Panin VM. Drosophila Dystroglycan is a target of O-mannosyltransferase activity of two protein O-mannosyltransferases, Rotated Abdomen and Twisted. Glycobiology. 2010;20(3):381-94. doi: 10.1093/glycob/cwp189. PubMed PMID: 19969597; PMCID: PMC2912551.

31. Dwyer CA, Katoh T, Tiemeyer M, Matthews RT. Neurons and glia modify receptor protein-tyrosine phosphatase zeta (RPTPzeta)/phosphacan with cell-specific O-mannosyl glycans in the developing brain. J Biol Chem. 2015;290(16):10256-73. doi: 10.1074/jbc.M114.614099. PubMed PMID: 25737452; PMCID: PMC4400340.

32. Bleckmann C, Geyer H, Lieberoth A, Splittstoesser F, Liu Y, Feizi T, Schachner M, Kleene R, Reinhold V, Geyer R. O-glycosylation pattern of CD24 from mouse brain. Biological chemistry. 2009;390(7):627-45.

33. Pacharra S, Hanisch F-G, Breloy I. Neurofascin 186 is O-mannosylated within and outside of the mucin domain. Journal of proteome research. 2012;11(8):3955-64.

34. Hanisch F-G, Faissner A, Breloy I. The Lecticans of Mammalian Brain Perineural Net Are O-Mannosylated2013.

35. Halim A, Larsen ISB, Neubert P, Joshi HJ, Petersen BL, Vakhrushev SY, Strahl S, Clausen H. Discovery of a nucleocytoplasmic O-mannose glycoproteome in yeast. Proceedings of the National Academy of Sciences. 2015;112(51):15648-53.

36. Kleizen B, Braakman I. A sweet send-off. science. 2013;340(6135):930-1.

37. Xu C, Ng DT. Glycosylation-directed quality control of protein folding. Nature reviews Molecular cell biology. 2015;16(12):742-52.

38. Xu C, Wang S, Thibault G, Ng DT. Futile protein folding cycles in the ER are terminated by the unfolded protein O-mannosylation pathway. Science. 2013;340(6135):978-81.

39. Loibl M, Strahl S. Protein O-mannosylation: what we have learned from baker's yeast. Biochimica et Biophysica Acta (BBA)-Molecular Cell Research. 2013;1833(11):2438-46.

40. Sanders SL, Gentzsch M, Tanner W, Herskowitz I. O-Glycosylation of Axl2/Bud10p by Pmt4p is required for its stability, localization, and function in daughter cells. The Journal of cell biology. 1999;145(6):1177-88.

41. Briggs DC, Yoshida-Moriguchi T, Zheng T, Venzke D, Anderson ME, Strazzulli A, Moracci M, Yu L, Hohenester E, Campbell KP. Structural basis of laminin binding to the LARGE glycans on dystroglycan. Nature chemical biology. 2016;12(10):810-4.

42. Yurchenco PD. Basement membranes: cell scaffoldings and signaling platforms. Cold Spring Harbor perspectives in biology. 2011;3(2):a004911.

43. Godfrey C, Foley AR, Clement E, Muntoni F. Dystroglycanopathies: coming into focus. Current opinion in genetics & development. 2011;21(3):278-85.

44. van Reeuwijk J, Janssen M, van den Elzen C, De Bernabé DB-V, Sabatelli P, Merlini L, Boon M, Scheffer H, Brockington M, Muntoni F. POMT2 mutations cause α-dystroglycan hypoglycosylation and Walker-Warburg syndrome. Journal of medical genetics. 2005;42(12):907-12.

45. Wallace SE, Conta JH, Winder TL, Willer T, Eskuri JM, Haas R, Patterson K, Campbell KP, Moore SA, Gospe SM, Jr. A novel missense mutation in POMT1 modulates the severe congenital muscular dystrophy phenotype associated with POMT1 nonsense mutations. Neuromuscul Disord. 2014;24(4):312-20. doi: 10.1016/j.nmd.2014.01.001. PubMed PMID: 24491487; PMCID: PMC3959257.

46. Sun T, Hevner RF. Growth and folding of the mammalian cerebral cortex: from molecules to malformations. Nature Reviews Neuroscience. 2014;15(4):217-32.

47. McConnell SK. Constructing the cerebral cortex: neurogenesis and fate determination. Neuron. 1995;15(4):761-8.

48. Zhao S, Frotscher M. Go or stop? Divergent roles of Reelin in radial neuronal migration. The Neuroscientist. 2010;16(4):421-34.

49. Shitamukai A, Matsuzaki F. Control of asymmetric cell division of mammalian neural progenitors. Development, growth & differentiation. 2012;54(3):277-86.

50. Vuillaumier-Barrot S, Bouchet-Séraphin C, Chelbi M, Devisme L, Quentin S, Gazal S, Laquerrière A, Fallet-Bianco C, Loget P, Odent S. Identification of mutations in TMEM5 and ISPD as a cause of severe cobblestone lissencephaly. The American Journal of Human Genetics. 2012;91(6):1135-43.

51. Halfter W, Dong S, Yip Y-P, Willem M, Mayer U. A critical function of the pial basement membrane in cortical histogenesis. Journal of Neuroscience. 2002;22(14):6029-40.

52. Hu H, Li J, Gagen CS, Gray NW, Zhang Z, Qi Y, Zhang P. Conditional knockout of protein O-mannosyltransferase 2 reveals tissue-specific roles of O-mannosyl

glycosylation in brain development. Journal of Comparative Neurology. 2011;519(7):1320-37.

53. Myshrall TD, Moore SA, Ostendorf AP, Satz JS, Kowalczyk T, Nguyen H, Daza RA, Lau C, Campbell KP, Hevner RF. Dystroglycan on radial glia end feet is required for pial basement membrane integrity and columnar organization of the developing cerebral cortex. Journal of Neuropathology & Experimental Neurology. 2012;71(12):1047-63.

54. Bartels MF, Winterhalter PR, Yu J, Liu Y, Lommel M, Mohrlen F, Hu H, Feizi T, Westerlind U, Ruppert T, Strahl S. Protein O-Mannosylation in the Murine Brain: Occurrence of Mono-O-Mannosyl Glycans and Identification of New Substrates. PLoS One. 2016;11(11):e0166119. doi: 10.1371/journal.pone.0166119. PubMed PMID: 27812179; PMCID: PMC5094735.

55. Südhof TC. Synaptic neurexin complexes: a molecular code for the logic of neural circuits. Cell. 2017;171(4):745-69.

56. Franco SJ, Martinez-Garay I, Gil-Sanz C, Harkins-Perry SR, Müller U. Reelin regulates cadherin function via Dab1/Rap1 to control neuronal migration and lamination in the neocortex. Neuron. 2011;69(3):482-97.

57. Matsunaga Y, Noda M, Murakawa H, Hayashi K, Nagasaka A, Inoue S, Miyata T, Miura T, Kubo K-i, Nakajima K. Reelin transiently promotes N-cadherin–dependent neuronal adhesion during mouse cortical development. Proceedings of the National Academy of Sciences. 2017;114(8):2048-53.

58. Lommel M, Winterhalter PR, Willer T, Dahlhoff M, Schneider MR, Bartels MF, Renner-Müller I, Ruppert T, Wolf E, Strahl S. Protein O-mannosylation is crucial for E-cadherin–mediated cell adhesion. Proceedings of the National Academy of Sciences. 2013;110(52):21024-9.

59. Nuernberger M, Weth F, Redies C. Layer-specific expression of multiple cadherins in the developing visual cortex (V1) of the ferret. Cerebral Cortex. 2009;19(2):388-401.

60. Cappello S, Gray MJ, Badouel C, Lange S, Einsiedler M, Srour M, Chitayat D, Hamdan FF, Jenkins ZA, Morgan T. Mutations in genes encoding the cadherin receptor-ligand pair DCHS1 and FAT4 disrupt cerebral cortical development. Nature genetics. 2013;45(11):1300.

61. Killen AC, Barber M, Paulin JJ, Ranscht B, Parnavelas JG, Andrews WD. Protective role of Cadherin 13 in interneuron development. Brain Structure and Function. 2017;222(8):3567-85.

62. Li R, Liang Y, Zheng S, He Q, Yang L. The atypical cadherin flamingo determines the competence of neurons for activity-dependent fine-scale topography. Molecular Brain. 2019;12(1):1-8.

63. Xu P, Guo L, Tang X, Xu H, Fan X. ERβ may contribute to the maintaining of radial glia cells polarity through cadherins during corticogenesis. Medical hypotheses. 2011;77(6):974-6.

64. Südhof TC. Towards an understanding of synapse formation. Neuron. 2018;100(2):276-93.

65. Sato S, Omori Y, Katoh K, Kondo M, Kanagawa M, Miyata K, Funabiki K, Koyasu T, Kajimura N, Miyoshi T. Pikachurin, a dystroglycan ligand, is essential for photoreceptor ribbon synapse formation. Nature neuroscience. 2008;11(8):923.

66. Omori Y, Araki F, Chaya T, Kajimura N, Irie S, Terada K, Muranishi Y, Tsujii T, Ueno S, Koyasu T. Presynaptic dystroglycan–pikachurin complex regulates the proper synaptic connection between retinal photoreceptor and bipolar cells. Journal of Neuroscience. 2012;32(18):6126-37.

67. Hu H, Li J, Zhang Z, Yu M. Pikachurin interaction with dystroglycan is diminished by defective O-mannosyl glycosylation in congenital muscular dystrophy models and rescued by LARGE overexpression. Neuroscience letters. 2011;489(1):10-5.

68. Wright KM, Lyon KA, Leung H, Leahy DJ, Ma L, Ginty DD. Dystroglycan organizes axon guidance cue localization and axonal pathfinding. Neuron. 2012;76(5):931-44. doi: 10.1016/j.neuron.2012.10.009. PubMed PMID: 23217742; PMCID: PMC3526105.

69. Dwyer CA, Baker E, Hu H, Matthews RT. RPTPζ/phosphacan is abnormally glycosylated in a model of muscle–eye–brain disease lacking functional POMGnT1. Neuroscience. 2012;220:47-61.

70. Ulbricht U, Brockmann MA, Aigner A, Eckerich C, Müller S, Fillbrandt R, Westphal M, Lamszus K. Expression and function of the receptor protein tyrosine phosphatase ζ and its ligand pleiotrophin in human astrocytomas. Journal of Neuropathology & Experimental Neurology. 2003;62(12):1265-75.

71. González-Castillo C, Ortuño-Sahagún D, Guzmán-Brambila C, Pallàs M, Rojas-Mayorquín AE. Pleiotrophin as a central nervous system neuromodulator, evidences from the hippocampus. Frontiers in cellular neuroscience. 2015;8:443.

72. Kanekiyo K, Inamori K-i, Kitazume S, Sato K, Maeda J, Higuchi M, Kizuka Y, Korekane H, Matsuo I, Honke K. Loss of branched O-mannosyl glycans in astrocytes accelerates remyelination. Journal of Neuroscience. 2013;33(24):10037-47.

73. Kwok JC, Afshari F, Garcia-Alias G, Fawcett JW. Proteoglycans in the central nervous system: plasticity, regeneration and their stimulation with chondroitinase ABC. Restorative neurology and neuroscience. 2008;26(2, 3):131-45.

74. Lyalin D, Koles K, Roosendaal SD, Repnikova E, Van Wechel L, Panin VM. The twisted gene encodes Drosophila protein O-mannosyltransferase 2 and genetically interacts with the rotated abdomen gene encoding Drosophila protein O-mannosyltransferase 1. Genetics. 2006;172(1):343-53. doi: 10.1534/genetics.105.049650. PubMed PMID: 16219785; PMCID: PMC1456162.

75. Wairkar YP, Fradkin LG, Noordermeer JN, DiAntonio A. Synaptic defects in a Drosophila model of congenital muscular dystrophy. J Neurosci. 2008;28(14):3781-9. doi: 10.1523/JNEUROSCI.0478-08.2008. PubMed PMID: 18385336; PMCID: PMC6671091.

76. Shcherbata HR, Yatsenko AS, Patterson L, Sood VD, Nudel U, Yaffe D, Baker D, Ruohola-Baker H. Dissecting muscle and neuronal disorders in a Drosophila model of muscular dystrophy. EMBO J. 2007;26(2):481-93. doi: 10.1038/sj.emboj.7601503. PubMed PMID: 17215867; PMCID: PMC1783456.

77. Ueyama M, Akimoto Y, Ichimiya T, Ueda R, Kawakami H, Aigaki T, Nishihara S. Increased apoptosis of myoblasts in Drosophila model for the Walker-Warburg syndrome. PloS one. 2010;5(7):e11557.

78. Haines N, Seabrooke S, Stewart BA. Dystroglycan and protein O-mannosyltransferases 1 and 2 are required to maintain integrity of Drosophila larval muscles. Molecular biology of the cell. 2007;18(12):4721-30.

79. Lyalin D. The role of O-mannosyl glycans in Drosophila development: Texas A & M University; 2012.

80. Moremen KW, Tiemeyer M, Nairn AV. Vertebrate protein glycosylation: diversity, synthesis and function. Nature reviews Molecular cell biology. 2012;13(7):448-62.

81. Martin PT. Congenital muscular dystrophies involving the O-mannose pathway. Curr Mol Med. 2007;7(4):417-25. doi: 10.2174/156652407780831601. PubMed PMID: 17584082; PMCID: PMC2855644.

82. Willer T, Prados B, Falcón-Pérez JM, Renner-Müller I, Przemeck GK, Lommel M, Coloma A, Valero MC, de Angelis MH, Tanner W. Targeted disruption of the Walker–Warburg syndrome gene Pomt1 in mouse results in embryonic lethality. Proceedings of the National Academy of Sciences. 2004;101(39):14126-31.

83. Mercuri E, Muntoni F. Muscular dystrophies. The Lancet. 2013;381(9869):845-860.

84. Vester-Christensen MB, Halim A, Joshi HJ, Steentoft C, Bennett EP, Levery SB, Vakhrushev SY, Clausen H. Mining the O-mannose glycoproteome reveals cadherins as major O-mannosylated glycoproteins. Proc Natl Acad Sci U S A. 2013;110(52):21018-23. doi: 10.1073/pnas.1313446110. PubMed PMID: 24101494; PMCID: PMC3876253.

85. Li J, Yu M, Feng G, Hu H, Li X. Breaches of the pial basement membrane are associated with defective dentate gyrus development in mouse models of congenital muscular dystrophies. Neurosci Lett. 2011;505(1):19-24. doi: 10.1016/j.neulet.2011.09.040. PubMed PMID: 21970971; PMCID: PMC3243927.

86. Martín-Blanco E, García-Bellido A. Mutations in the rotated abdomen locus affect muscle development and reveal an intrinsic asymmetry in Drosophila. Proceedings of the National Academy of Sciences. 1996;93(12):6048-52.

87. Ichimiya T, Manya H, Ohmae Y, Yoshida H, Takahashi K, Ueda R, Endo T, Nishihara S. The twisted abdomen phenotype of Drosophila POMT1 and POMT2 mutants coincides with their heterophilic protein O-mannosyltransferase activity. J Biol Chem. 2004;279(41):42638-47. doi: 10.1074/jbc.M404900200. PubMed PMID: 15271988.

88. Nolo R, Abbott LA, Bellen HJ. Senseless, a Zn finger transcription factor, is necessary and sufficient for sensory organ development in Drosophila. Cell. 2000;102(3):349-62.

89. Christoforou CP, Greer CE, Challoner BR, Charizanos D, Ray RP. The detached locus encodes Drosophila Dystrophin, which acts with other components of the Dystrophin Associated Protein Complex to influence intercellular signalling in developing wing veins. Developmental biology. 2008;313(2):519-32.

90. Han C, Wang D, Soba P, Zhu S, Lin X, Jan LY, Jan Y-N. Integrins regulate repulsion-mediated dendritic patterning of Drosophila sensory neurons by restricting dendrites in a 2D space. Neuron. 2012;73(1):64-78.

91. Rothwell WF, Sullivan W. Fluorescent analysis of Drosophila embryos. Drosophila protocols. 2000:141-57.

92. Grueber WB, Ye B, Yang CH, Younger S, Borden K, Jan LY, Jan YN. Projections of Drosophila multidendritic neurons in the central nervous system: links with peripheral dendrite morphology. Development. 2007;134(1):55-64. doi: 10.1242/dev.02666. PubMed PMID: 17164414.

93. Grueber WB, Jan LY, Jan YN. Tiling of the Drosophila epidermis by multidendritic sensory neurons. Development. 2002;129(12):2867-78.

94. Crisp S, Evers JF, Fiala A, Bate M. The development of motor coordination in Drosophila embryos. Development. 2008;135(22):3707-17.

95. Pereanu W, Spindler S, Im E, Buu N, Hartenstein V. The emergence of patterned movement during late embryogenesis of Drosophila. Developmental neurobiology. 2007;67(12):1669-85.

96. Baker R, Nakamura N, Chandel I, Howell B, Lyalin D, Panin VM. Protein O-Mannosyltransferases Affect Sensory Axon Wiring and Dynamic Chirality of Body Posture in the Drosophila Embryo. J Neurosci. 2018;38(7):1850-65. doi: 10.1523/JNEUROSCI.0346-17.2017. PubMed PMID: 29167399; PMCID: PMC5815462.

97. Neuhaus-Follini A, Bashaw GJ. Crossing the embryonic midline: molecular mechanisms regulating axon responsiveness at an intermediate target. Wiley Interdisciplinary Reviews: Developmental Biology. 2015;4(4):377-89.

98. Noordermeer JN, Kopczynski CC, Fetter RD, Bland KS, Chen W-Y, Goodman CS. Wrapper, a novel member of the Ig superfamily, is expressed by midline glia and is required for them to ensheath commissural axons in Drosophila. Neuron. 1998;21(5):991-1001.

99. Landgraf M, Sánchez-Soriano N, Technau GM, Urban J, Prokop A. Charting the Drosophila neuropile: a strategy for the standardised characterisation of genetically amenable neurites. Developmental biology. 2003;260(1):207-25.

100. Jacobs JR. The midline glia of Drosophila: a molecular genetic model for the developmental functions of glia. Progress in neurobiology. 2000;62(5):475-508.

101. Ayoob JC, Terman JR, Kolodkin AL. Drosophila Plexin B is a Sema-2a receptor required for axon guidance. Development. 2006;133(11):2125-35.

102. Wu Z, Sweeney LB, Ayoob JC, Chak K, Andreone BJ, Ohyama T, Kerr R, Luo L, Zlatic M, Kolodkin AL. A combinatorial semaphorin code instructs the initial steps of sensory circuit assembly in the Drosophila CNS. Neuron. 2011;70(2):281-98.

103. Organisti C, Hein I, Grunwald Kadow IC, Suzuki T. Flamingo, a seven-pass transmembrane cadherin, cooperates with Netrin/Frazzled in Drosophila midline guidance. Genes Cells. 2015;20(1):50-67. doi: 10.1111/gtc.12202. PubMed PMID: 25440577.

104. Gorczyca DA, Younger S, Meltzer S, Kim SE, Cheng L, Song W, Lee HY, Jan LY, Jan YN. Identification of Ppk26, a DEG/ENaC channel functioning with Ppk1 in a mutually dependent manner to guide locomotion behavior in Drosophila. Cell reports. 2014;9(4):1446-58.

105. Song W, Onishi M, Jan LY, Jan YN. Peripheral multidendritic sensory neurons are necessary for rhythmic locomotion behavior in Drosophila larvae. Proceedings of the National Academy of Sciences. 2007;104(12):5199-204.

106. Clark MQ, Zarin AA, Carreira-Rosario A, Doe CQ. Neural circuits driving larval locomotion in Drosophila. Neural development. 2018;13(1):1-10.

107. Caldwell JC, Miller MM, Wing S, Soll DR, Eberl DF. Dynamic analysis of larval locomotion in Drosophila chordotonal organ mutants. Proceedings of the National Academy of Sciences. 2003;100(26):16053-8.

108. Morikawa RK, Kanamori T, Yasunaga K-i, Emoto K. Different levels of the Tripartite motif protein, Anomalies in sensory axon patterning (Asap), regulate distinct axonal projections of Drosophila sensory neurons. Proceedings of the National Academy of Sciences. 2011;108(48):19389-94.

109. Lee T, Luo L. Mosaic analysis with a repressible cell marker for studies of gene function in neuronal morphogenesis. Neuron. 1999;22(3):451-61.

110. Sarov M, Barz C, Jambor H, Hein MY, Schmied C, Suchold D, Stender B, Janosch S, Kj VV, Krishnan R. A genome-wide resource for the analysis of protein localisation in Drosophila. Elife. 2016;5:e12068.

111. Hwang RY, Zhong L, Xu Y, Johnson T, Zhang F, Deisseroth K, Tracey WD. Nociceptive neurons protect Drosophila larvae from parasitoid wasps. Current Biology. 2007;17(24):2105-16.

112. Zhong L, Hwang RY, Tracey WD. Pickpocket is a DEG/ENaC protein required for mechanical nociception in Drosophila larvae. Current Biology. 2010;20(5):429-34.

113. Zlatic M, Li F, Strigini M, Grueber W, Bate M. Positional cues in the Drosophila nerve cord: semaphorins pattern the dorso-ventral axis. PLoS biology. 2009;7(6).

114. Oliva C, Soldano A, Mora N, De Geest N, Claeys A, Erfurth M-L, Sierralta J, Ramaekers A, Dascenco D, Ejsmont RK. Regulation of Drosophila brain wiring by neuropil interactions via a slit-Robo-RPTP signaling complex. Developmental cell. 2016;39(2):267-78.

115. Leyten Q, Gabreëls F, Renier W, Ter Laak H. Congenital muscular dystrophy: a review of the literature. Clinical neurology and neurosurgery. 1996;98(4):267-80.

116. Di Costanzo S, Balasubramanian A, Pond HL, Rozkalne A, Pantaleoni C, Saredi S, Gupta VA, Sunu CM, Yu TW, Kang PB. POMK mutations disrupt muscle development leading to a spectrum of neuromuscular presentations. Human molecular genetics. 2014;23(21):5781-92.

117. Ensslen-Craig SE, Brady-Kalnay SM. Receptor protein tyrosine phosphatases regulate neural development and axon guidance. Developmental biology. 2004;275(1):12-22.

118. Stoker AW, editor. RPTPs in axons, synapses and neurology. Seminars in cell & developmental biology; 2015: Elsevier.

119. Deng W-M, Schneider M, Frock R, Castillejo-Lopez C, Gaman EA, Baumgartner S, Ruohola-Baker H. Dystroglycan is required for polarizing the epithelial cells and the oocyte in Drosophila. Development. 2003;130(1):173-84.

120. Desai CJ, Krueger NX, Saito H, Zinn K. Competition and cooperation among receptor tyrosine phosphatases control motoneuron growth cone guidance in Drosophila. Development. 1997;124(10):1941-52.

121. Desai C, Purdy J. The neural receptor protein tyrosine phosphatase DPTP69D is required during periods of axon outgrowth in Drosophila. Genetics. 2003;164(2):575-88.

122. Robertson Sears HC. The receptor tyrosine phosphatase Ptp69D and the receptor tyrosine kinase Pvr in Drosophila nervous system development: Massachusetts Institute of Technology; 2004.

123. Poe AR, Tang L, Wang B, Li Y, Sapar ML, Han C. Dendritic space-filling requires a neuronal type-specific extracellular permissive signal in Drosophila. Proceedings of the National Academy of Sciences. 2017;114(38):E8062-E71.

124. Krueger NX, Van Vactor D, Wan HI, Gelbart WM, Goodman CS, Saito H. The transmembrane tyrosine phosphatase DLAR controls motor axon guidance in Drosophila. Cell. 1996;84(4):611-22.

125. Desai CJ, Gindhart Jr JG, Goldstein LS, Zinn K. Receptor tyrosine phosphatases are required for motor axon guidance in the Drosophila embryo. Cell. 1996;84(4):599-609.

126. Schindelholz B, Knirr M, Warrior R, Zinn K. Regulation of CNS and motor axon guidance in Drosophila by the receptor tyrosine phosphatase DPTP52F. Development. 2001;128(21):4371-82.

127. Jeon M, Nguyen H, Bahri S, Zinn K. Redundancy and compensation in axon guidance: genetic analysis of the Drosophila Ptp10D/Ptp4E receptor tyrosine phosphatase subfamily. Neural development. 2008;3(1):3.

128. Sun Q, Bahri S, Schmid A, Chia W, Zinn K. Receptor tyrosine phosphatases regulate axon guidance across the midline of the Drosophila embryo. Development. 2000;127(4):801-12.

129. Goth CK, Vakhrushev SY, Joshi HJ, Clausen H, Schjoldager KT. Fine-Tuning Limited Proteolysis: A Major Role for Regulated Site-Specific O-Glycosylation. Trends Biochem Sci. 2018;43(4):269-84. doi: 10.1016/j.tibs.2018.02.005. PubMed PMID: 29506880.

130. Hansen LH, Madsen TD, Goth CK, Clausen H, Chen Y, Dzhoyashvili N, Iyer SR, Sangaralingham SJ, Burnett JC, Rehfeld JF. Discovery of O-glycans on atrial natriuretic peptide (ANP) that affect both its proteolytic degradation and potency at its cognate receptor. Journal of Biological Chemistry. 2019;294(34):12567-78.

131. Chandel I, Ten Hagen KG, Panin V. Sweet rescue or surrender of the failing heart? Journal of Biological Chemistry. 2019;294(34):12579-80.

132. Garrity PA, Lee C-H, Salecker I, Robertson HC, Desai CJ, Zinn K, Zipursky SL. Retinal axon target selection in Drosophila is regulated by a receptor protein tyrosine phosphatase. Neuron. 1999;22(4):707-17.

133. Pulido R, Krueger NX, Serra-Pagès C, Saito H, Streuli M. Molecular Characterization of the Human Transmembrane Protein-tyrosine Phosphatase δ EVIDENCE FOR TISSUE-SPECIFIC EXPRESSION OF ALTERNATIVE HUMAN TRANSMEMBRANE PROTEIN-TYROSINE PHOSPHATASE δ ISOFORMS. Journal of Biological Chemistry. 1995;270(12):6722-8.

134. Streuli M, Krueger N, Ariniello P, Tang M, Munro J, Blattler W, Adler D, Disteche C, Saito H. Expression of the receptor-linked protein tyrosine phosphatase LAR: proteolytic cleavage and shedding of the CAM-like extracellular region. The EMBO Journal. 1992;11(3):897-907.

135. Coles CH, Jones EY, Aricescu AR, editors. Extracellular regulation of type IIa receptor protein tyrosine phosphatases: mechanistic insights from structural analyses. Seminars in cell & developmental biology; 2015: Elsevier.

136. Johnson KG, Van Vactor D. Receptor protein tyrosine phosphatases in nervous system development. Physiological reviews. 2003;83(1):1-24.

137. Pulido R, Serra-Pages C, Tang M, Streuli M. The LAR/PTP delta/PTP sigma subfamily of transmembrane protein-tyrosine-phosphatases: multiple human LAR, PTP delta, and PTP sigma isoforms are expressed in a tissue-specific manner and associate with the LAR-interacting protein LIP. 1. Proceedings of the National Academy of Sciences. 1995;92(25):11686-90.

138. Stoker AW. Isoforms of a novel cell adhesion molecule-like protein tyrosine phosphatase are implicated in neural development. Mechanisms of development. 1994;46(3):201-17.

139. Coles CH, Mitakidis N, Zhang P, Elegheert J, Lu W, Stoker AW, Nakagawa T, Craig AM, Jones EY, Aricescu AR. Structural basis for extracellular cis and trans RPTPσ signal competition in synaptogenesis. Nature communications. 2014;5(1):1-12.

140. Coles CH, Shen Y, Tenney AP, Siebold C, Sutton GC, Lu W, Gallagher JT, Jones EY, Flanagan JG, Aricescu AR. Proteoglycan-specific molecular switch for RPTPσ clustering and neuronal extension. Science. 2011;332(6028):484-8.

141. Sarrazin S, Lamanna WC, Esko JD. Heparan sulfate proteoglycans. Cold Spring Harbor perspectives in biology. 2011;3(7):a004952.

142. Suster ML, Bate M. Embryonic assembly of a central pattern generator without sensory input. Nature. 2002;416(6877):174-8.

143. Hughes CL, Thomas JB. A sensory feedback circuit coordinates muscle activity in Drosophila. Molecular and Cellular Neuroscience. 2007;35(2):383-96.

144. Nakamura N, Lyalin D, Panin VM. Protein O-mannosylation in animal development and physiology: from human disorders to Drosophila phenotypes. Semin Cell Dev Biol. 2010;21(6):622-30. doi: 10.1016/j.semcdb.2010.03.010. PubMed PMID: 20362685; PMCID: PMC2917527.

145. Jaeken J, Matthijs G. Congenital disorders of glycosylation: a rapidly expanding disease family. Annu Rev Genomics Hum Genet. 2007;8:261-78. doi: 10.1146/annurev.genom.8.080706.092327. PubMed PMID: 17506657.

146. Roberts DB. Drosophila: a practical approach: Oxford University Press, USA; 1998.

147. Penjweini R, Loew HG, Hamblin MR, Kratky KW. Long-term monitoring of live cell proliferation in presence of PVP-Hypericin: a new strategy using ms pulses of LED and the fluorescent dye CFSE. Journal of microscopy. 2012;245(1):100-8.

148. Chandel I, Baker R, Nakamura N, Panin V. Live Imaging and Analysis of Muscle Contractions in Drosophila Embryo. Journal of visualized experiments: JoVE. 2019(149).

149. Heckscher ES, Zarin AA, Faumont S, Clark MQ, Manning L, Fushiki A, Schneider-Mizell CM, Fetter RD, Truman JW, Zwart MF. Even-skipped+ interneurons are core components of a sensorimotor circuit that maintains left-right symmetric muscle contraction amplitude. Neuron. 2015;88(2):314-29.

APPENDIX A

MASS SPECTROMETRY PEAKS FOR SER/THR RESIDUES ON EXTRACELLULAR DOMAIN OF RPTP69D

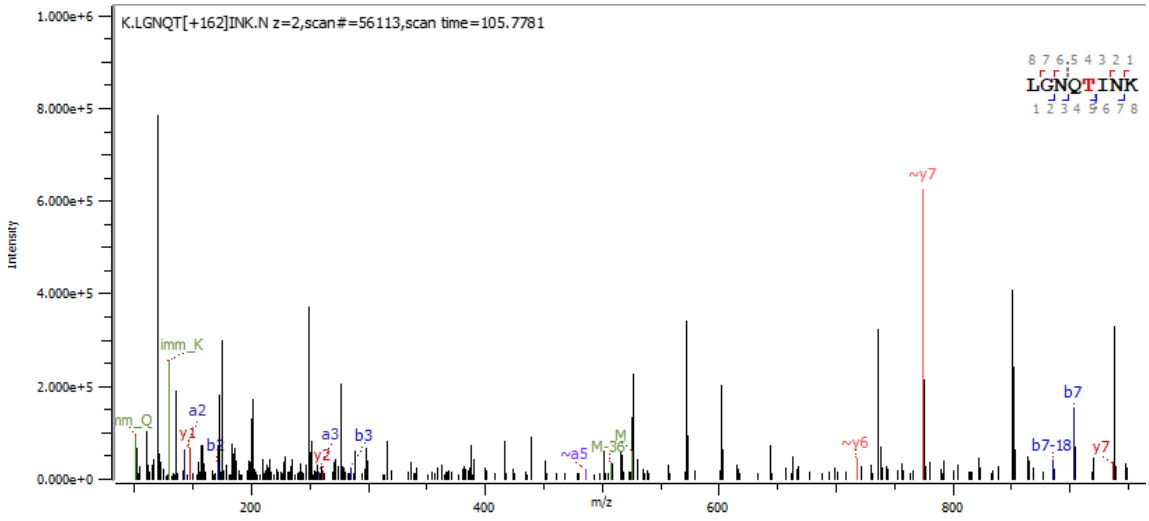

Figure 29. MS peak for T60. b7 and y7 ions represent that peptide fragment with the additional hexose.

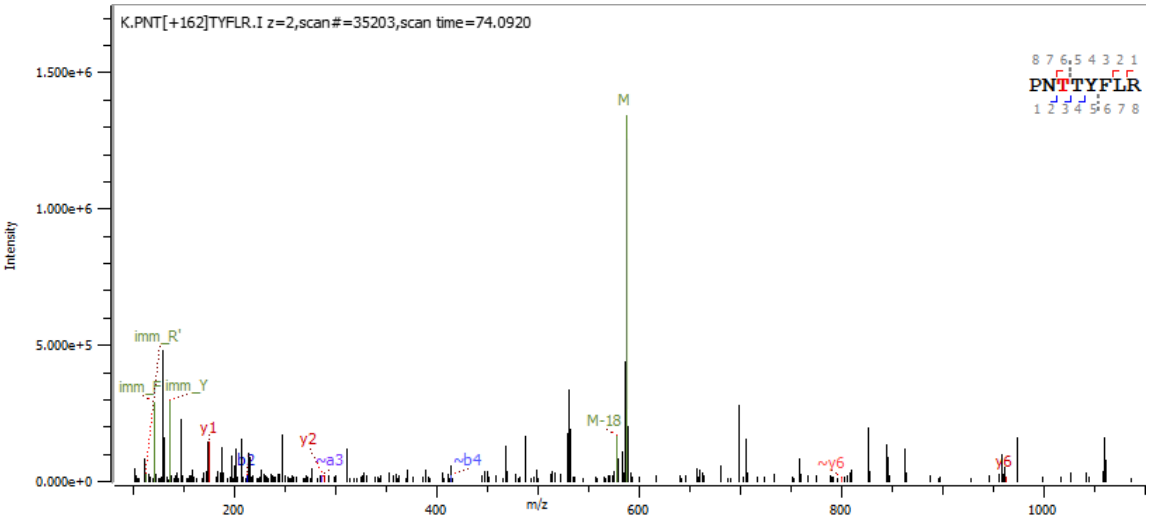

Figure 30. MS peak for T303/304. Minimal fragment ions, Can't tell which residue may be modified with current data.

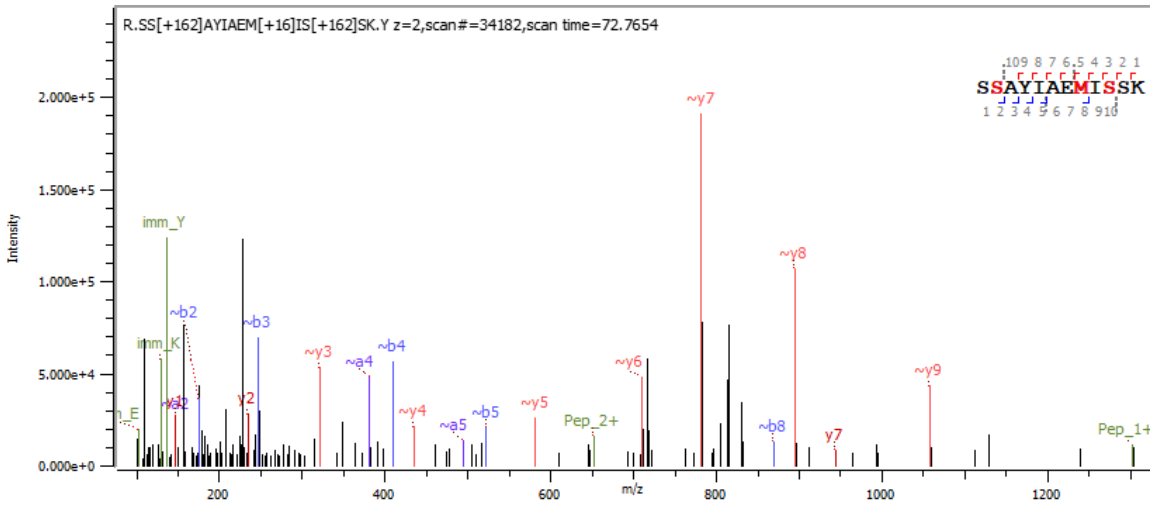

Figure 31. MS peaks for S626/627. Excellent fragmentation across the glycopeptide.